On the Signatures of Magnetic Reconnection at Current Sheets using Cluster and MMS Multi-satellite Constellation Observations

Stefan Eriksson
Laboratory for Atmospheric and Space Physics, Boulder, Colorado

Image: Petr Horálek, hybrid solar eclipse on 20 April 2023, https://www.petrhoralek.com/?p=23566

On the Signatures of Magnetic Reconnection at Current Sheets using Cluster and MMS Multi-satellite Constellation Observations

Stefan Eriksson
Laboratory for Atmospheric and Space Physics, Boulder, Colorado

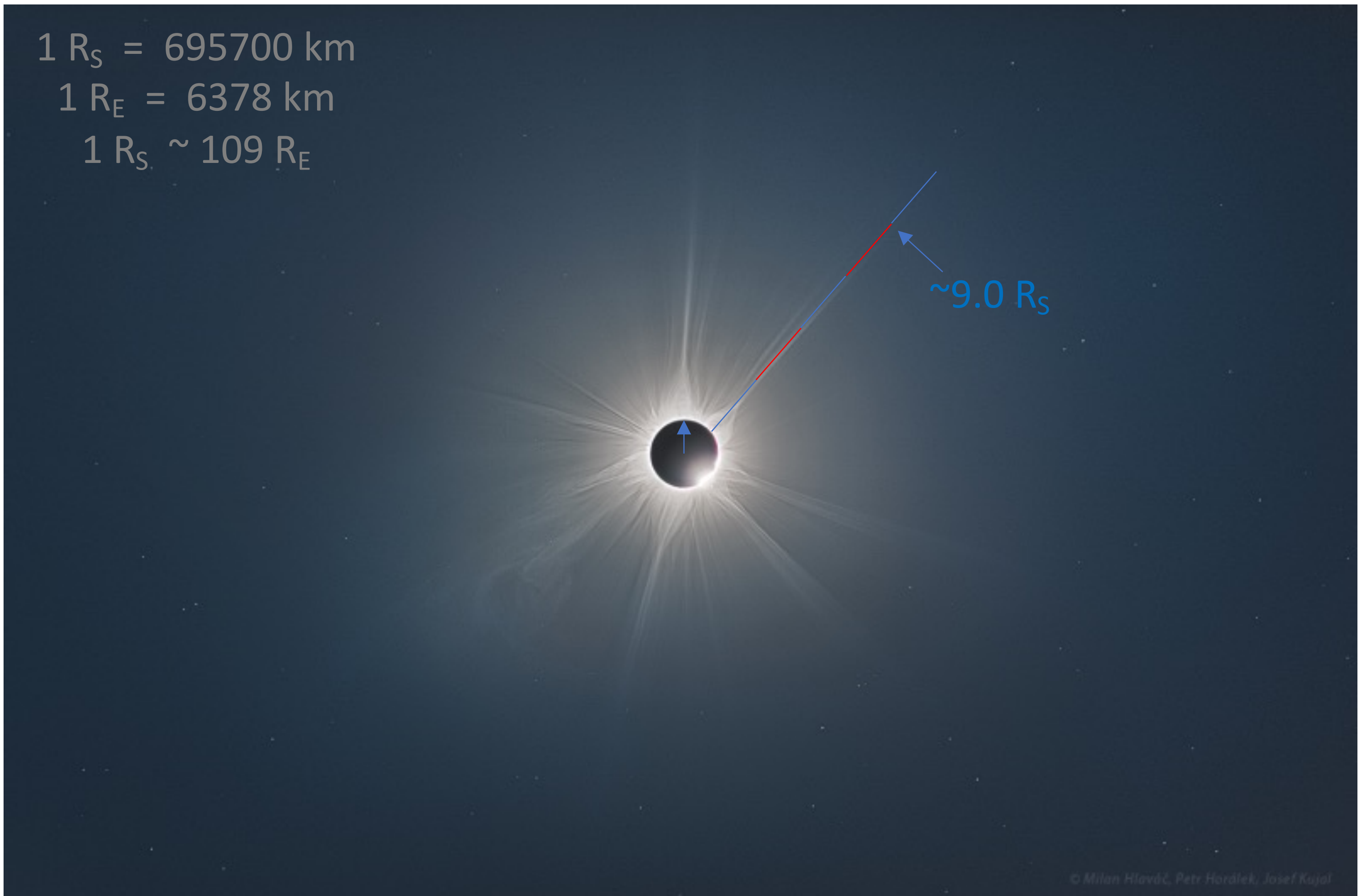

Image: Petr Horálek, hybrid solar eclipse on 20 April 2023, https://www.petrhoralek.com/?p=23566

On the Signatures of Magnetic Reconnection at Current Sheets using Cluster and MMS Multi-satellite Constellation Observations

Stefan Eriksson
Laboratory for Atmospheric and Space Physics, Boulder, Colorado

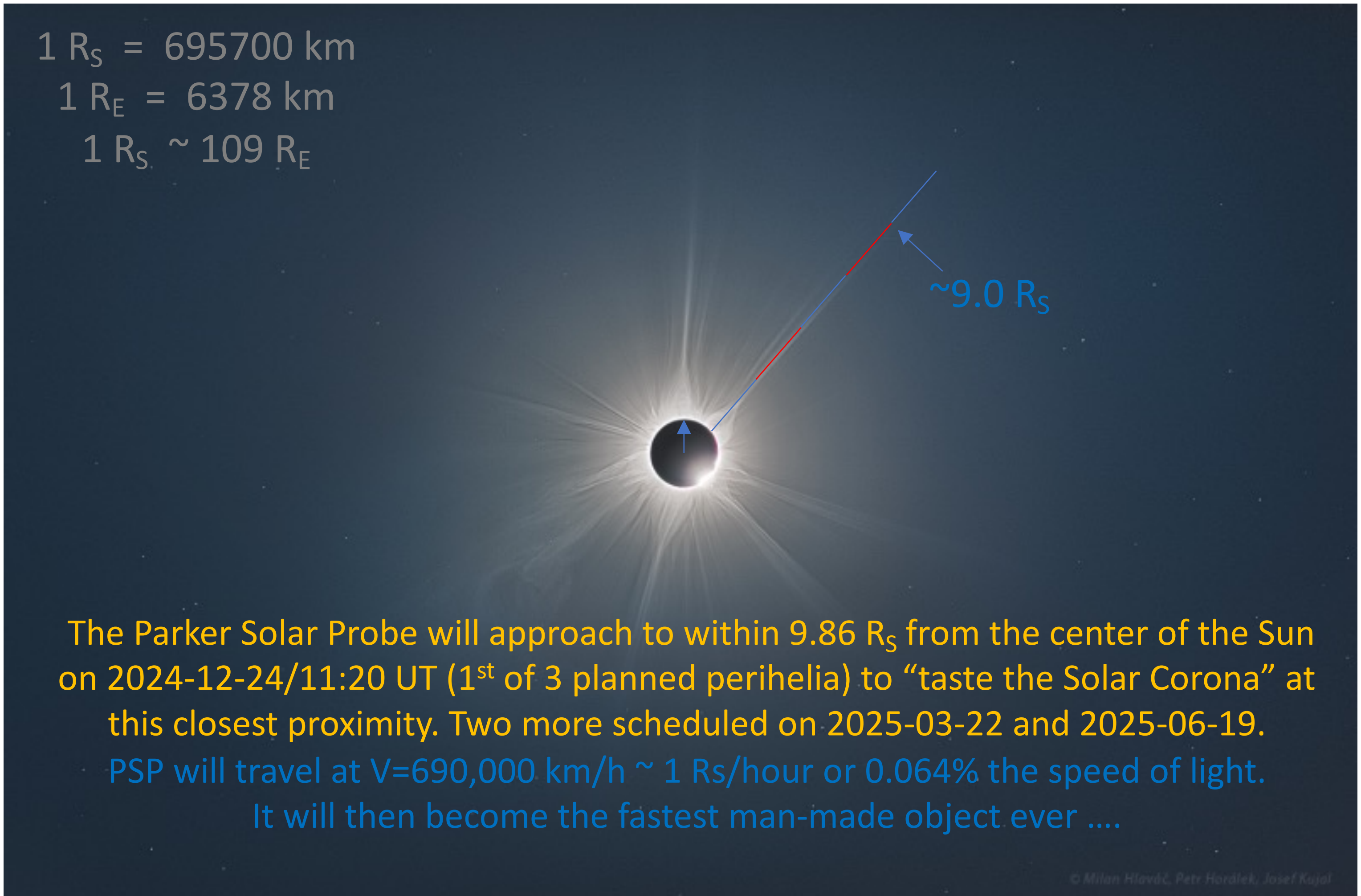

Image: Petr Horálek, hybrid solar eclipse on 20 April 2023, https://www.petrhoralek.com/?p=23566

On the Signatures of Magnetic Reconnection at Current Sheets using Cluster and MMS Multi-satellite Constellation Observations

Stefan Eriksson
Laboratory for Atmospheric and Space Physics, Boulder, Colorado

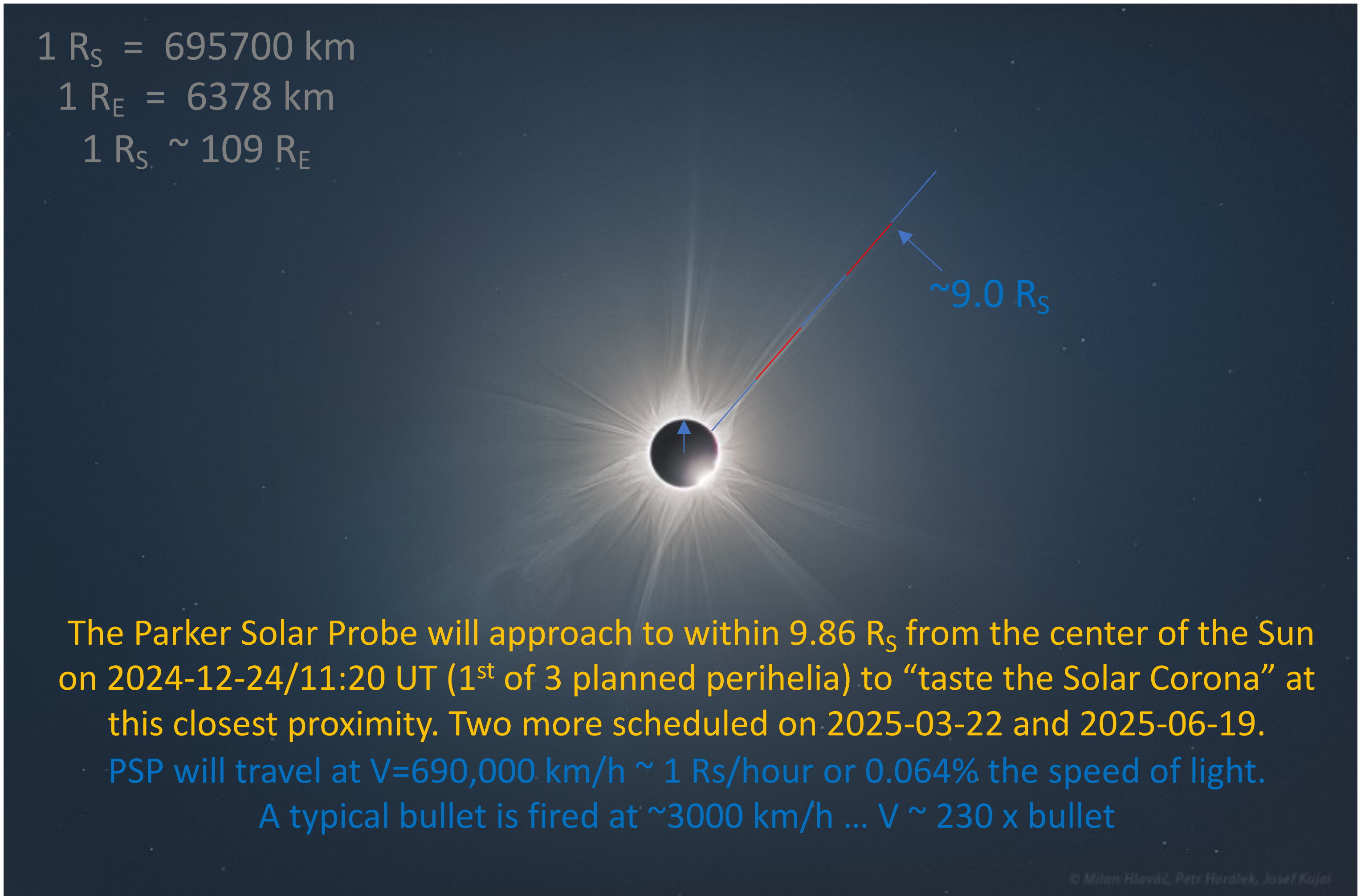

Image: Petr Horálek, hybrid solar eclipse on 20 April 2023, https://www.petrhoralek.com/?p=23566

On the Signatures of Magnetic Reconnection at Current Sheets using Cluster and MMS Multi-satellite Constellation Observations

Stefan Eriksson

Laboratory for Atmospheric and Space Physics, Boulder, Colorado

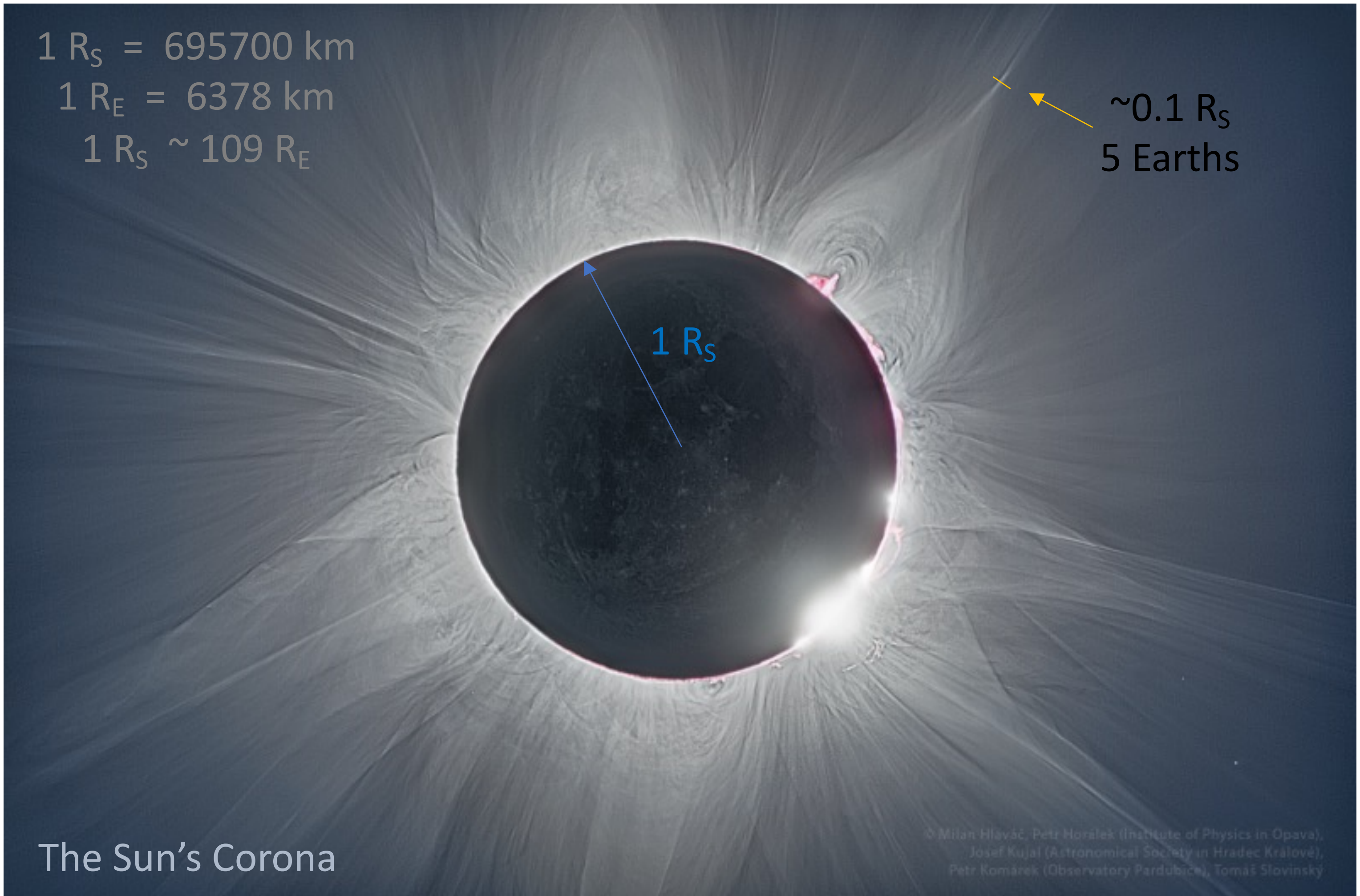

Image: Petr Horálek *et al*, hybrid solar eclipse on 20 April 2023, https://www.petrhoralek.com/?p=23566

On the Signatures of Magnetic Reconnection at Current Sheets using Cluster and MMS Multi-satellite Constellation Observations

Stefan Eriksson
Laboratory for Atmospheric and Space Physics, Boulder, Colorado

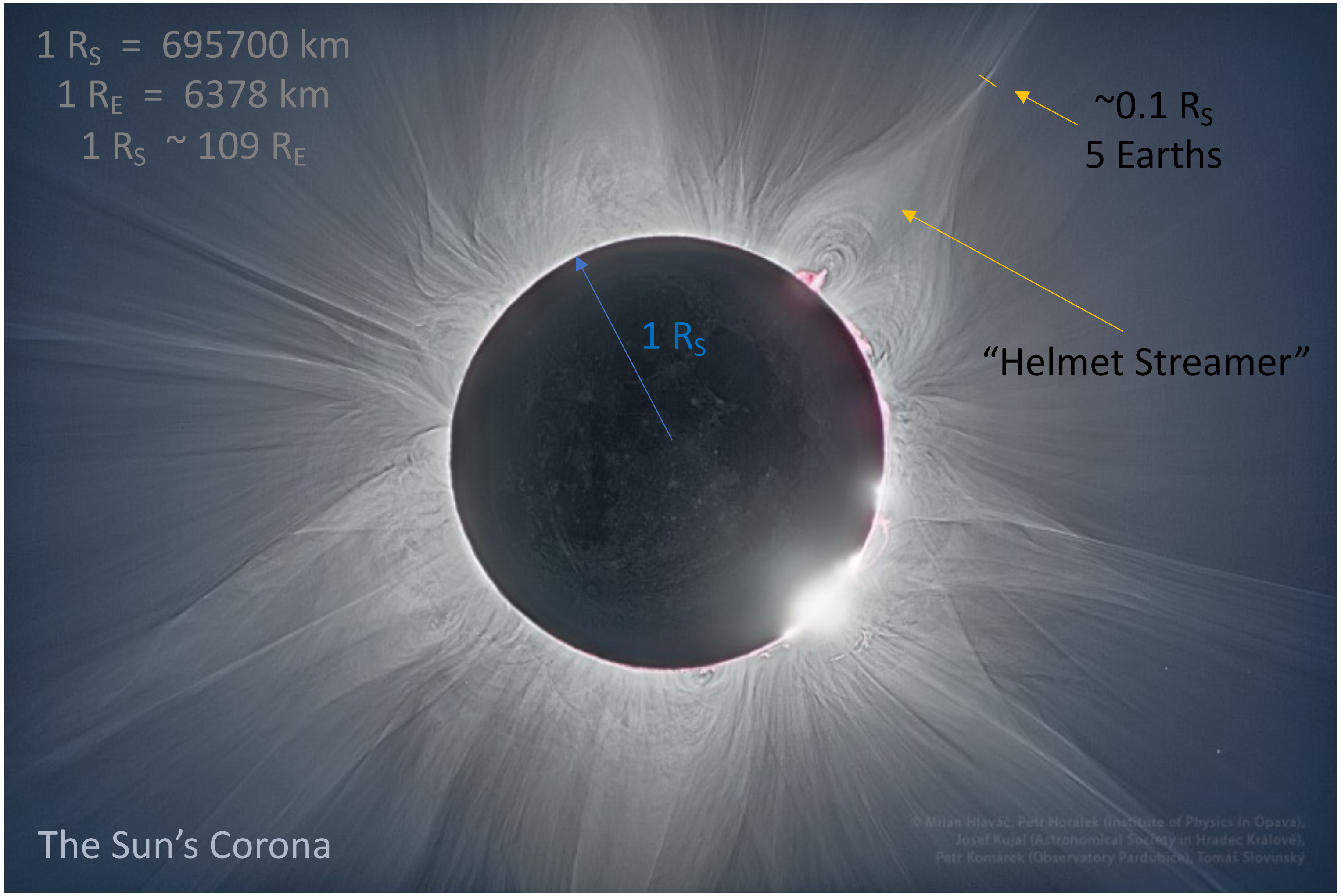

Image: Petr Horálek *et al*, hybrid solar eclipse on 20 April 2023, https://www.petrhoralek.com/?p=23566

On the Signatures of Magnetic Reconnection at Current Sheets using Cluster and MMS Multi-satellite Constellation Observations

Stefan Eriksson

Laboratory for Atmospheric and Space Physics, Boulder, Colorado

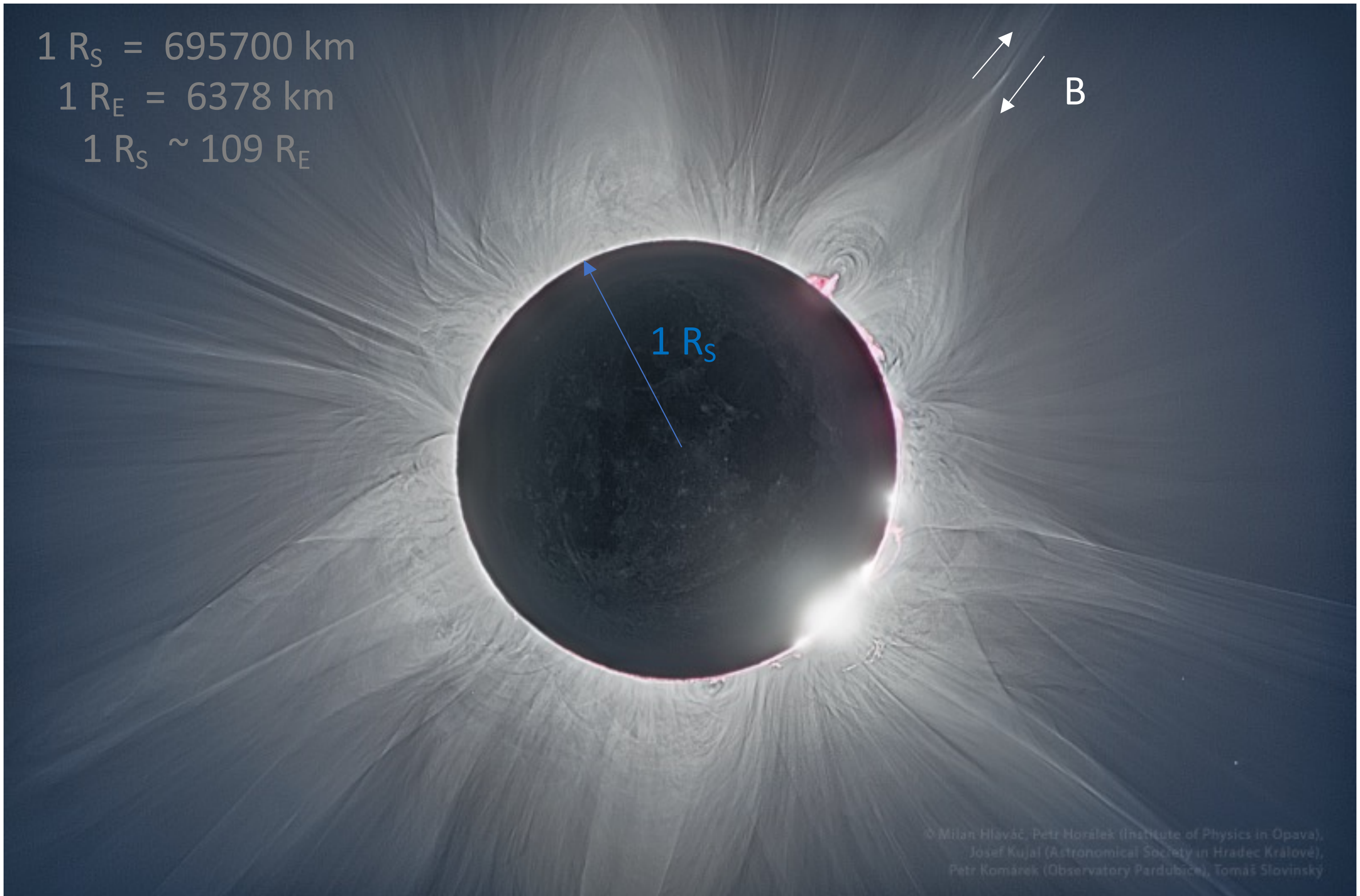

Image: Petr Horálek *et al*, hybrid solar eclipse on 20 April 2023, https://www.petrhoralek.com/?p=23566

Overview

- **Current sheets:** ***Magnetic field rotations [$J=\nabla\times B/\mu_0$] from the very wide Heliospheric Current Sheet to "narrow" M'pause***
- Multi-spacecraft missions: *A brief introduction to tedrahedron formations and the Curlometer technique*
- Near-Earth space regimes & boundaries
- The magnetic reconnection process at current sheets:

  (a) Schematic overviews, 2D vs 3D & ion (di) scale

  (b) "To be or not to be" frozen-in? The G.O.L. vs Hall ☺

  (c) Reconnection rate v_{in}/v_{out}
- Observations of Reconnection Jets:

  (a) Cluster in the solar wind vs "timing normal" concept

  (b) MMS at the magnetopause: J from "curlB" vs J=Ne(Vi-Ve)
- Summary

Heliospheric Current Sheet

SMITH: REVIEW

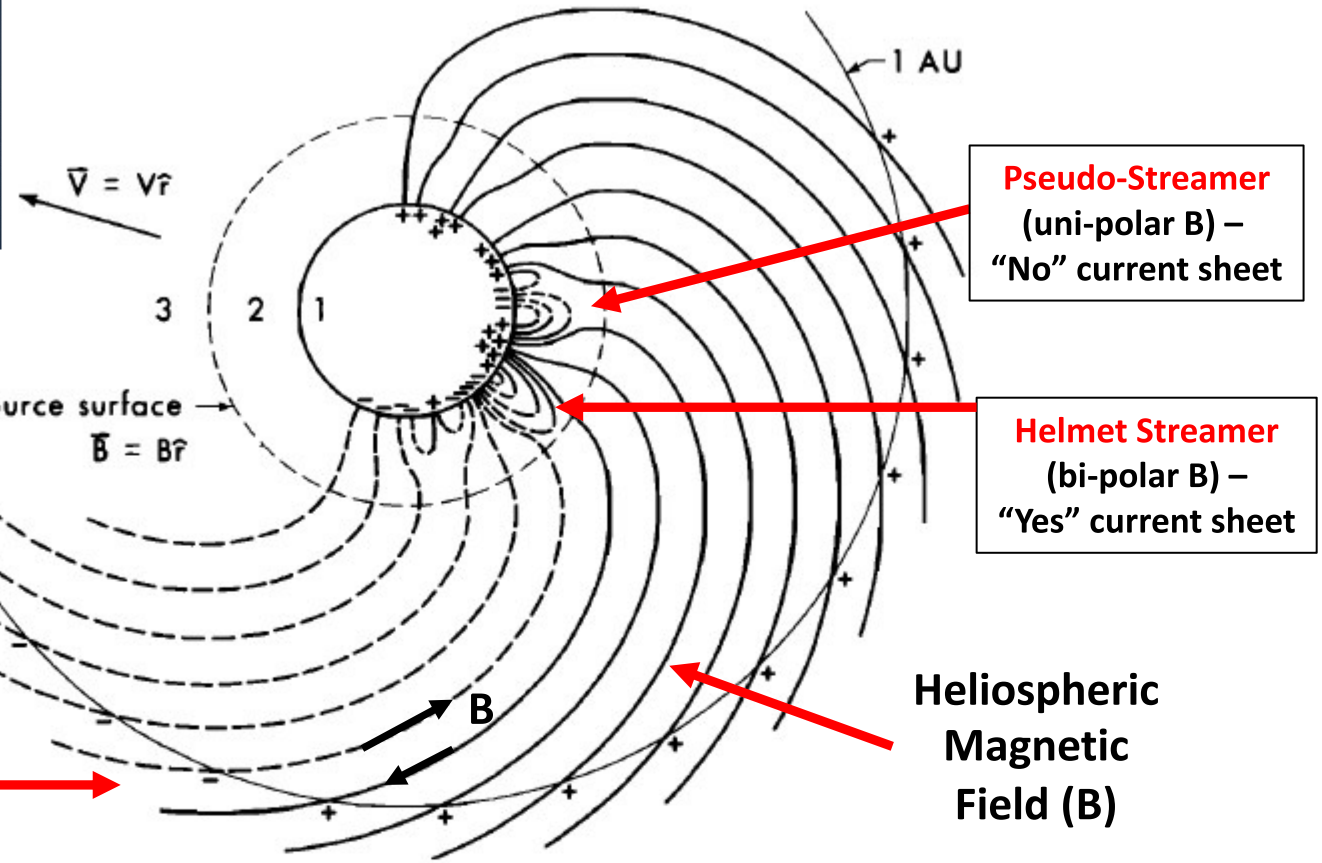

Figure 7. Schematic of the solar wind magnetic field source surface. The photospheric magnetic field, routinely observed by ground-based magnetographs, is extrapolated upward using a magnetic potential to the “source surface” at which the field is required to become radial. The differing magnetic polarities along the photosphere associated with both low- and high-latitude fields are indicated. Only the largest-scale fields reach the source surface. Both positive and negative fields are shown. From *Schatten* [1972].

Smith, The heliospheric current sheet, J. Geophys. Res., 106, A8, 15,819-15,831, 2001

Heliospheric Current Sheet

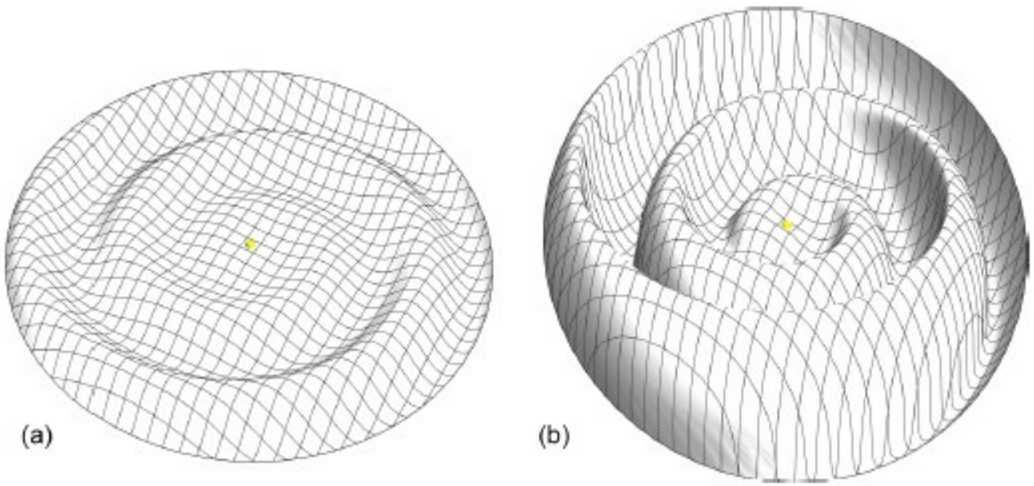

Figure 5. Shape of the "ballerina skirt" model of the heliocentric current sheet defined by $\cos\theta^* = \cos\theta$. Topology at $t = 0$ and for $\theta_{t0} = 5°$ **(a)** and $\theta_{t0} = 30°$ **(b)**.

Lhotka, C. & Y. Narita, Kinematic models of the interplanetary magnetic field, Annales Geophysicae, 37, 299–314, 2019

Ref	HCS min (km)	HCS max (km)	<HCS> (km)
19 HCSs (1)	3500	12000	9100 (median)
212 HCSs (2)	-	-	64000 (average) ~10 R_E

1. Winterhalter et al., The heliospheric plasma sheet, J. Geophys. Res., 99, A4, 6667-6680, 1994
2. Lepping et al, Large-scale properties and solar connection of the heliospheric current and plasma sheets: WIND observations, Geophys. Res. Lett., 1996.

Earth's Magnetopause Current

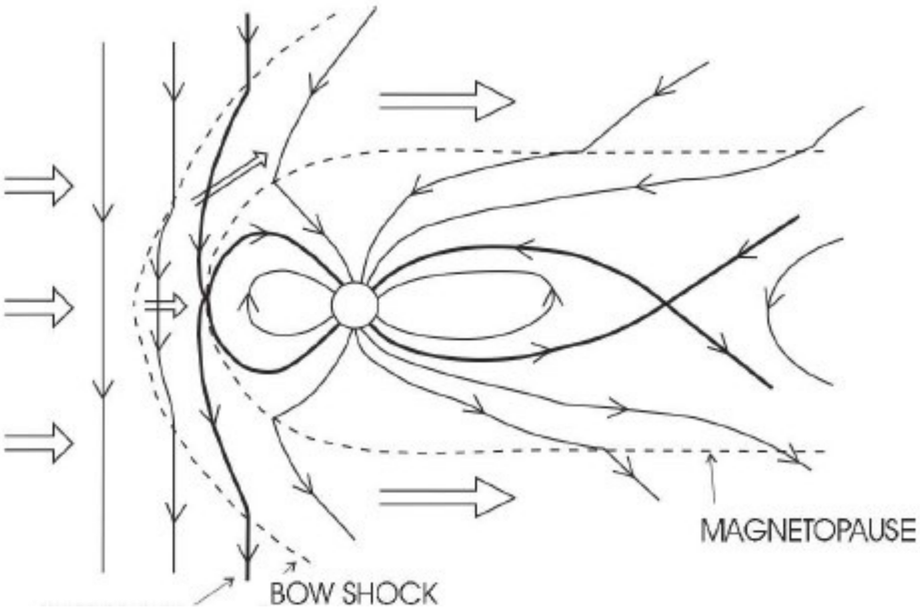

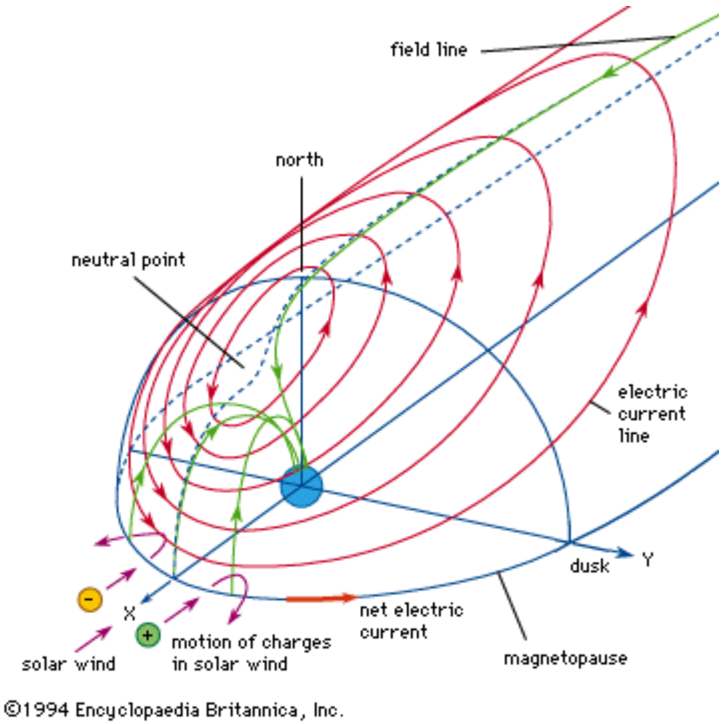

Principles of Heliophysics, V2.0

https://www.britannica.com/science/geomagnetic-field/The-magnetopause-current

The Earth's magnetopause current layer is typically ~200-600 km thick.

[Le & Russell, The thickness and structure of high beta magnetopause current layer, *Geophys. Res. Lett.*, 1994]

Overview

- **Current sheets:** ***Magnetic field rotations [$J = \nabla \times B/\mu_0$] from the very wide Heliospheric Current Sheet to "narrow" M'pause***
- **Multi-spacecraft missions:** ***A brief introduction to tedrahedron formations and the Curlometer technique***
- Near-Earth space regimes & boundaries
- The magnetic reconnection process at current sheets:
  - *(a) Schematic overviews, 2D vs 3D & ion (di) scale*
  - *(b) "To be or not to be" frozen-in? The G.O.L. vs Hall ☺*
  - *(c) Reconnection rate v_{in}/v_{out}*
- Observations of Reconnection Jets:
  - *(a) Cluster in the solar wind vs "timing normal" concept*
  - *(b) MMS at the magnetopause: J from "curlB" vs J=Ne(Vi-Ve)*
- Summary

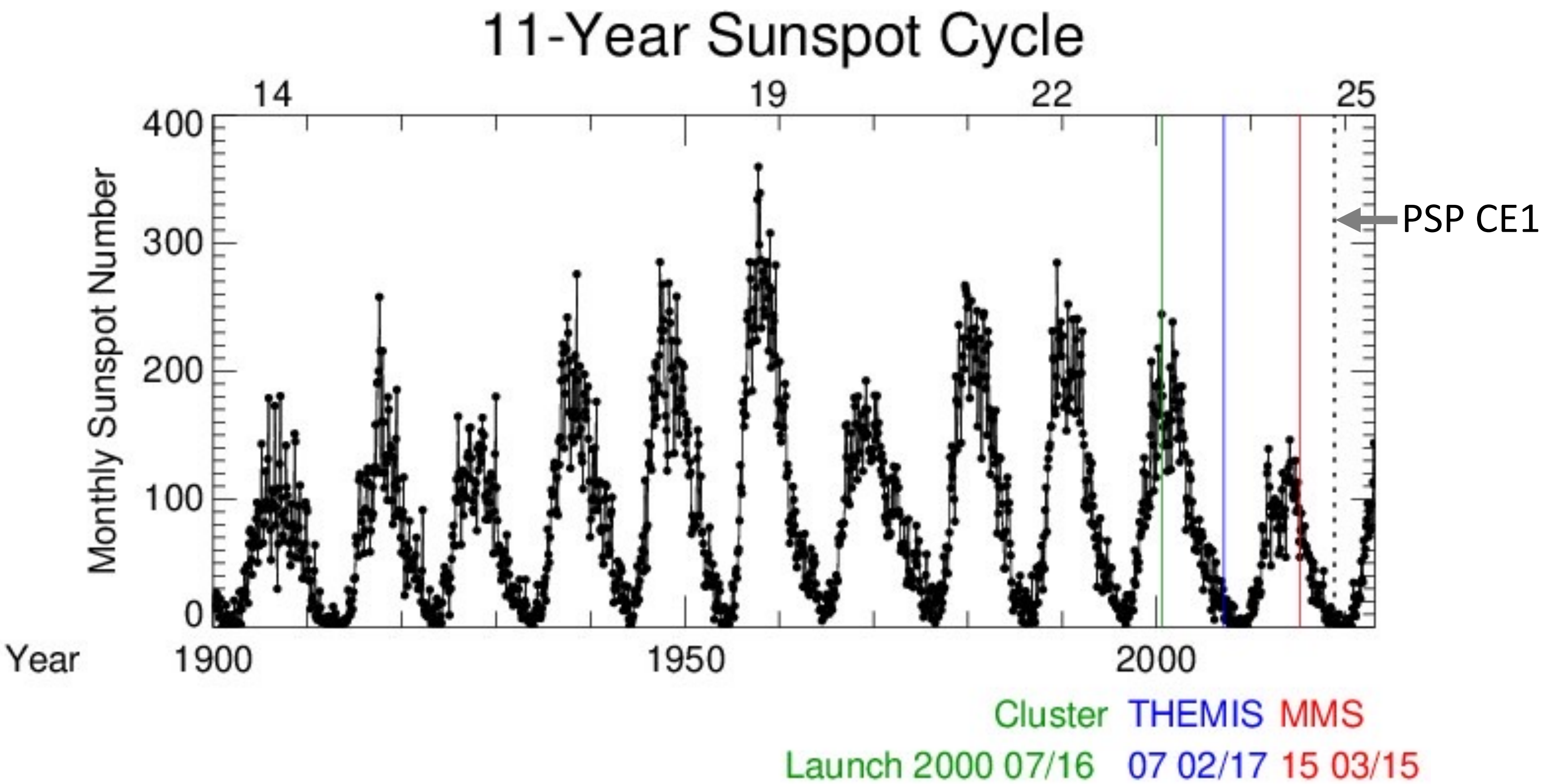

Cluster: 4 s/c - first (ion-scale) tetrahedron formation mission (ESA/NASA)

THEMIS: 5 s/c – no tetrahedron requirement (NASA)

MMS: 4 s/c – first <u>electron-scale</u> tetrahedron mission (NASA)

HelioSwarm: 9 s/c multi-scale turbulence mission (NASA: Launch~2028)

Source: WDC-SILSO, Royal Observatory of Belgium, Brussels https://www.sidc.be/silso/datafiles

The four-spacecraft Cluster mission

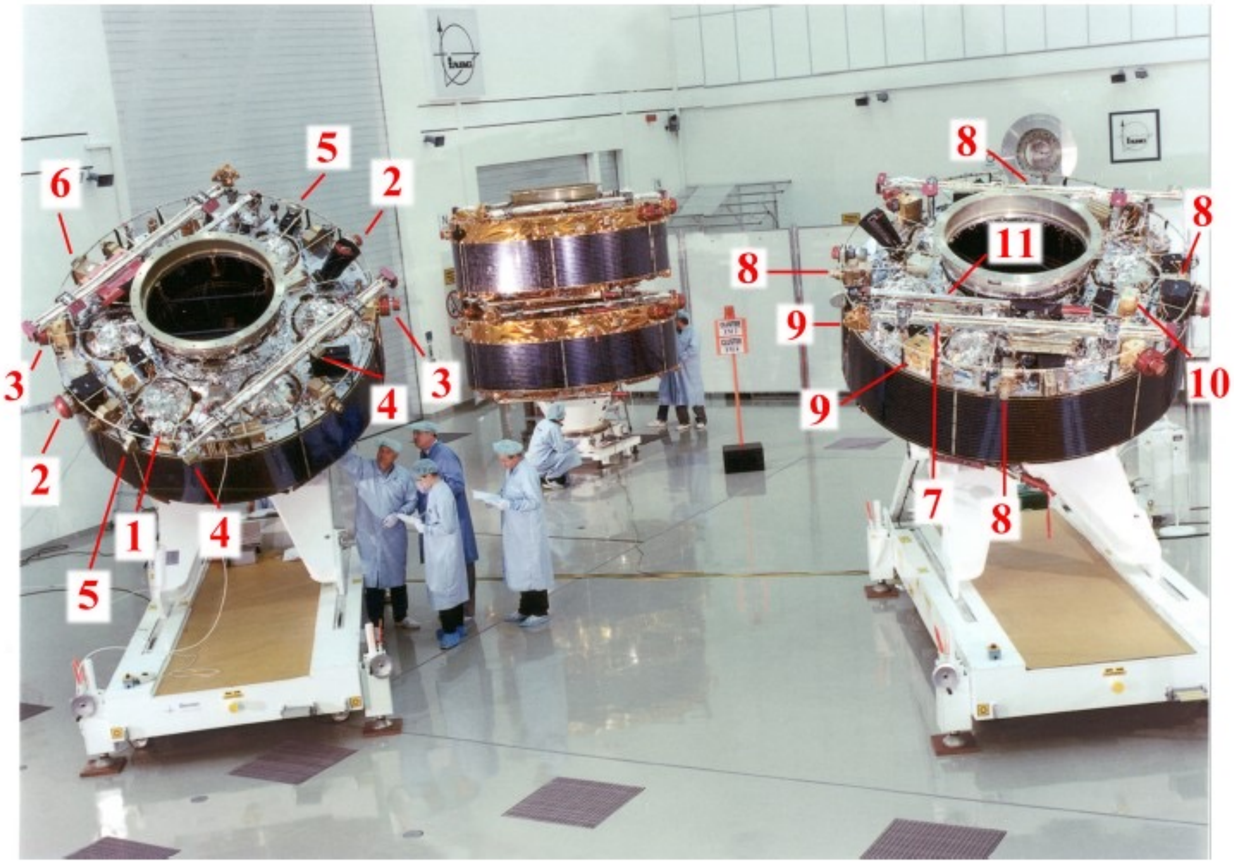

Cluster II is an ESA space mission with NASA participation, to study the Earth's magneto-sphere from a 4 x 19.6 R_E elliptical orbit.

This mission is composed of four identical spacecraft flying for the very first time in a tetrahedron formation.

The Cluster II spacecraft launched in pairs in July and August 2000 from Baikonur, Kazakhstan.

First scientific measurements made on February 1, 2001. As of March 2023, its mission has been extended until September 2024.

Fig. 3. Position of the 11 instruments on the spacecraft. ASPOC (1), CIS (2), EDI (3), FGM (4), PEACE (5), RAPID (6), DWP (7), EFW (8), STAFF (9), WBD (10), WHISPER (11)

Escoubet et al, The Cluster mission, Annales Geophysicae (2001);
Escoubet et al, Recent highlights from Cluster, the first 3-D magnetospheric mission, Ann. Geophys. (2015)

What is a Tetrahedron?

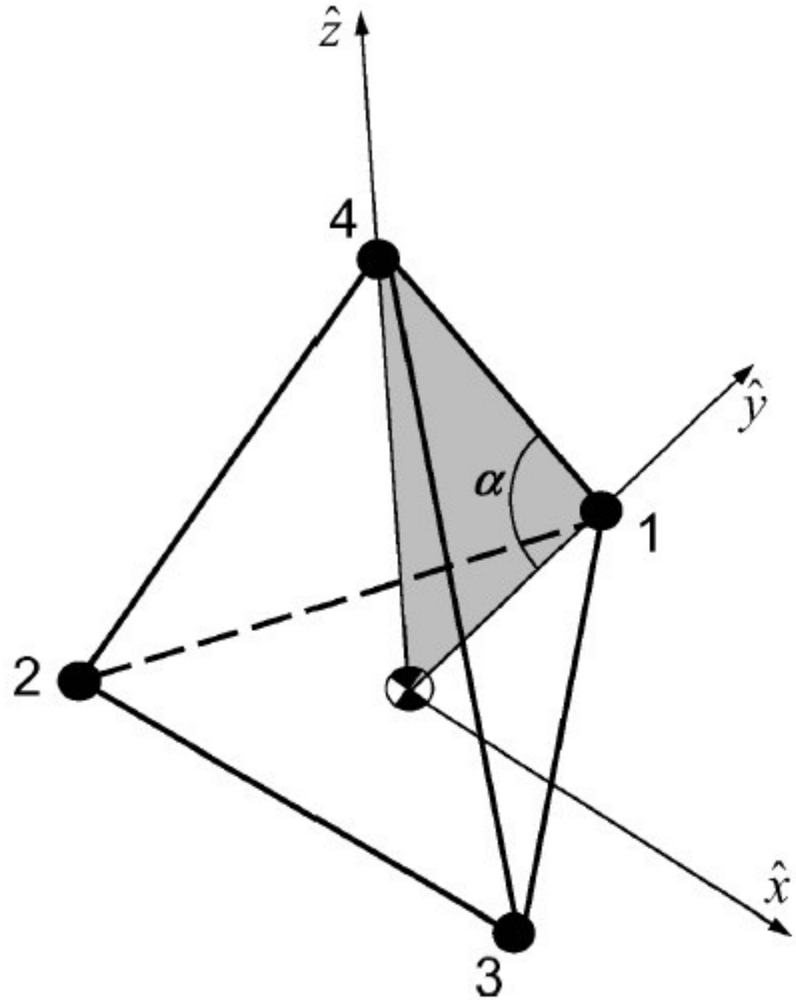

Fig. 5 Regular tetrahedron illustrating *V* frame and internal angle α.

Clemente, D. C., and E. M. Atkins, Optimization of a Tetrahedral Satellite Formation, JOURNAL OF SPACECRAFT AND ROCKETS, 42, 4, 2005, DOI:10.2514/1.9776

What is a Tetrahedron?

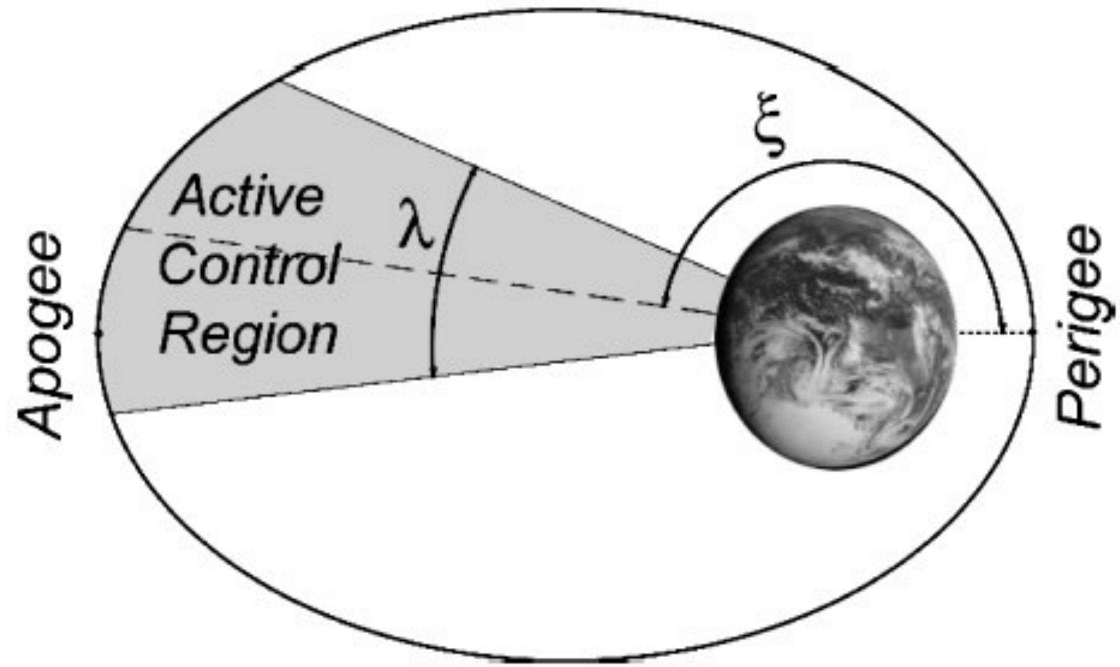

Fig. 2 Location and width of active control region for an elliptical orbit.

Clemente, D. C., and E. M. Atkins, Optimization of a Tetrahedral Satellite Formation, JOURNAL OF SPACECRAFT AND ROCKETS, 42, 4, 2005, DOI:10.2514/1.9776

Why fly a Tetrahedron mission?

There is a need to know the current density (**J**) in space due to its importance in many space plasma applications, such as magnetic reconnection.

The MMS FPI instrument measurements of electron velocity (**V**e at 30 ms cadence) is very high-quality, such that a local (s/c) measurement can be obtained as **J**=n*e*(**V**i-**V**e) at the ion cadence (interpolation of **V**e to **V**i 150-ms cadence).

However, before MMS, those high-quality measurements were not available, and the need to estimate **J** from a tetrahedron formation, **<u>curlometer technique</u>** is/was crucial.

Tetrahedron allows the **<u>gradients</u>** of any vector/matrix to be evaluated. E.g., divergence of **B** ($\nabla \cdot \mathbf{B} = 0$) or electron pressure tensor ($\nabla \cdot \mathbf{Pe}$).

The Curlometer Technique

At low frequencies (much less than the plasma frequency) the electrical current density and the magnetic flux vector in a plasma are related by Ampere's law,

$$\mu_0 \mathbf{J} = \mathbf{Curl\ B} \qquad (1)$$

For a cartesian coordinate system, for instance, taking the z component of the equation yields

$$\frac{\partial B_x}{\partial y} - \frac{\partial B_y}{\partial x} = \mu_0 J_z \qquad (2)$$

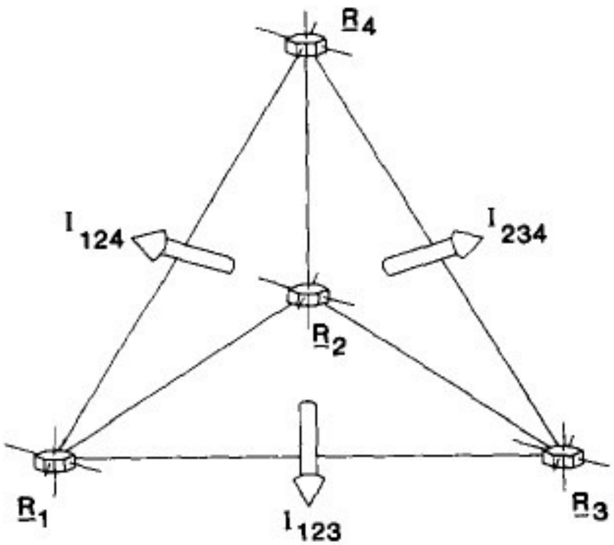

Fig. 1: The CLUSTER spacecraft tetrahedron.

A typical configuration of the CLUSTER spacecraft is depicted in Figure 1. In general the tetradhedron formed will not be regular. Each spacecraft measures a time series of **B** at each vertex of the tetrahedron. The vector separation of spacecraft i and j is $\Delta \mathbf{R}_{ij}$ and the vector field difference between the spacecraft is $\Delta \mathbf{B}_{ij}$. One can produce difference estimates for each component of **J** so long as a least three of the separation vectors are linearly independent as follows.

It is useful to have a procedure for current calculation that is coordinate-independent. The integral definition of the **curl B**, arising from Stokes' theorem, gives

M. W. Dunlop et al., ANALYSIS OF MULTIPOINT MAGNETOMETER DATA, Adv. Space Res. Vol. 8, No. 9—10, 1988.

The Curlometer Technique

$\mu_0 \mathbf{J}\cdot(\Delta\mathbf{R}i \times \Delta\mathbf{R}j) = \Delta\mathbf{B}i\cdot\Delta\mathbf{R}j - \Delta\mathbf{B}j\cdot\Delta\mathbf{R}i$

where **J** represents the **average current density** in the s/c volume and Δ**B**i is the difference in **B** between s/c 1 (ref s/c) and s/c i=2,3,4.

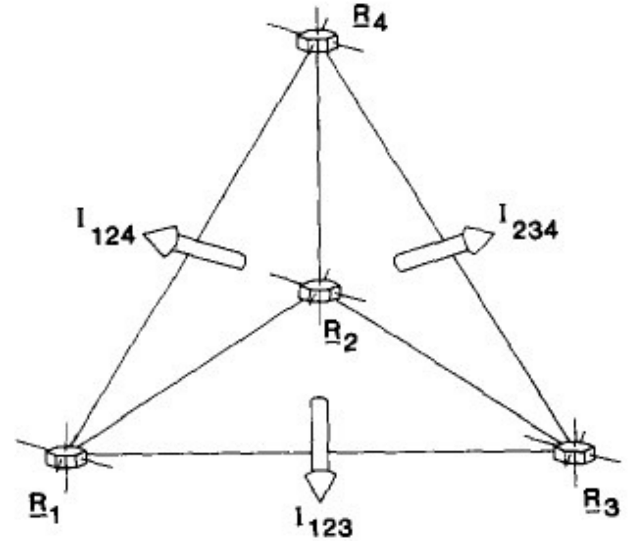

Δ**R**i is the vector separation of s/c 1 (ref s/c) and s/c i=2,3,4.

By cyclically taking i and j through values 2,3,4 one derives a set of three equations for three independent components of curl **B**.

M. W. Dunlop et al., ANALYSIS OF MULTIPOINT MAGNETOMETER DATA, Adv. Space Res. Vol. 8, No. 9—10, 1988.
Dunlop, M. W., et al. (2021). Curlometer technique and applications. Journal of Geophysical Research: Space Physics, 126, e2021JA029538. https://doi.org/10.1029/2021JA029538

Overview

- **Current sheets:** ***Magnetic field rotations [$J=\nabla\times B/\mu_0$] from the very wide Heliospheric Current Sheet to "narrow" M'pause***
- **Multi-spacecraft missions:** ***A brief introduction to tedrahedron formations and the Curlometer technique***
- **Near-Earth space regimes & boundaries**
- The magnetic reconnection process at current sheets:

  (a) Schematic overviews, 2D vs 3D & ion (di) scale

  (b) "To be or not to be" frozen-in? The G.O.L. vs Hall ☺

  (c) Reconnection rate v_{in}/v_{out}
- Observations of Reconnection Jets:

  (a) Cluster in the solar wind vs "timing normal" concept

  (b) MMS at the magnetopause: J from "curlB" vs J=Ne(Vi-Ve)
- Summary

The four-spacecraft Cluster mission: Orbit configurations

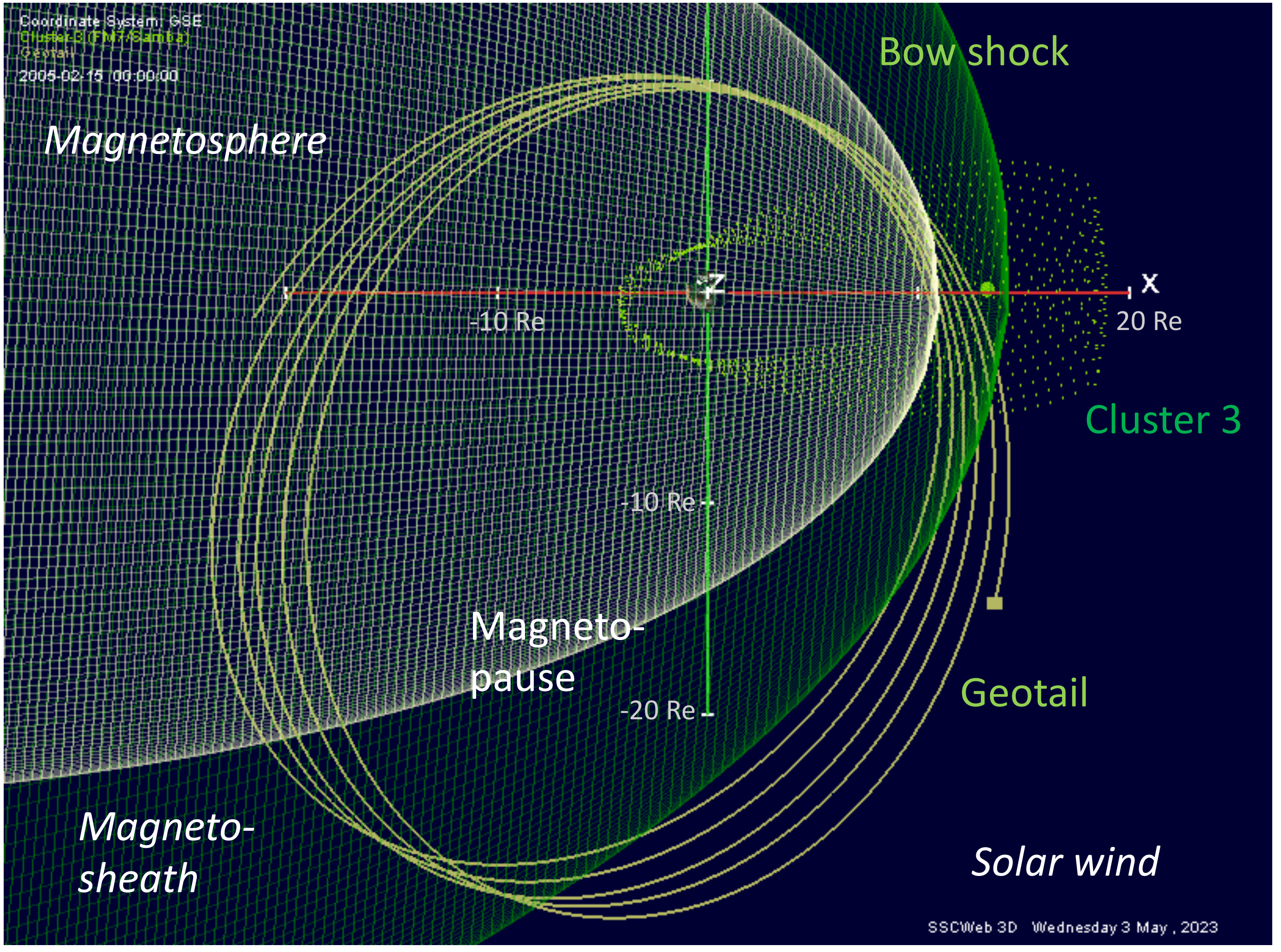

2005-02-15 to 2005-03-15: 4.0 x 19.6 R_E

Near-Earth Space Plasma Boundaries

Magnetosphere (A):
Hot and tenuous plasma in the Earth's geomagnetic field

Magnetopause (1):
*Current density (**J**) boundary layer that resists (**J**x**B** force) the oncoming (shocked) solar wind plasma*

Magnetosheath (B):
The region of turbulent and shocked ('slow') solar wind plasma

Bow shock (2):
Transition layer from super-Alfvenic (M_A>1) to sub-Alfvenic (M_A<1) plasma motion

Solar wind (C):
Solar origin B and M_A>1 plasma streaming away from the Sun

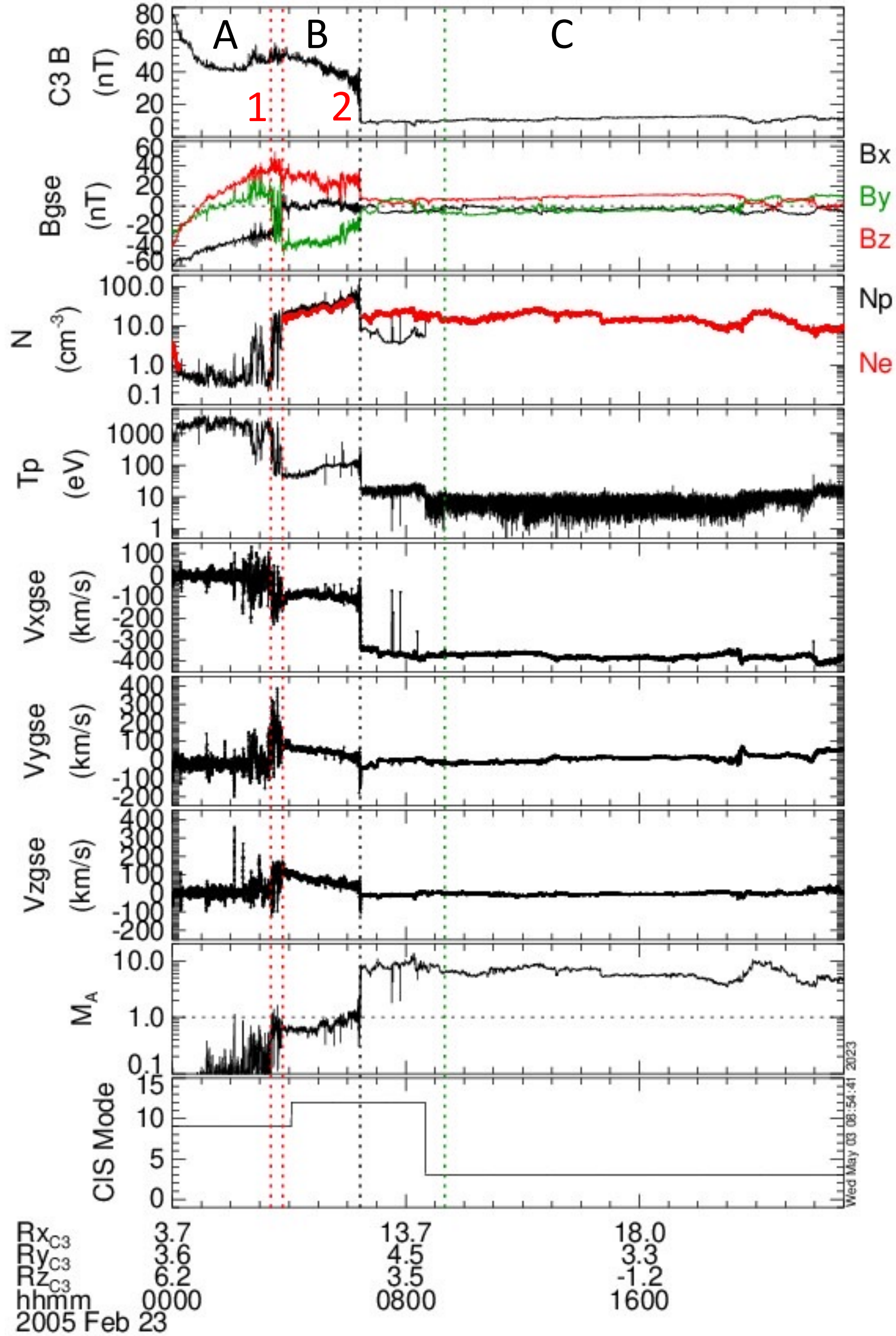

Near-Earth Space Plasma Boundaries

Magnetosphere (A):
Hot and tenuous plasma in the Earth's geomagnetic field

Magnetopause (1):
*Current density (**J**) boundary layer that resists (**J**x**B** force) the oncoming (shocked) solar wind plasma*

Magnetosheath (B):
The region of turbulent and shocked ('slow') solar wind plasma

Bow shock (2):
Transition layer from super-Alfvenic (M_A>1) to sub-Alfvenic (M_A<1) plasma motion

Solar wind (C):
Solar origin B and M_A>1 plasma streaming away from the Sun

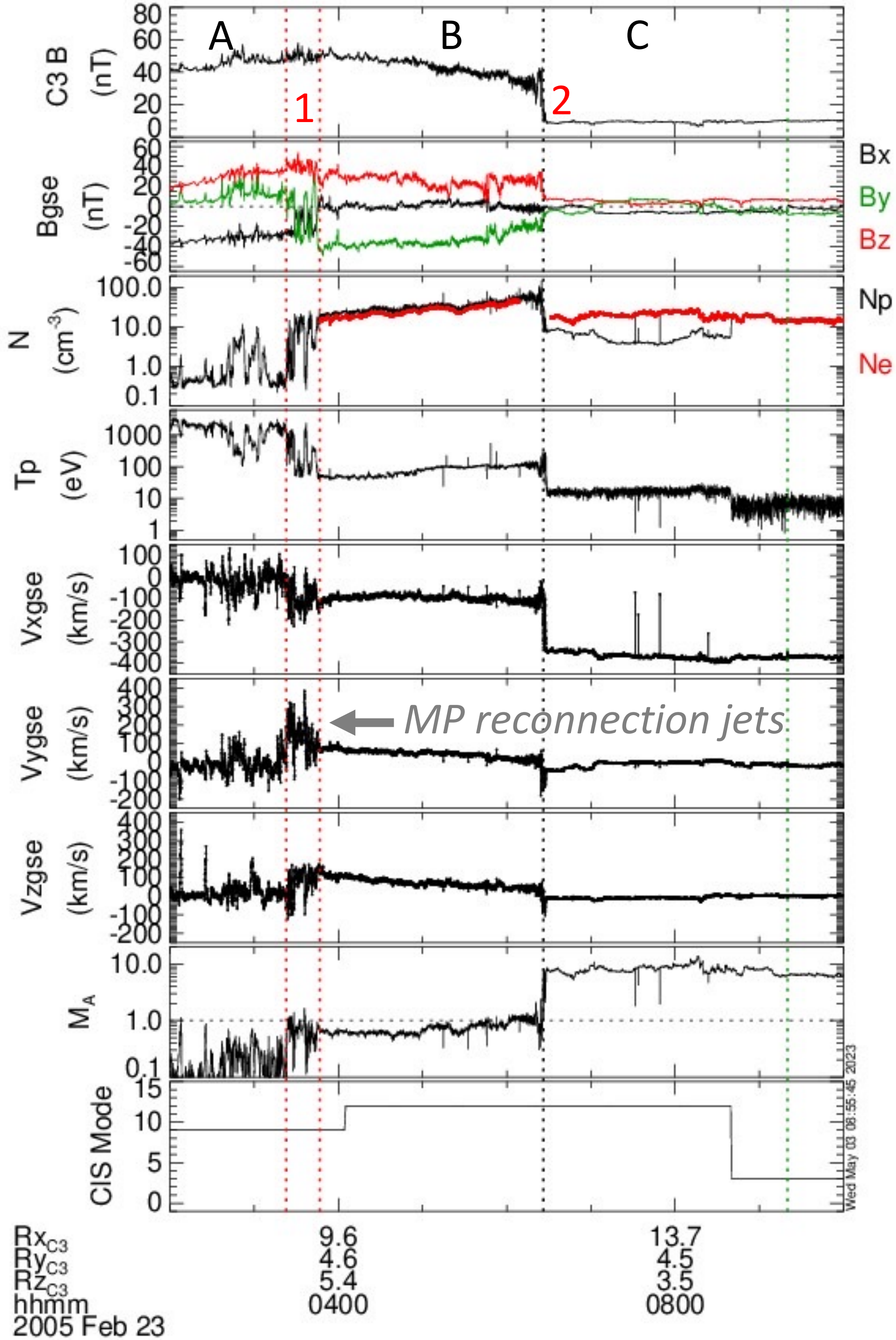

Overview

- **Current sheets:** ***Magnetic field rotations [$J=\nabla\times B/\mu_0$] from the very wide Heliospheric Current Sheet to "narrow" M'pause***
- **Multi-spacecraft missions:** ***A brief introduction to tedrahedron formations and the Curlometer technique***
- **Near-Earth space regimes & boundaries**
- **The magnetic reconnection process at current sheets:**

    (a) Schematic overviews, 2D vs 3D & ion (di) scale

    (b) "To be or not to be" frozen-in? The G.O.L. vs Hall ☺

    (c) Reconnection rate v_{in}/v_{out}
- Observations of Reconnection Jets:

    (a) Cluster in the solar wind vs "timing normal" concept

    (b) MMS at the magnetopause: J from "curlB" vs J=Ne(Vi-Ve)
- Summary

Magnetic Reconnection at Current Sheets

- **Ideal MHD**: frozen-in field lines – "At its simplest, the *frozen-in-field-line theorem* states that if two fluid elements lie on a common field line at one time, then they lie on a common field line at all times past and future." [*Principles of Heliophysics, p55]*

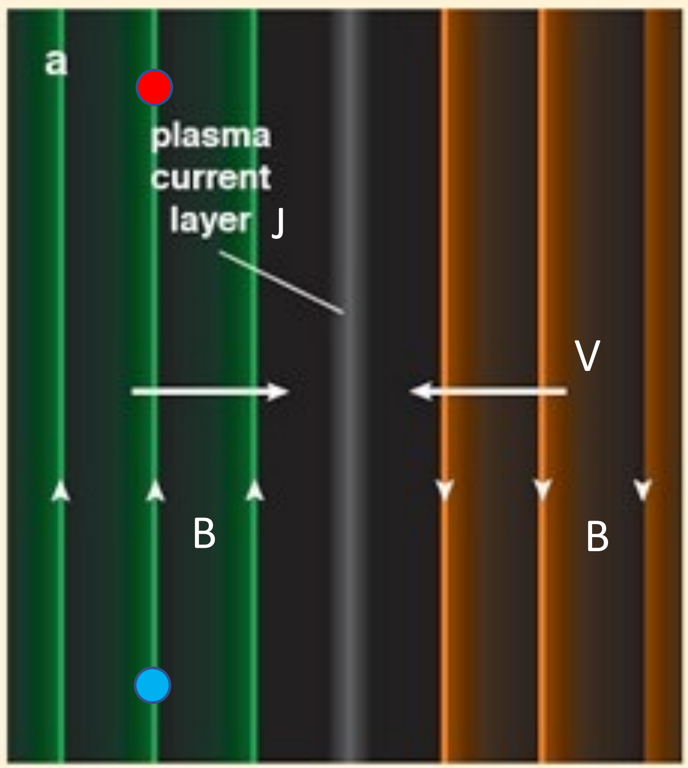

$$\nabla \times \boldsymbol{B} = \mu_0 \boldsymbol{J} + \mu_0 \epsilon_0 \frac{\partial \boldsymbol{E}}{\partial t}$$

Burch, J.L., & J.F. Drake (2009). Reconnecting Magnetic Fields, American Scientist, Sept-Oct., vol. 97, number 5, doi:10.1511/2009.80.392

Magnetic Reconnection at Current Sheets

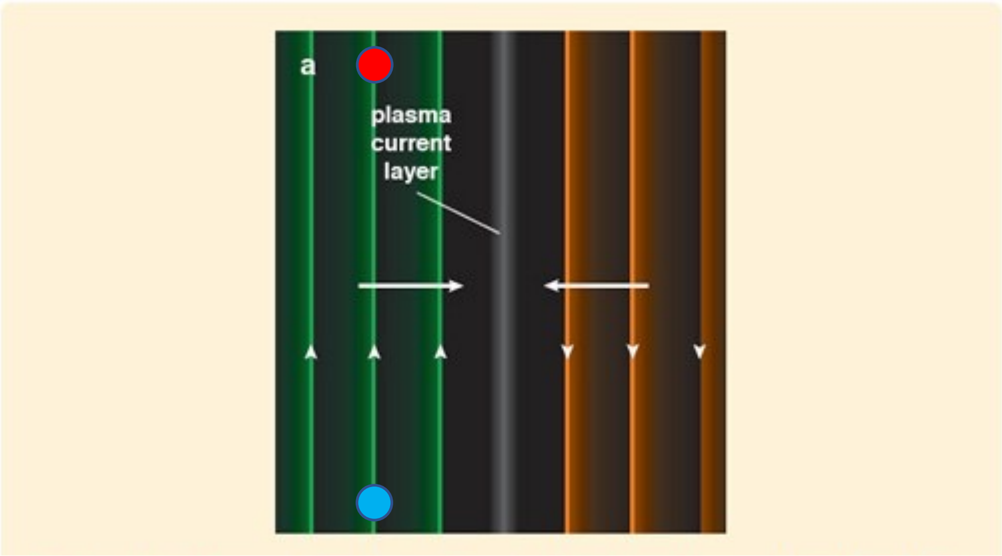

- "Failure of the "field-line" concept … is captured by the term *reconnection* … this term can be used to refer to the **changing connectivity** in a vacuum potential field …or… the **decoupling of particle motions from the background magnetic field** … we can say that **reconnection occurs whenever the approximation of frozen-in flux fails**."

Burch, J.L., & J.F. Drake (2009). Reconnecting Magnetic Fields, American Scientist, Sept-Oct., vol. 97, number 5, doi:10.1511/2009.80.392

Magnetic Reconnection at Current Sheets

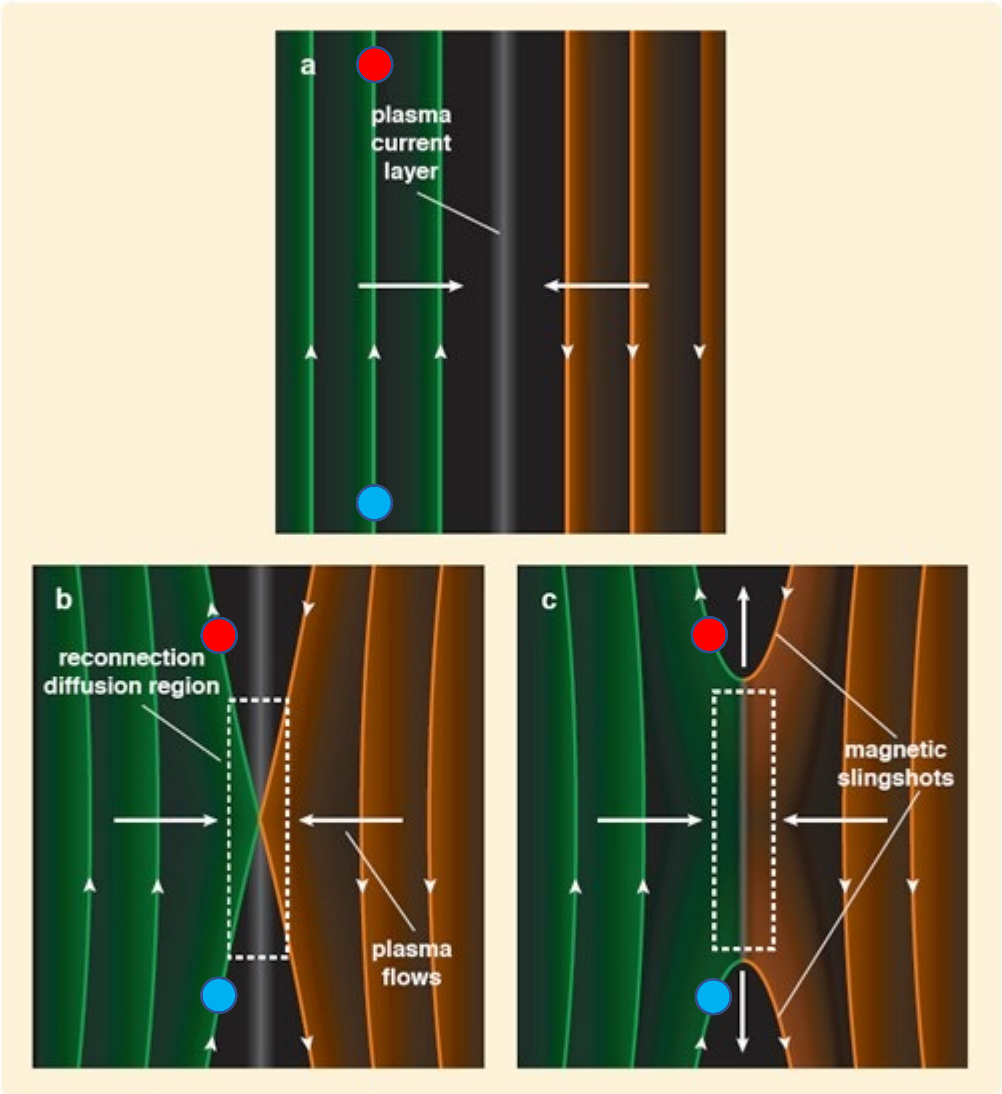

- "Failure of the "field-line" concept … is captured by the term *reconnection* … this term can be used to refer to the **changing connectivity** in a vacuum potential field …or… the **decoupling of particle motions from the background magnetic field** … we can say that **<u>reconnection occurs whenever the approximation of frozen-in flux fails</u>**."

Burch, J.L., & J.F. Drake (2009). Reconnecting Magnetic Fields, American Scientist, Sept-Oct., vol. 97, number 5, doi:10.1511/2009.80.392

Magnetic Reconnection at Current Sheets

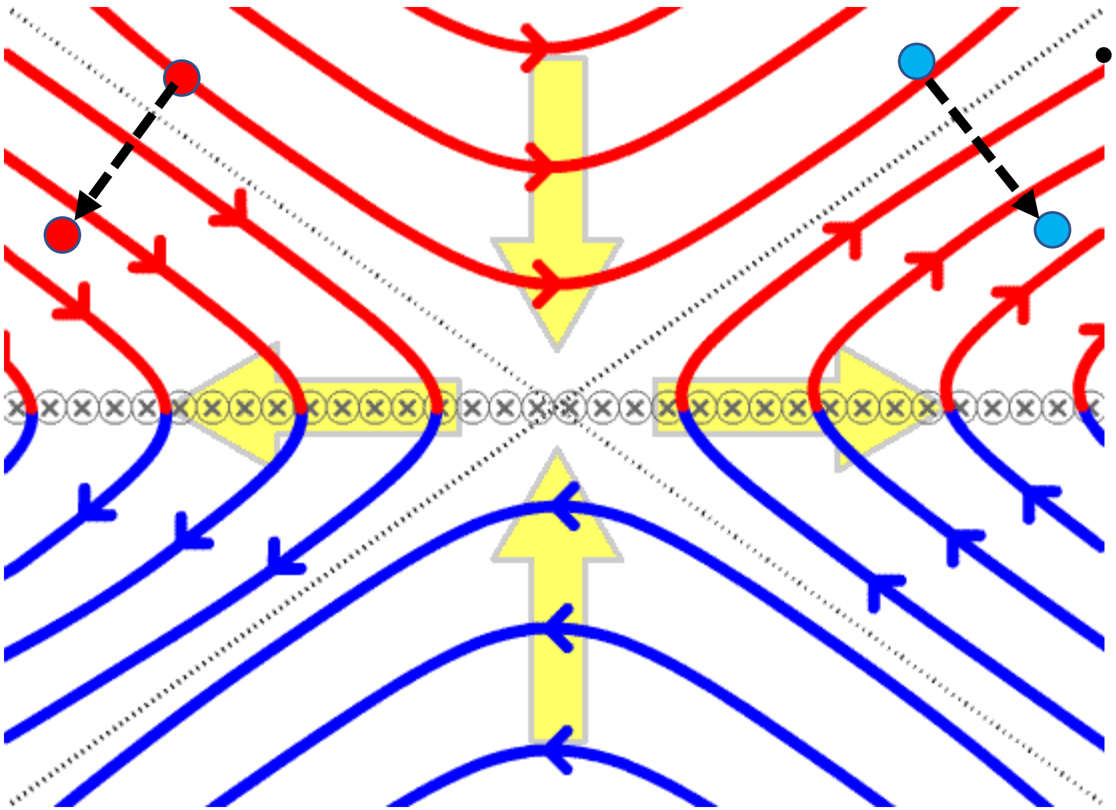

- "Failure of the "field-line" concept ... is captured by the term *reconnection* ... this term can be used to refer to the **changing connectivity** in a vacuum potential field ...or... the **decoupling of particle motions from the background magnetic field** ... we can say that **reconnection occurs whenever the approximation of frozen-in flux fails**."

Particles "frozen-in" with a magnetic field (**B**) gyrate about it. When **B** moves, then particles move along with it at the **V** = (**E** x **B**)/B² drift (yellow arrows).
In this case, there must be an electric field **E** = -**V** x **B** pointing out of the plane.

2-D versus 3-D

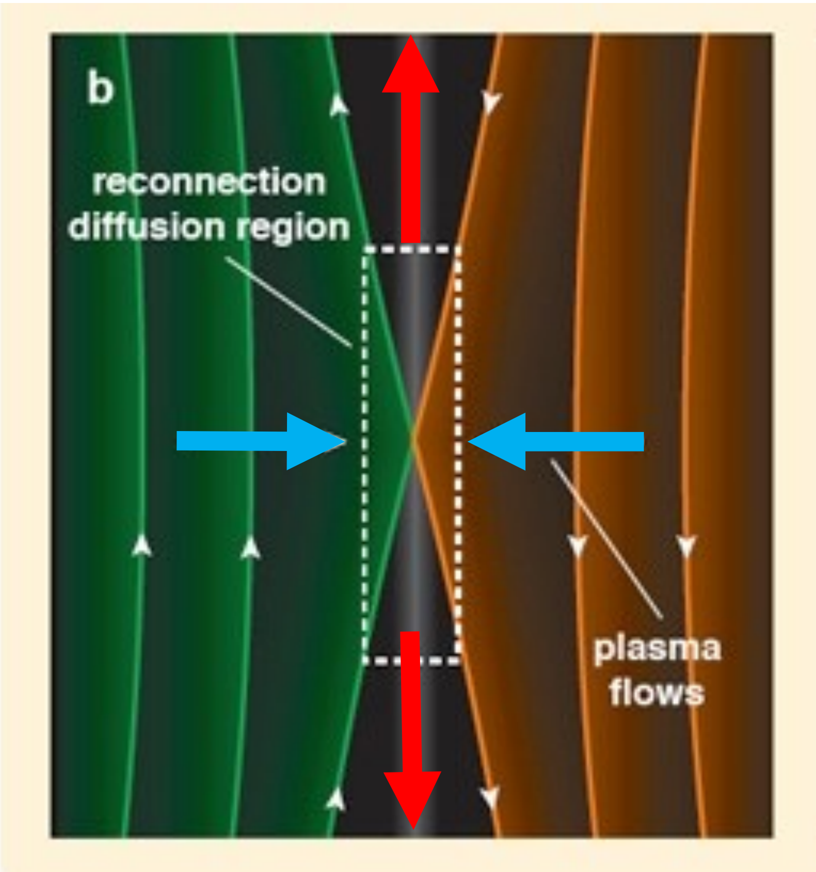

Burch, J.L., & J.F. Drake (2009). Reconnecting Magnetic Fields, American Scientist, Sept-Oct., vol. 97, number 5, doi:10.1511/2009.80.392

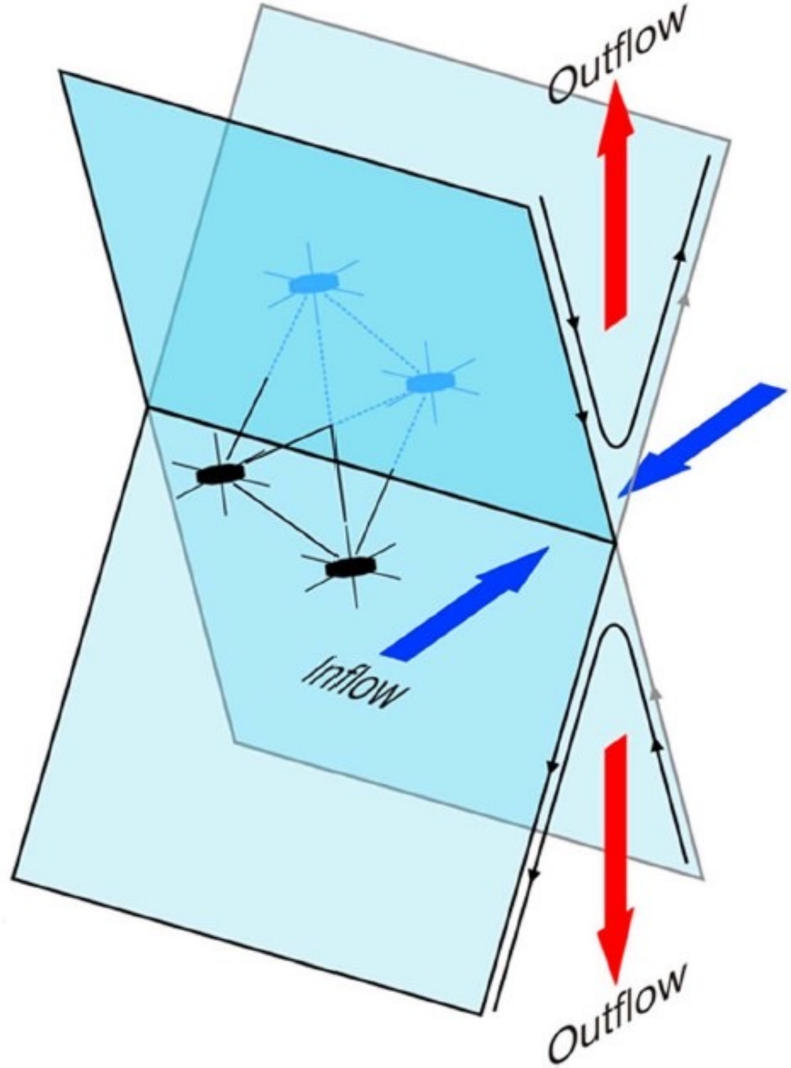

Gross, N. A., and W. J. Hughes (2015), A Decade of Questions About Magnetic Reconnection, Space Weather, 13, 606–610, doi:10.1002/2015SW001220

Magnetic Reconnection at Current Sheets

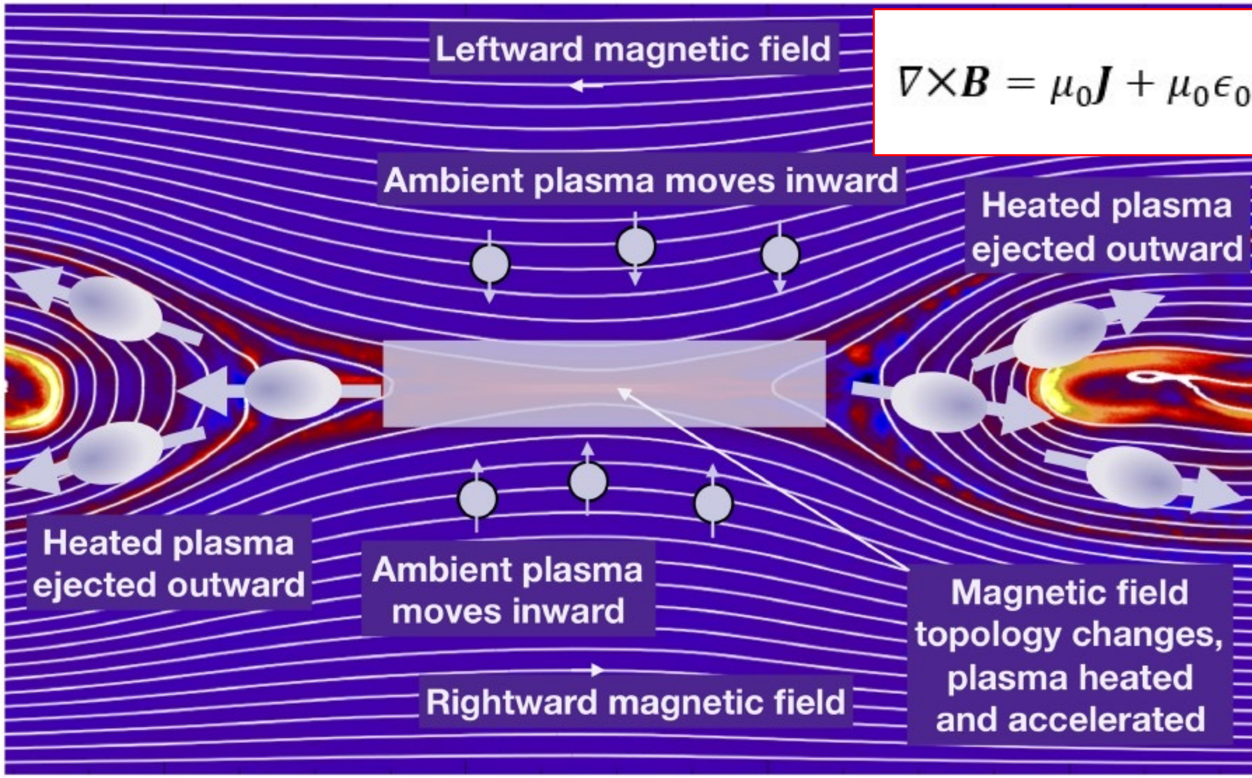

$$\nabla\times\boldsymbol{B} = \mu_0\boldsymbol{J} + \mu_0\epsilon_0\frac{\partial\boldsymbol{E}}{\partial t}$$

Current J shown in color

Hesse, M., & Cassak, P. A. (2020). Magnetic reconnection in the space sciences: Past, present, and future. Journal of Geophysical Research: Space Physics, 125, e2018JA025935. https://doi.org/10.1029/2018JA025935

Magnetic Reconnection at Current Sheets

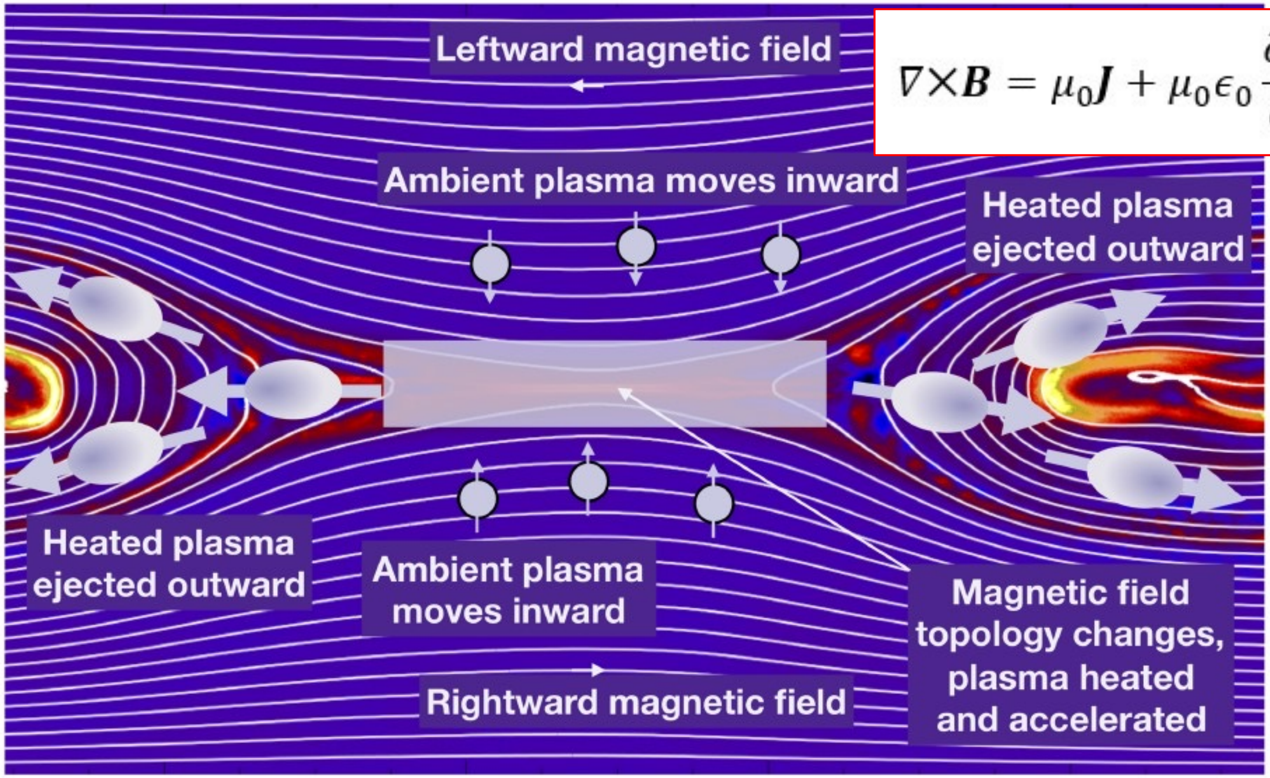

$$\nabla \times \boldsymbol{B} = \mu_0 \boldsymbol{J} + \mu_0 \epsilon_0 \frac{\partial \boldsymbol{E}}{\partial t}$$

Current J shown in color

Reconnection diffusion region* is where the charged particles (i and e) are no longer "frozen-in" to **B**, or **E** ≠ -**v** x **B** and the full particle motion is not a simple gyration about **B**

*It is really a *finite volume of space* – not an "X-point" or "X-line" per se.

Hesse, M., & Cassak, P. A. (2020). Magnetic reconnection in the space sciences: Past, present, and future. Journal of Geophysical Research: Space Physics, 125, e2018JA025935. https://doi.org/10.1029/2018JA025935

Magnetic Reconnection at Current Sheets

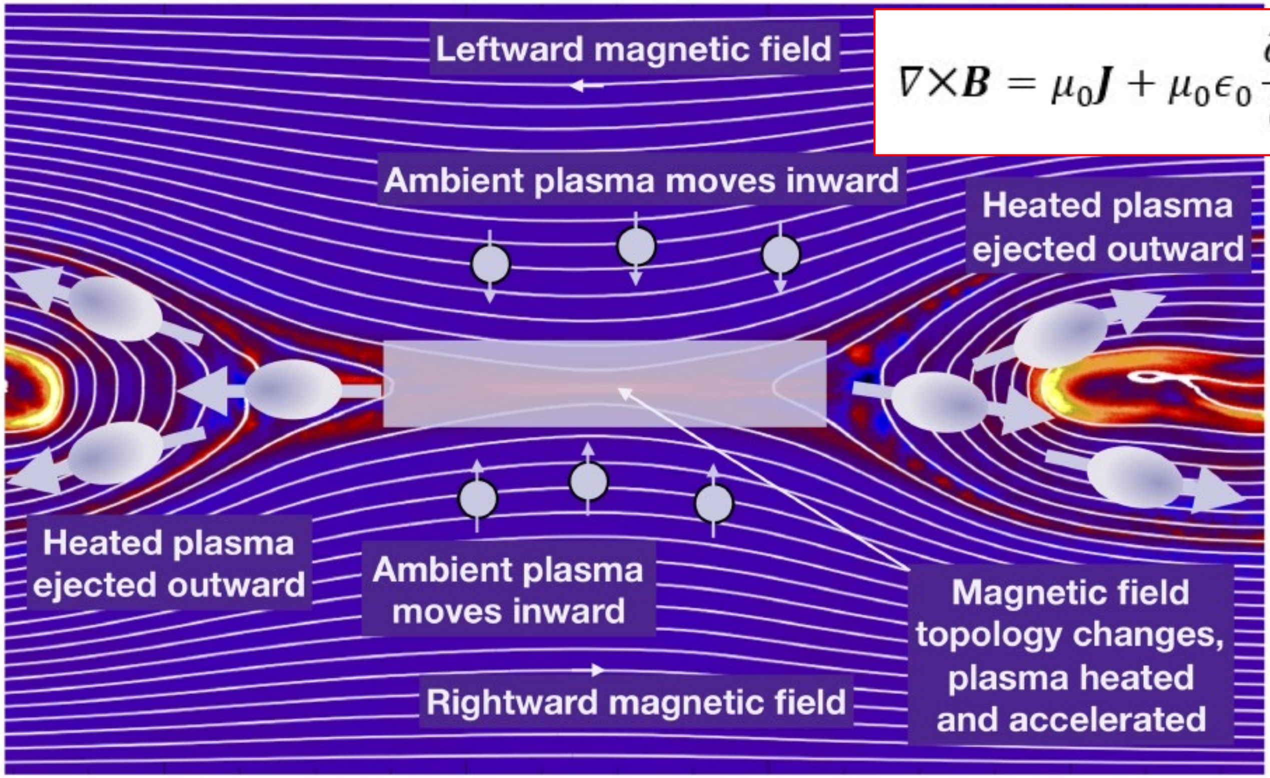

$$\nabla \times \boldsymbol{B} = \mu_0 \boldsymbol{J} + \mu_0 \epsilon_0 \frac{\partial \boldsymbol{E}}{\partial t}$$

Current J shown in color

Reconnection jet regions: Newly reconnected fields are strongly bent. This magnetic tension force acts on the plasma (left & right) and results in two plasma jet regions.

Hesse, M., & Cassak, P. A. (2020). Magnetic reconnection in the space sciences: Past, present, and future. Journal of Geophysical Research: Space Physics, 125, e2018JA025935. https://doi.org/10.1029/2018JA025935

Magnetic Reconnection

Particle-In-Cell (PIC) kinetic (ion and electron) simulations

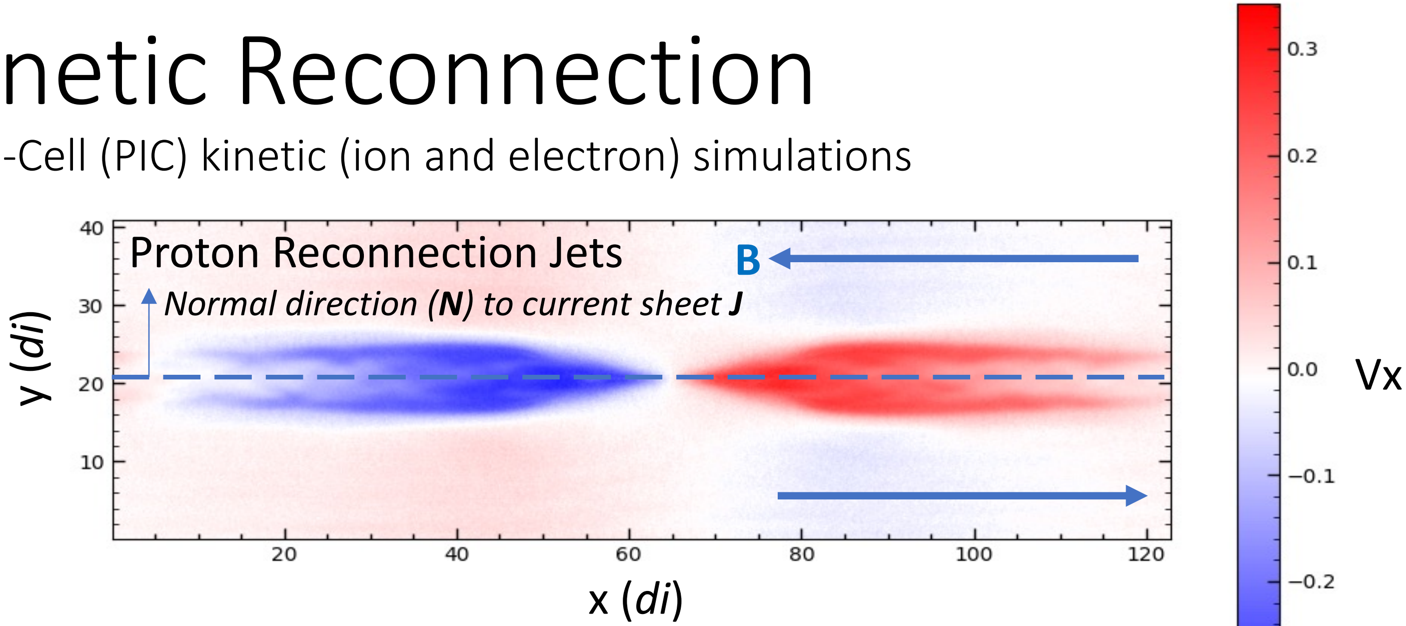

$$\nabla \times \boldsymbol{B} = \mu_0 \boldsymbol{J} + \mu_0 \epsilon_0 \frac{\partial \boldsymbol{E}}{\partial t}$$ Ampere's Law

Two main approaches exist to simulate the time-evolution of a plasma due to the presence of magnetic and electric fields.

(1) Fluid methods (MHD) capture macroscopic system evolution. Inaccuracies develop at small scales such as magnetic reconnection problem.

(2) Kinetic methods (PIC) aims to describe the full motion of ions and electrons from Maxwell's equations and the Vlasov transport equation. Often computationally expensive to use 3-D in a "big box" with full mass ratio of proton to electrons m_p/m_e=1836.

Image provided by Prayash Pyakurel, SSL/UC Berkeley (P3D numerical code)

Magnetic Reconnection Ion Scale

PIC kinetic simulation

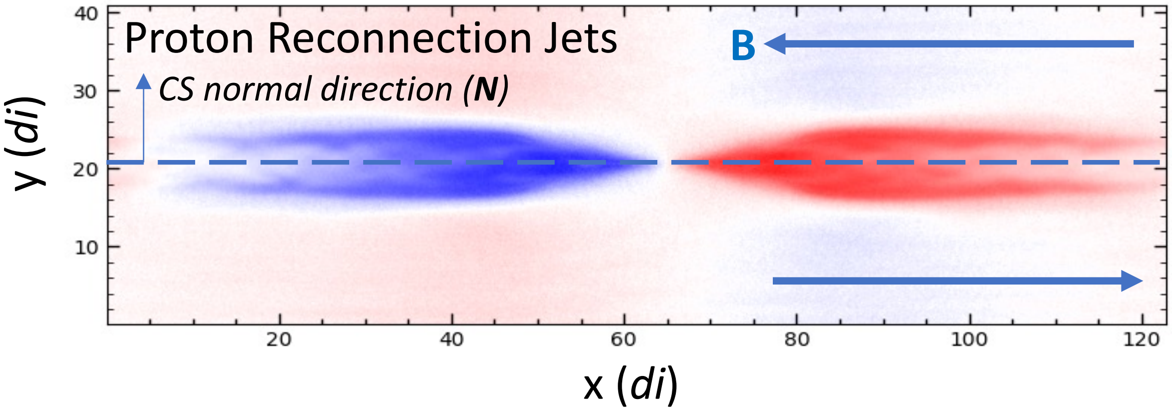

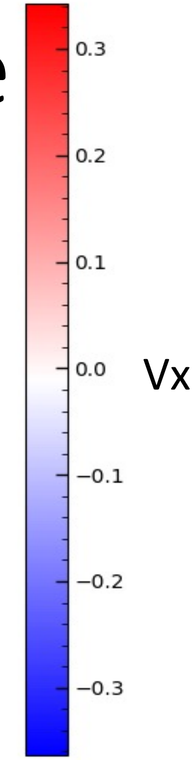

PIC simulations suggest that reconnection occurs when a current sheet thins down (external or internal drivers) to the "ion scale" 1 *di* = c/ω_{pi}

Here, **c** is speed of light and $\boldsymbol{\omega_{pi}^2 = N_p * e^2/m_p * \varepsilon_0}$ is the proton plasma frequency.

$\boldsymbol{\omega_{pi}}$ is a fundamental time-scale in plasma physics. It represents a typical electrostatic oscillation frequency of a plasma in response to a local and small charge separation.

A plasma is 'quasi-neutral' ($N=N_i \sim N_e$) such that a given small **charge displacement *x*** will generate an electric field $E_x = -\rho/\varepsilon_0$ for a charge density $\rho = e*N*\boldsymbol{x}$ that will act on the charged particles to return them to their original position.

From Newton's law: $m*d^2(\boldsymbol{x})/dt^2 = e*E_x = -e^2*N*\boldsymbol{x} / \varepsilon_0 = - m*\omega_{pi}^2\ \boldsymbol{x}$

Image provided by Prayash Pyakurel, SSL/UC Berkeley (P3D numerical code)

Magnetic Reconnection Ion Scale

PIC kinetic simulation

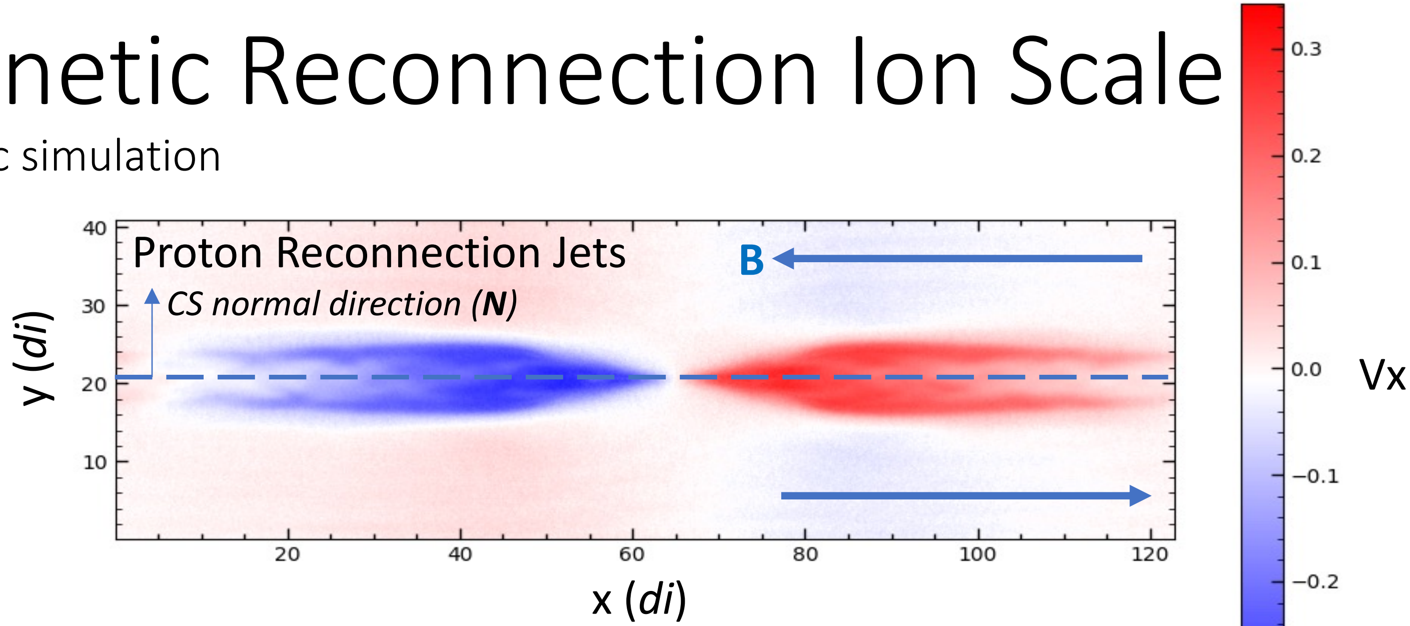

The *di* scale is known as "ion skin depth" and "ion inertial length"

1 *di* = c/ω_{pi} where **$\omega_{pi}^2 = N_p * e^2 / m_p * \varepsilon_0$**

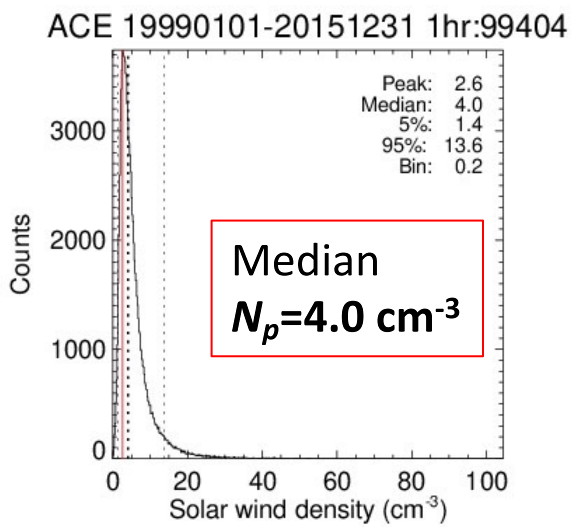

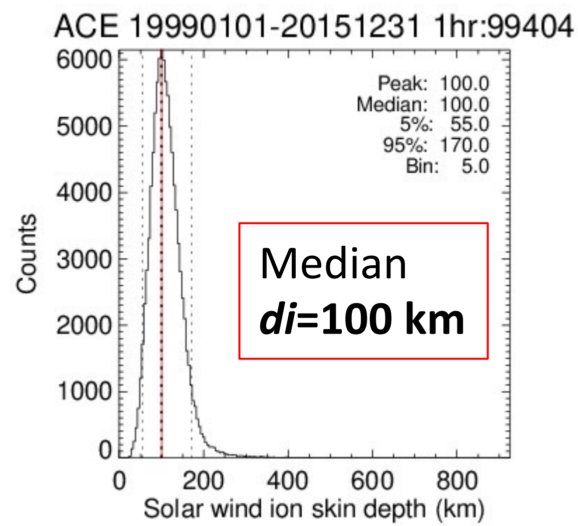

Image provided by Prayash Pyakurel, SSL/UC Berkeley (P3D numerical code)

Overview

- **Current sheets:** ***Magnetic field rotations [$J=\nabla\times B/\mu_0$] from the very wide Heliospheric Current Sheet to "narrow" M'pause***
- **Multi-spacecraft missions:** ***A brief introduction to tedrahedron formations and the Curlometer technique***
- **Near-Earth space regimes & boundaries**
- **The magnetic reconnection process at current sheets:**

  (a) Schematic overviews, 2D vs 3D & ion (di) scale

  (b) "To be or not to be" frozen-in? The G.O.L. vs Hall ☺

  (c) Reconnection rate v_{in}/v_{out}
- Observations of Reconnection Jets:

  (a) Cluster in the solar wind vs "timing normal" concept

  (b) MMS at the magnetopause: J from "curlB" vs J=Ne(Vi-Ve)
- Summary

Magnetic Reconnection – G.O.L.

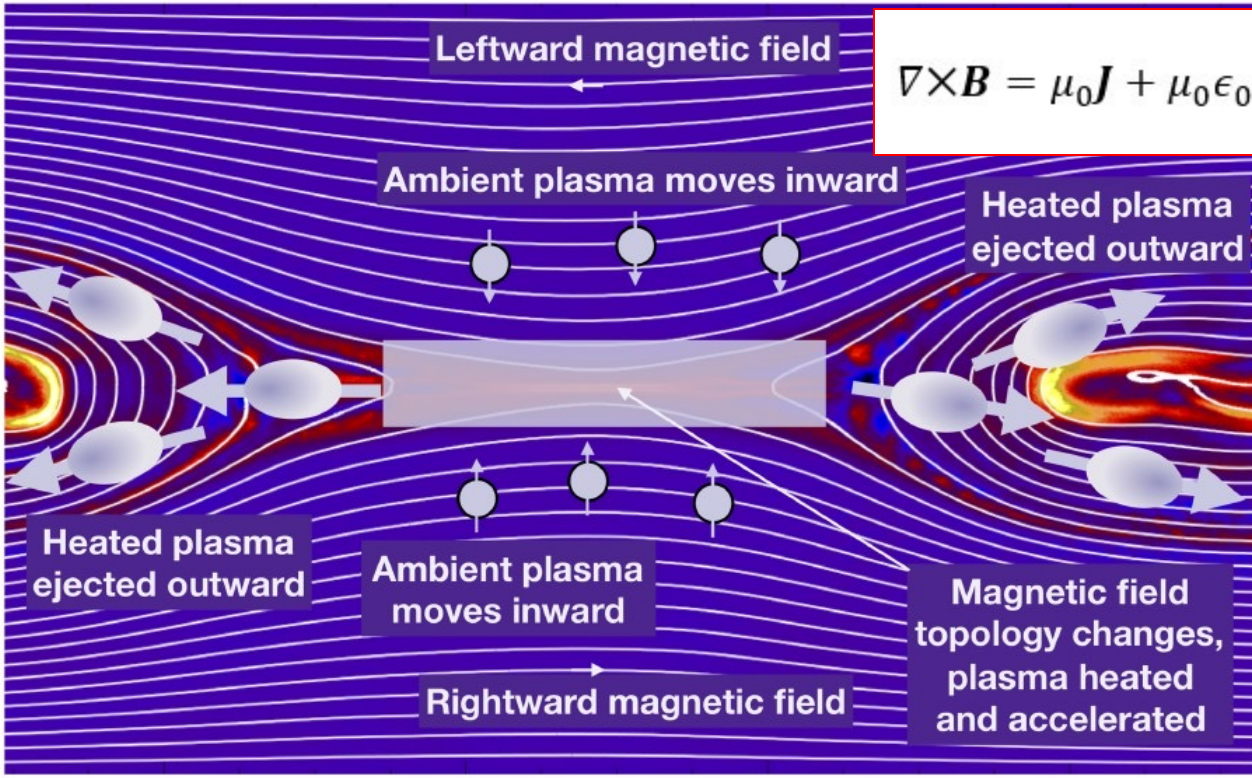

$$\nabla \times \boldsymbol{B} = \mu_0 \boldsymbol{J} + \mu_0 \epsilon_0 \frac{\partial \boldsymbol{E}}{\partial t}$$

Since **E** = -**v** x **B** (frozen-in condition) just outside the narrow current layer (both inflow regions), then there must be an electric field **E** of that magnitude also inside the localized diffusion region where **E** ≠ -**v** x **B** .

If **E** is ***<u>not</u>*** equal to -(**v** x **B**) there, *then what supports this **E** locally*?

We must explore the *particle motions and the forces acting on them* in this small current layer region where the in-plane **B** is weak (special case: |**B**|<<1).

Magnetic Reconnection – G.O.L.

PIC kinetic simulation

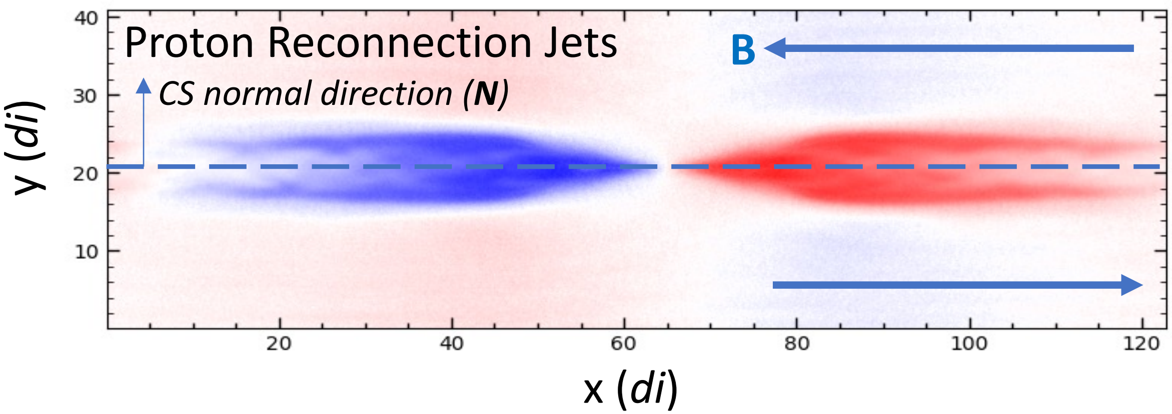

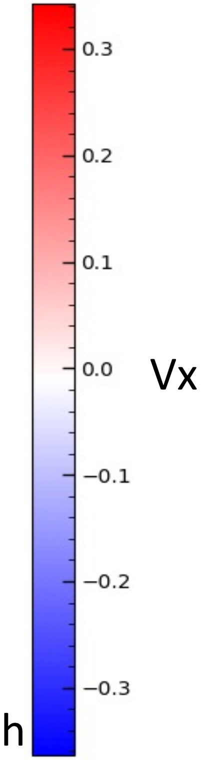

Generalized Ohm's Law: In order to deduce Ohm's Law for a plasma with magnetic field **B**, we consider at least <u>*two equations of motion*</u> – one each for electrons and ions - under the influence of the ***forces*** acting on the particles

Newton's 2nd Law of Motion for particles in collisionless plasma:

(1) $m_e \mathbf{a}_e = \mathbf{F}_{Ee} + \mathbf{F}_{Be} - \nabla p_e/n_e + m_e \mathbf{g}$ [$\mathbf{F}_{Ee} = -e\mathbf{E}$ and $\mathbf{F}_{Be} = -e(\mathbf{v}_e \times \mathbf{B})$]

(2) $m_i \mathbf{a}_i = \mathbf{F}_{Ei} + \mathbf{F}_{Bi} - \nabla p_i/n_i + m_i \mathbf{g}$ [$\mathbf{F}_{Ei} = e\mathbf{E}$ and $\mathbf{F}_{Bi} = e(\mathbf{v}_i \times \mathbf{B})$]

where $p_e=n_e k_B T_e$ and $p_i=n_i k_B T_i$ are electron and ion *scalar* pressures for an assumed isotropic plasma temperature. In anisotropic plasmas (e.g., $Te_{||}>Te_{perp}$) ∇p -> $\nabla\cdot\mathbf{P}$ where $\mathbf{P}=P_{ij}$ is a 3x3 pressure tensor.

E.g. H. Alfven & C.-G. Fälthammar, Cosmical Electrodynamics, Oxford University Press, 2nd Edition, 1963

Magnetic Reconnection – G.O.L.

PIC kinetic simulation

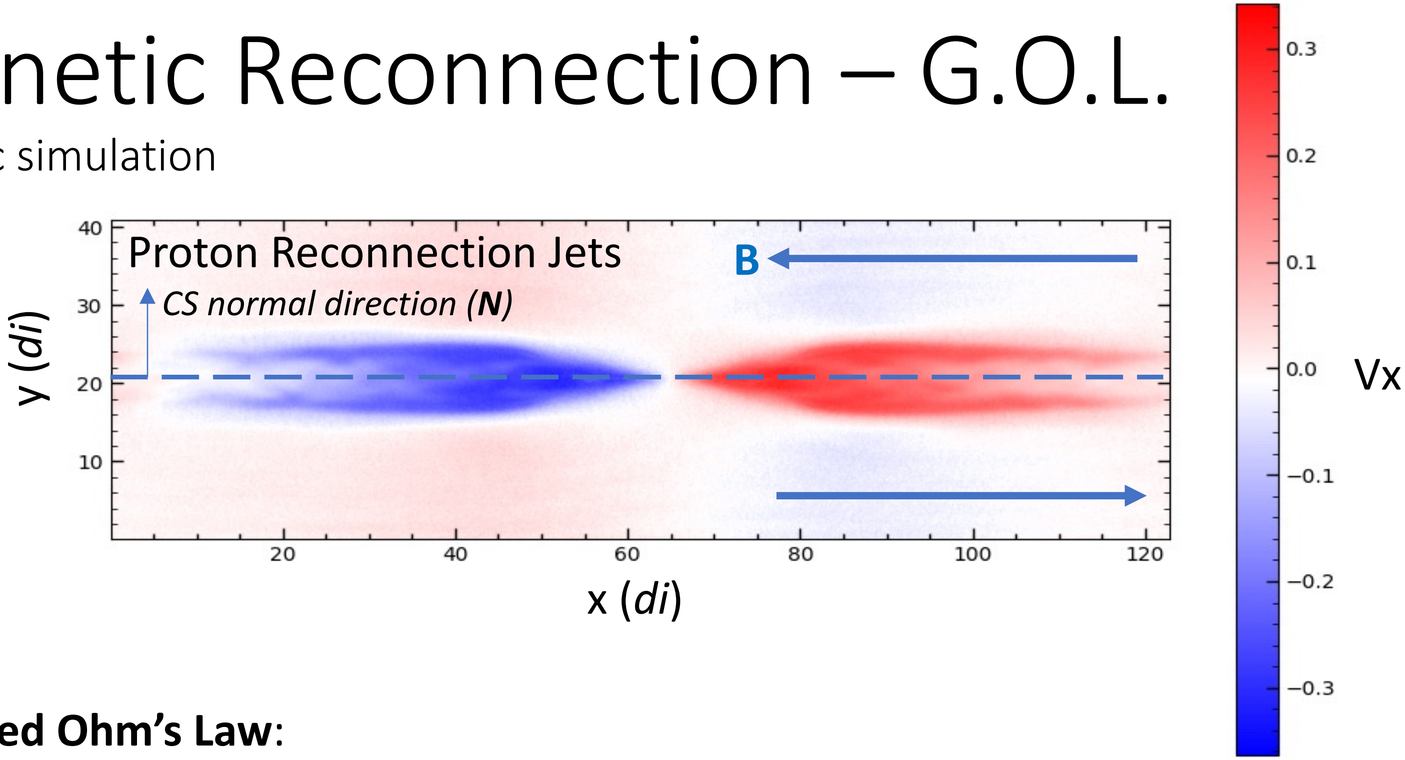

Generalized Ohm's Law:

Newton's 2nd law for a plasma with number density $n_i = n_e = n$ (quasi-neutral):

(1) $n m_e d\mathbf{v}_e/dt = -ne[\mathbf{E} + \mathbf{v}_e \times \mathbf{B}] - \nabla p_e + n m_e \mathbf{g}$

(2) $n m_i d\mathbf{v}_i/dt = ne[\mathbf{E} + \mathbf{v}_i \times \mathbf{B}] - \nabla p_i + n m_i \mathbf{g}$

Adding (1) + (2) using mass density $\rho = n(m_i + m_e)$, momentum $\rho\mathbf{v} = n(m_i\mathbf{v}_i + m_e\mathbf{v}_e)$, and current density $\mathbf{J} = ne(\mathbf{v}_i - \mathbf{v}_e)$ results in:

Plasma Equation of Motion: $\rho\, d\mathbf{v}/dt = \mathbf{J}\times\mathbf{B} - \nabla p + \rho\mathbf{g}$

E.g. H. Alfven & C.-G. Fälthammar, Cosmical Electrodynamics, Oxford University Press, 2nd Edition, 1963

Magnetic Reconnection – G.O.L.

PIC kinetic simulation

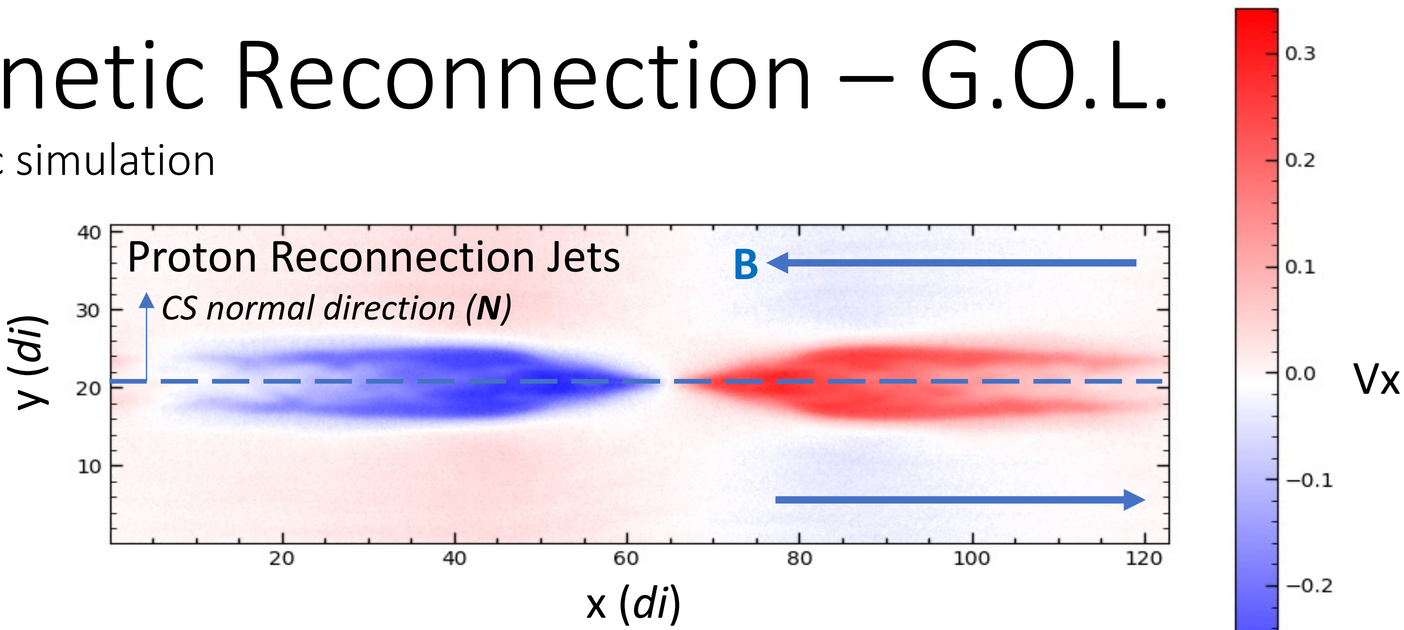

Generalized Ohm's Law:

Newton's 2nd law for a plasma with number density $n_i = n_e = n$ (quasi-neutral):

(1) $n m_e d\mathbf{v}_e/dt = -ne[\mathbf{E} + \mathbf{v}_e \times \mathbf{B}] - \nabla p_e + n m_e \mathbf{g}$

(2) $n m_i d\mathbf{v}_i/dt = ne[\mathbf{E} + \mathbf{v}_i \times \mathbf{B}] - \nabla p_i + n m_i \mathbf{g}$

Taking (Eq2)*$m_e/(m_i ne)$ ***minus*** (Eq1)*1/ne ***with*** $\mathbf{v}_i \sim \mathbf{v}$ and $\mathbf{v}_e \sim (\mathbf{v} - \mathbf{J}/ne)$ from $\mathbf{J} = ne(\mathbf{v}_i - \mathbf{v}_e)$ [$m_e \ll m_i$ limit] results in:

G.O.L. $\mathbf{E} + \mathbf{v} \times \mathbf{B} = \mathbf{J}\times\mathbf{B}/ne - [\nabla p_e - m_e \nabla p_i/m_i]/ne + m_e/ne^2\, d\mathbf{J}/dt$

E.g. H. Alfven & C.-G. Fälthammar, Cosmical Electrodynamics, Oxford University Press, 2nd Edition, 1963

Magnetic Reconnection – G.O.L.

PIC kinetic simulation

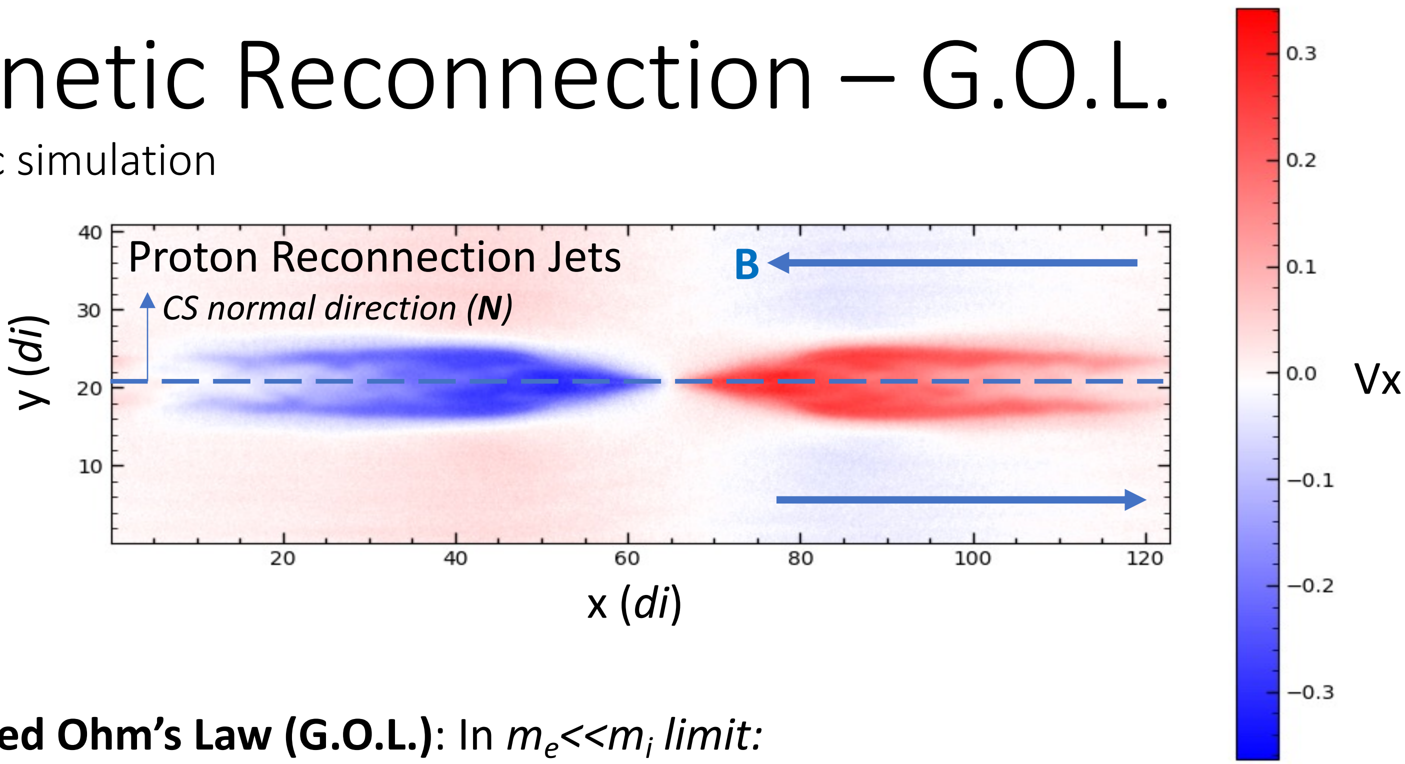

Generalized Ohm's Law (G.O.L.): In $m_e << m_i$ *limit:*

G.O.L. $\mathbf{E} + \mathbf{v} \times \mathbf{B} = \mathbf{J}\times\mathbf{B}/ne - \nabla\cdot\mathbf{P}_e/ne + m_e/ne^2\, d\mathbf{J}/dt$ [$\mathbf{P}_e$: electron pressure tensor]

E' = "Hall" – "electron pressure divergence" + "electron inertia" terms

In kinetic treatments of plasmas (non-MHD), the presence of a *non-ideal electric field* $\mathbf{E}' = \mathbf{E} + \mathbf{v} \times \mathbf{B} \neq 0$ in the frame of the moving particles ($\mathbf{v}=\mathbf{v}_i$ or $\mathbf{v}=\mathbf{v}_e$) will contribute to this violation of the "frozen-in" condition.

E.g. H. Alfven & C.-G. Fälthammar, Cosmical Electrodynamics, Oxford University Press, 2nd Edition, 1963

Magnetic Reconnection – G.O.L.

PIC kinetic simulation

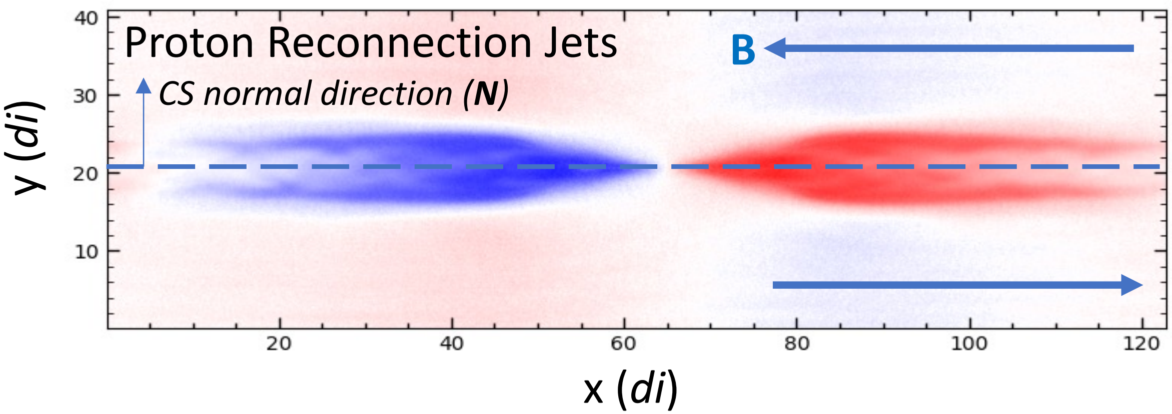

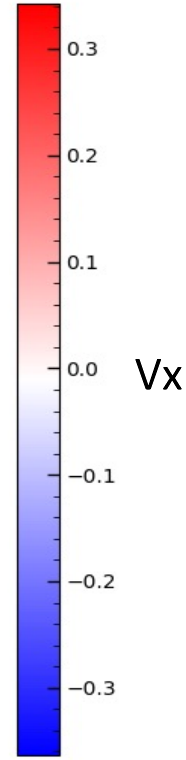

Generalized Ohm's Law (G.O.L.): In $m_e << m_i$ *limit:*

G.O.L. $\mathbf{E} + \mathbf{v} \times \mathbf{B} = \mathbf{J}\times\mathbf{B}/ne - \nabla\cdot\mathbf{P}_e/ne + m_e/ne^2\, d\mathbf{J}/dt$ [$\mathbf{P}_e$: electron pressure tensor]

E' = "Hall" – "electron pressure divergence" + "electron inertia" terms

The Objective of the MMS s/c constellation –> Explore the RHS terms of G.O.L. where electron scales are crucial to measure. High measurement cadence a requirement.

E.g. H. Alfven & C.-G. Fälthammar, Cosmical Electrodynamics, Oxford University Press, 2nd Edition, 1963

Magnetic Reconnection – G.O.L. terms

Symmetric PIC simulation

$$\mathbf{E} + \mathbf{v} \times \mathbf{B} = \mathbf{J}\times\mathbf{B}/ne - \nabla\cdot\mathbf{P}_e/ne + m_e/ne^2\, d\mathbf{J}/dt$$

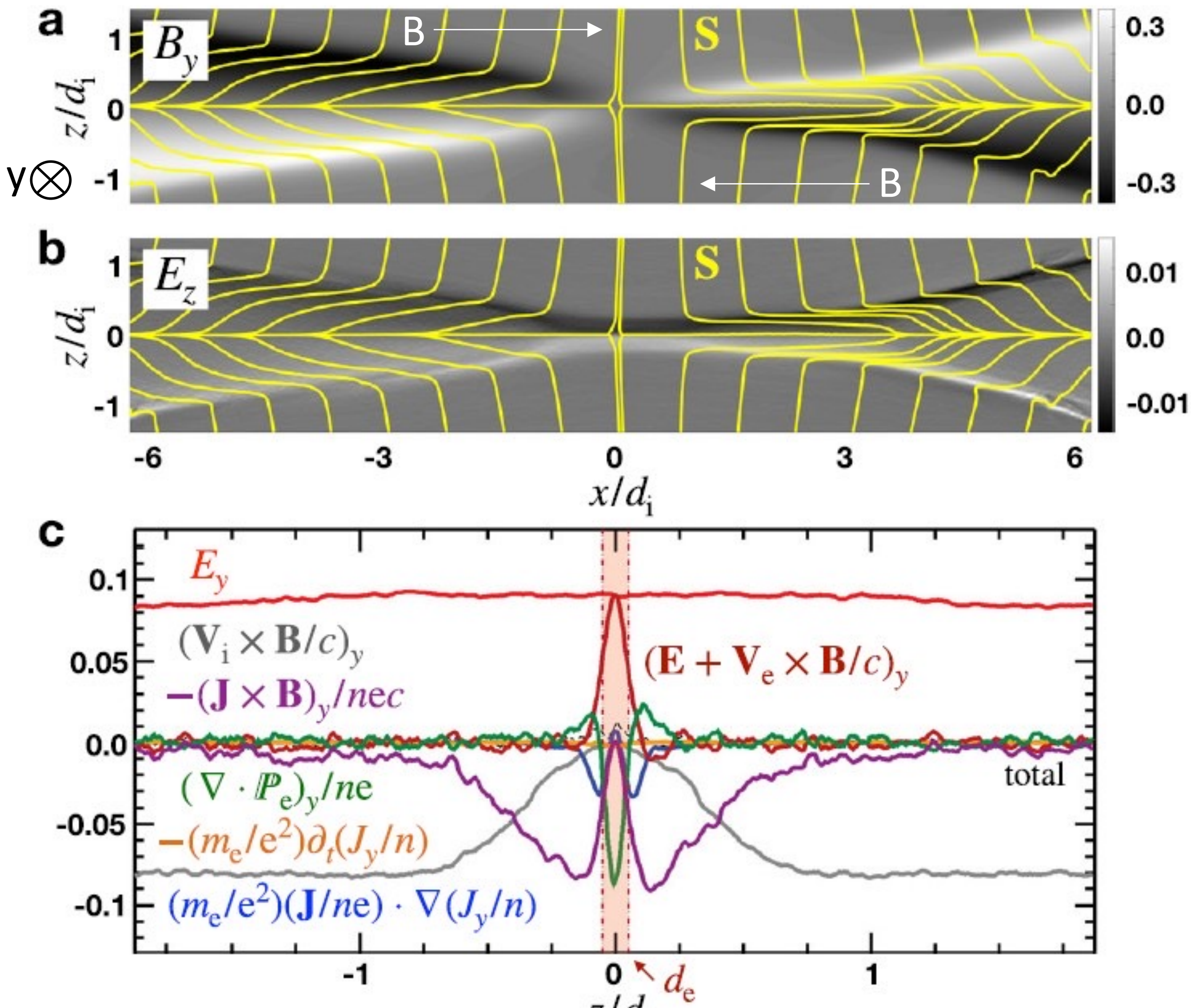

Yi-Hsin Liu, Paul Cassak, Xiaocan Li et al., First-principles theory of the rate of magnetic reconnection in magnetospheric and solar plasmas Nature Communications, 2022, https://doi.org/10.1038/s42005-022-00854-x

Magnetic Reconnection – G.O.L. terms

Symmetric PIC simulation

$\mathbf{E} + \mathbf{v} \times \mathbf{B} = \mathbf{J}\times\mathbf{B}/ne - \nabla\cdot\mathbf{P}_e/ne + m_e/ne^2\, d\mathbf{J}/dt$

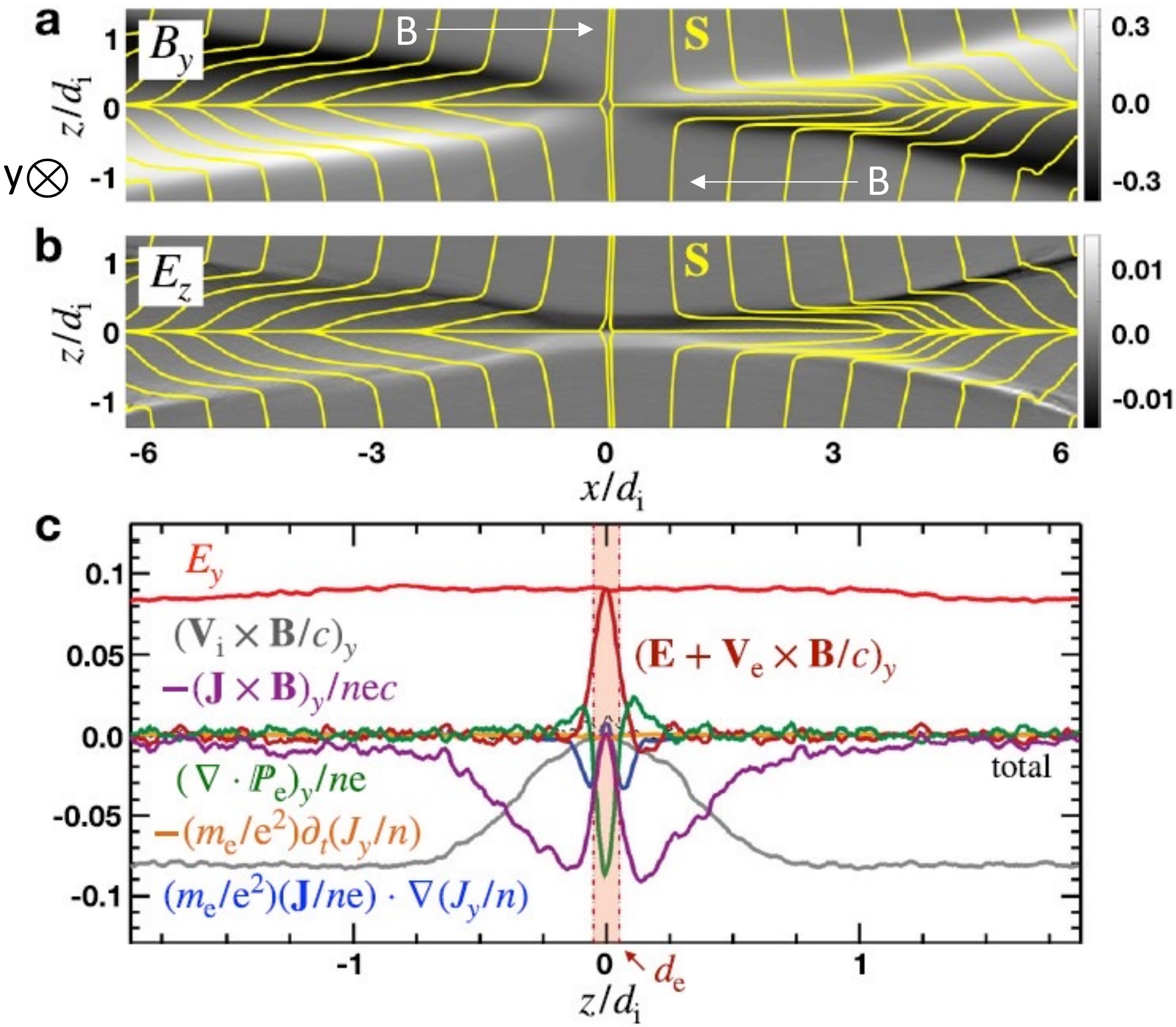

Note on scales:

m_p/m_e=1836

$d_e=c/\omega_{pe}$

$d_i=d_e$*SQRT(m_p/m_e)~43*d_i

Example solar wind:

d_i =100 km

d_e =2.3 km

Yi-Hsin Liu, Paul Cassak, Xiaocan Li et al., First-principles theory of the rate of magnetic reconnection in magnetospheric and solar plasmas Nature Communications, 2022, https://doi.org/10.1038/s42005-022-00854-x

Magnetic Reconnection – 3 Regions

Symmetric PIC simulation

$\mathbf{E} + \mathbf{v} \times \mathbf{B} = \mathbf{J}\mathrm{x}\mathbf{B}/ne - \nabla\cdot\mathbf{P}_e/ne + m_e/ne^2\, d\mathbf{J}/dt$

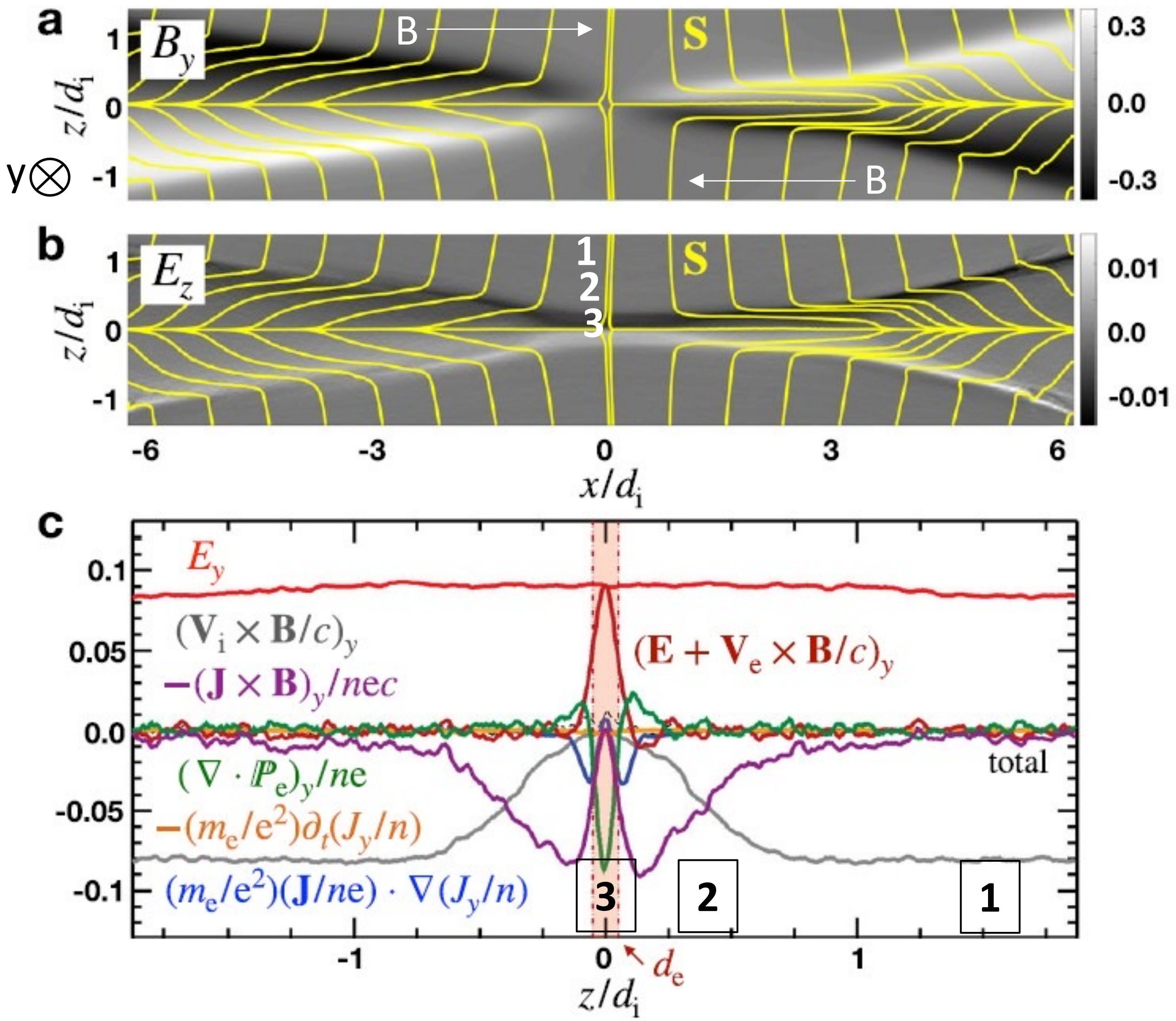

1. Upstream Inflow Region

E = -Vi x B

Plasma ExB inflow

i & e "frozen-in" to B

2. Ion Diffusion Region

E + Vi x B = JxB/ne

i "de-coupled" & e "frozen-in"

3. Electron Diffusion Region

E + Ve x B = $-\nabla\cdot\mathrm{P}_e/ne$

i & e "de-coupled"

Yi-Hsin Liu, Paul Cassak, Xiaocan Li et al., First-principles theory of the rate of magnetic reconnection in magnetospheric and solar plasmas Nature Communications, 2022, https://doi.org/10.1038/s42005-022-00854-x

Magnetic Reconnection – Hall E

Symmetric PIC simulation

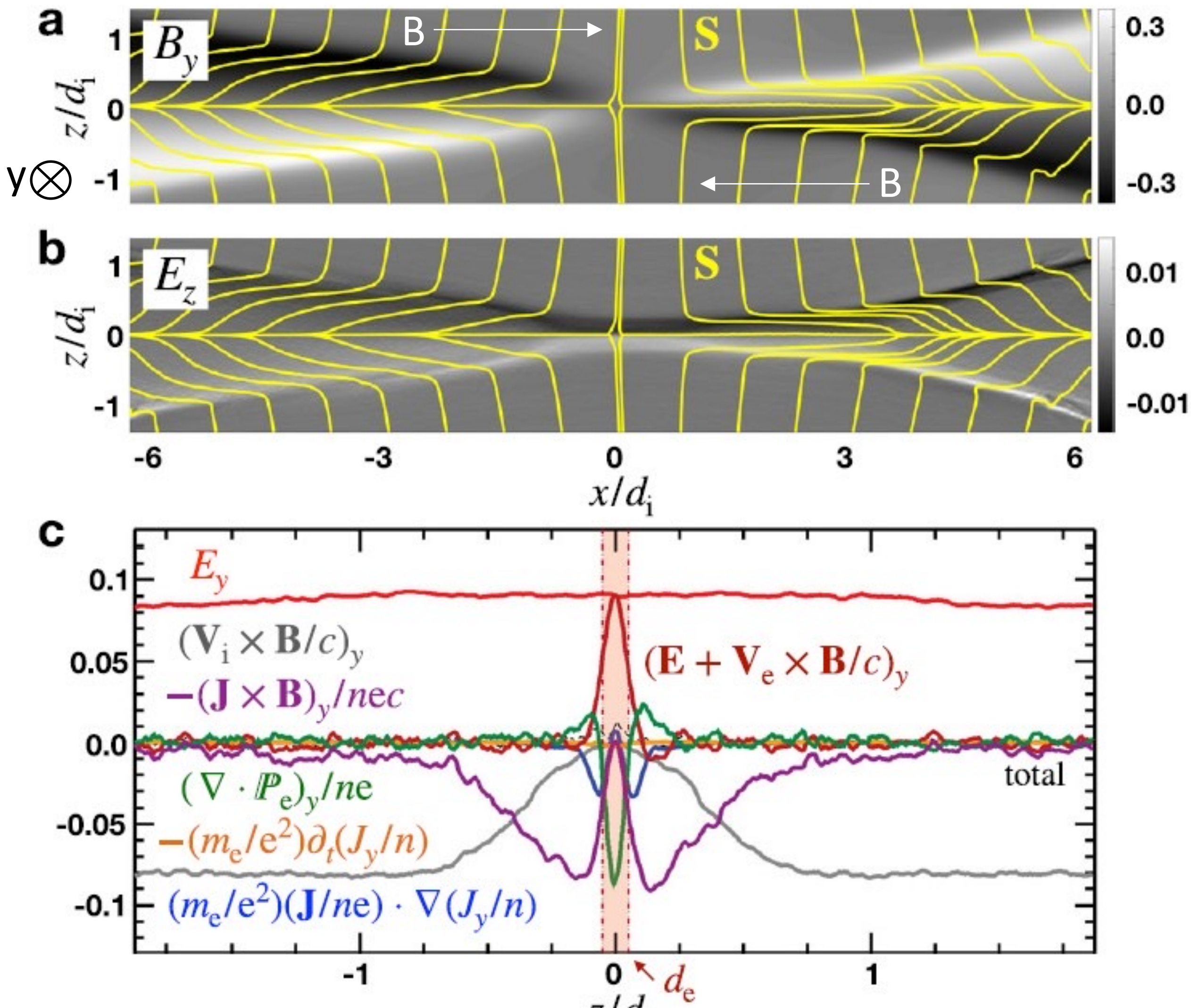

Since electrons decouple from **B** closer to the current layer than ions, an inward (Ez) polarization electric field is generated that prevents a large charge separation.

Yi-Hsin Liu, Paul Cassak, Xiaocan Li et al., First-principles theory of the rate of magnetic reconnection in magnetospheric and solar plasmas Nature Communications, 2022, https://doi.org/10.1038/s42005-022-00854-x

Magnetic Reconnection – Hall B

Symmetric PIC simulation

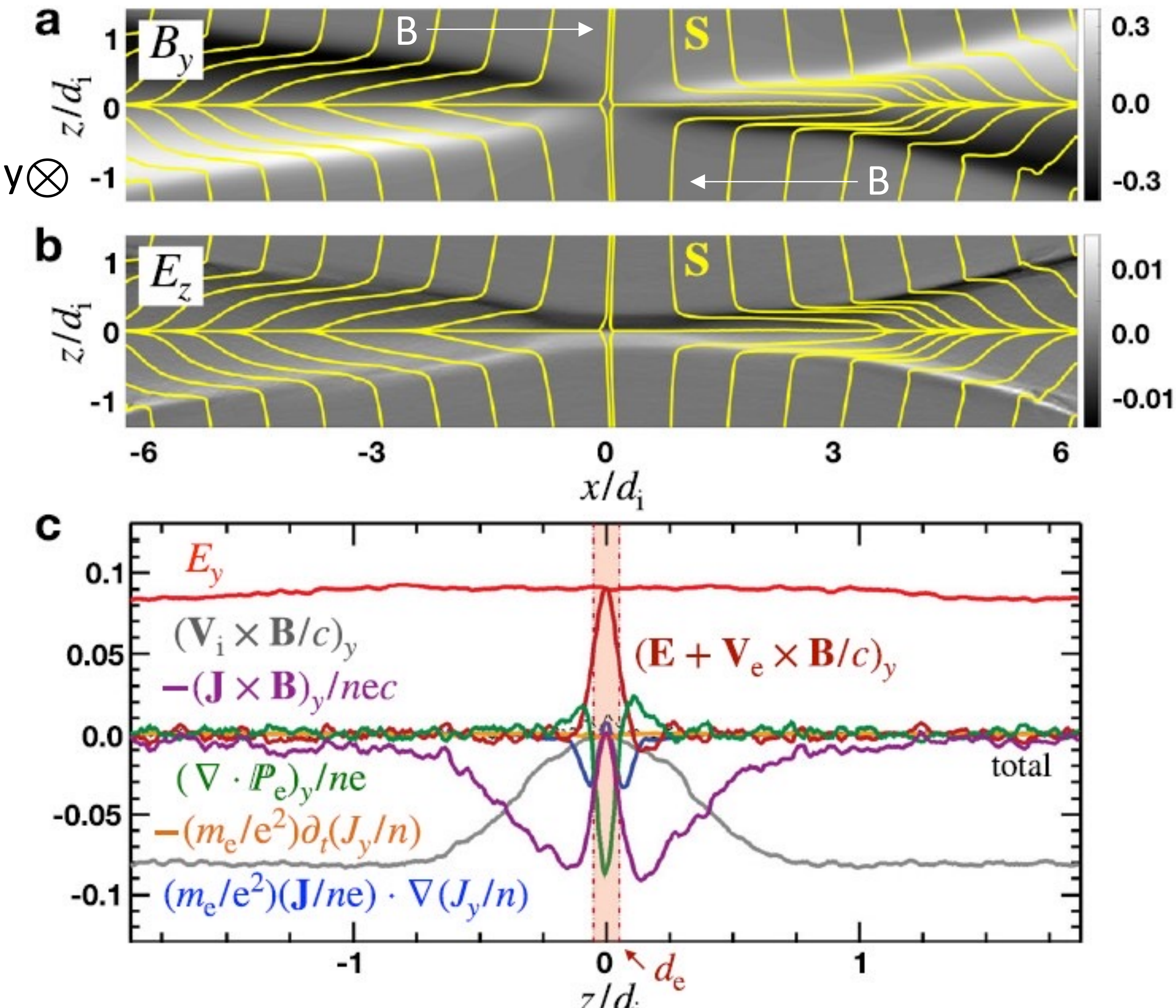

Likewise, a magnetic field (By) perturbation is generated from the inward and outward electron motions (current).

Yi-Hsin Liu, Paul Cassak, Xiaocan Li et al., First-principles theory of the rate of magnetic reconnection in magnetospheric and solar plasmas Nature Communications, 2022, https://doi.org/10.1038/s42005-022-00854-x

Magnetic Reconnection – Hall E & B

Symmetric PIC simulation

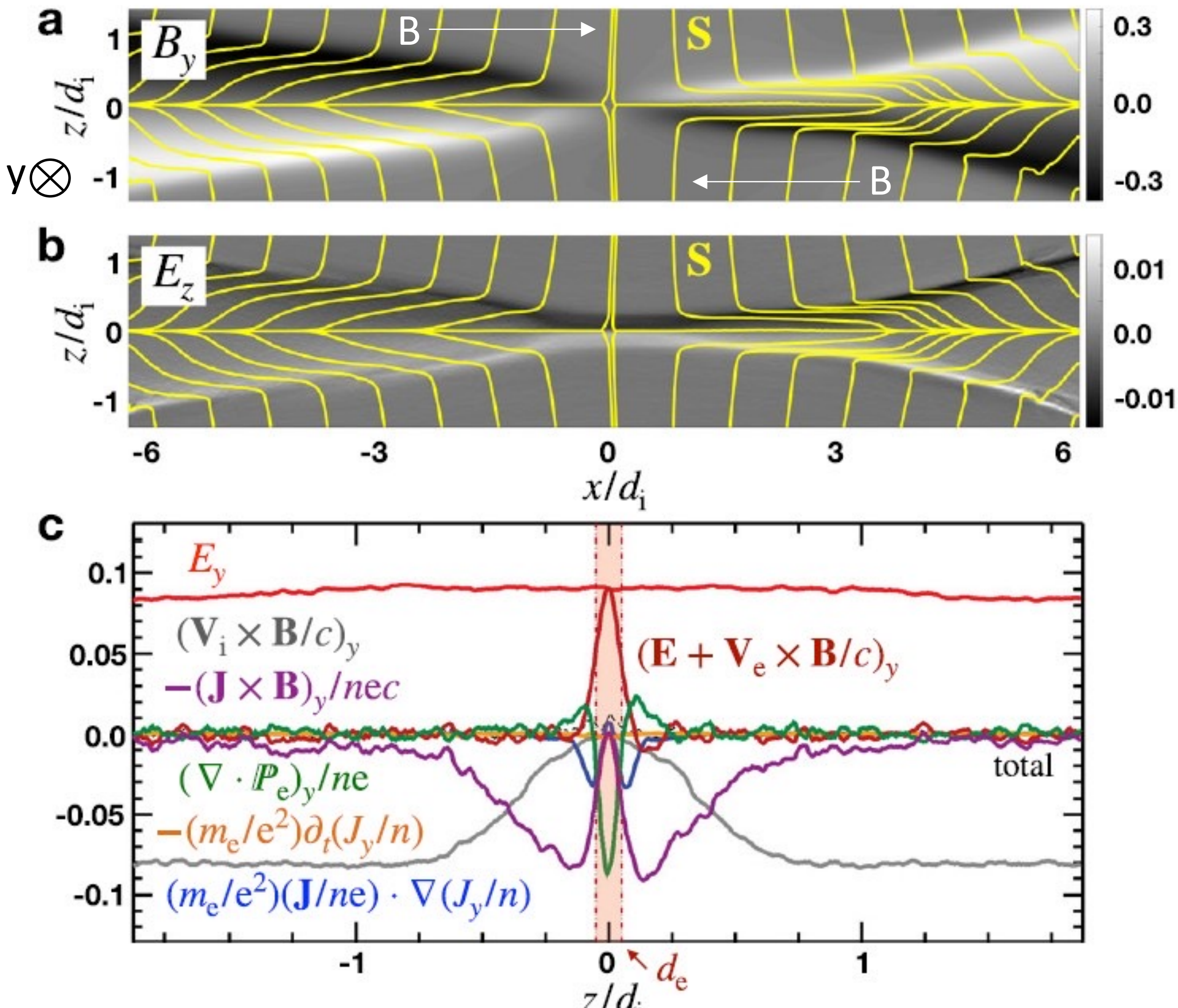

We refer to these effects of the Hall **J**x**B** term of the G.O.L. in the ion diffusion region as the ***Hall magnetic field and Hall electric field***.

Yi-Hsin Liu, Paul Cassak, Xiaocan Li et al., First-principles theory of the rate of magnetic reconnection in magnetospheric and solar plasmas Nature Communications, 2022, https://doi.org/10.1038/s42005-022-00854-x

Magnetic Reconnection – Hall E & B

Symmetric PIC simulation

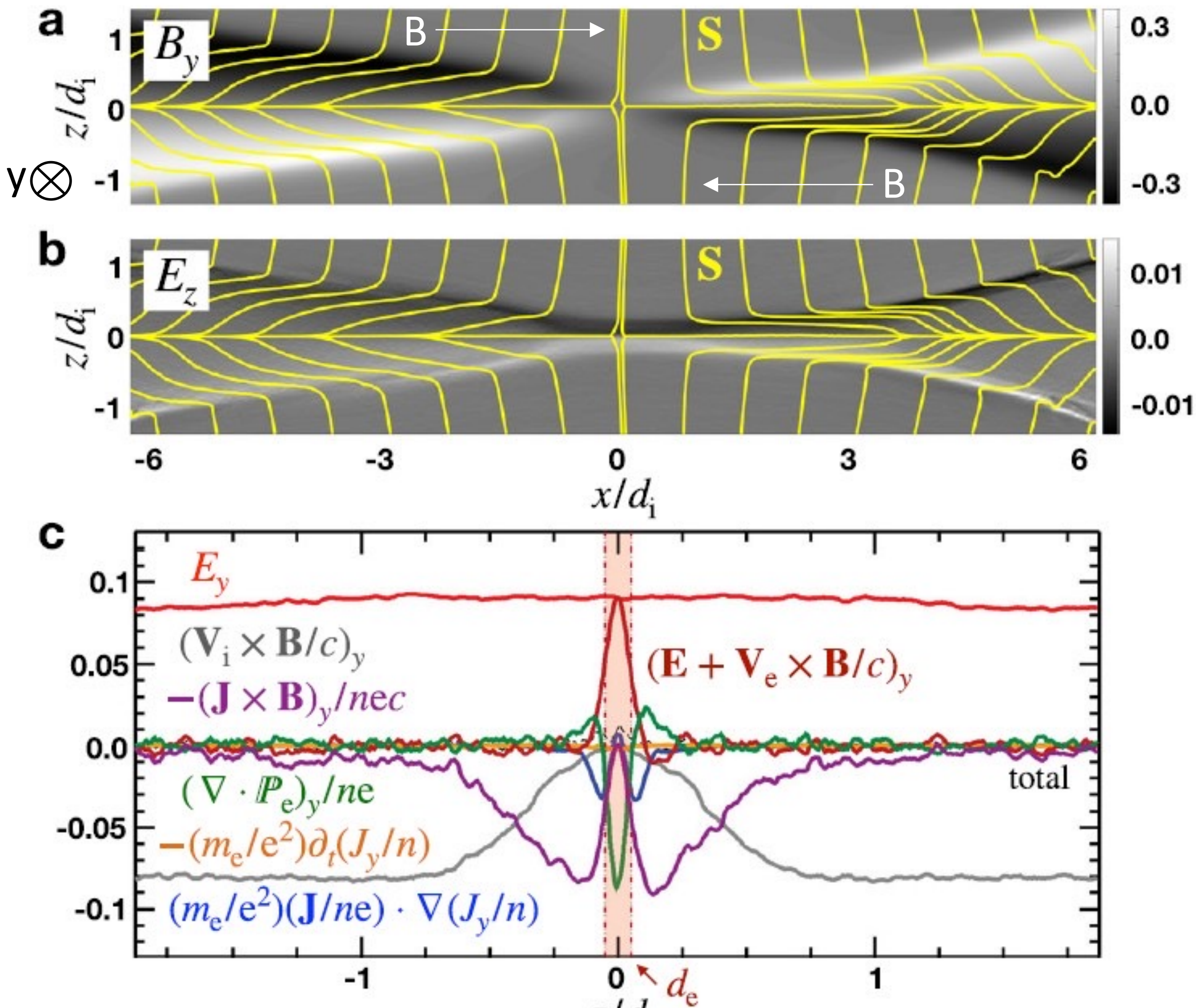

Streamlines **S** = **E** x **B**/μ_0 is the Poynting flux (directional energy flux) due to Hall Ez and By terms.

Yi-Hsin Liu, Paul Cassak, Xiaocan Li et al., First-principles theory of the rate of magnetic reconnection in magnetospheric and solar plasmas Nature Communications, 2022, https://doi.org/10.1038/s42005-022-00854-x

Magnetic Reconnection – Hall E & B

Asymmetric PIC simulation (dayside magnetopause) & **[x, y, z] <-> [L, M, N]**

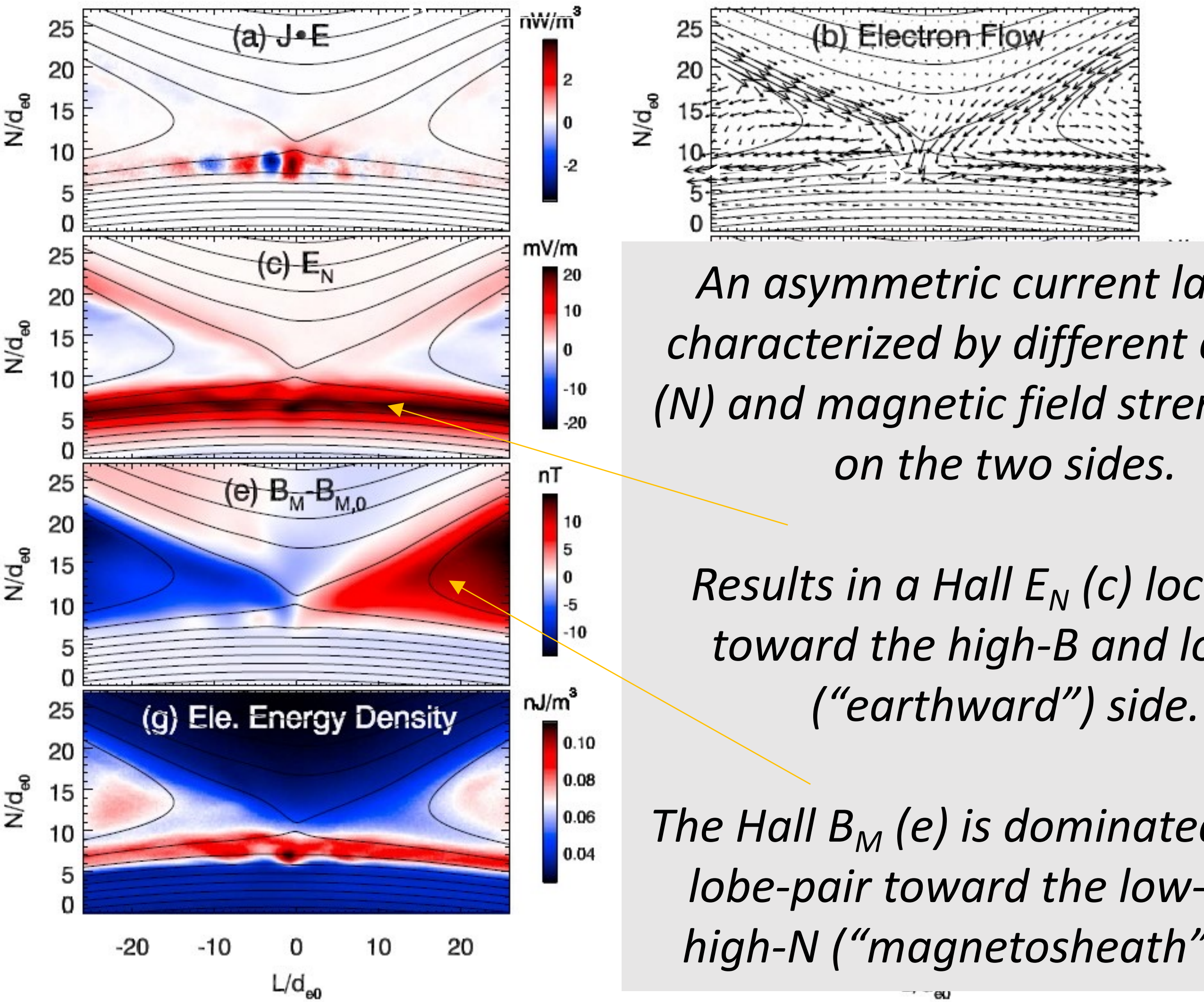

An asymmetric current layer is characterized by different density (N) and magnetic field strength (B) on the two sides.

Results in a Hall E_N (c) localized toward the high-B and low-N ("earthward") side.

The Hall B_M (e) is dominated by the lobe-pair toward the low-B and high-N ("magnetosheath") side.

Swisdak, M., Drake, J. F., Price, L., Burch, J. L., Cassak, P. A., & Phan, T.-D. (2018). Localized and intense energy conversion in the diffusion region of asymmetric magnetic reconnection. Geophysical Research Letters, 45, 5260–5267. https://doi.org/10.1029/2017GL076862

Magnetic Reconnection – Hall B Summary

Symmetric two-fluid simulation

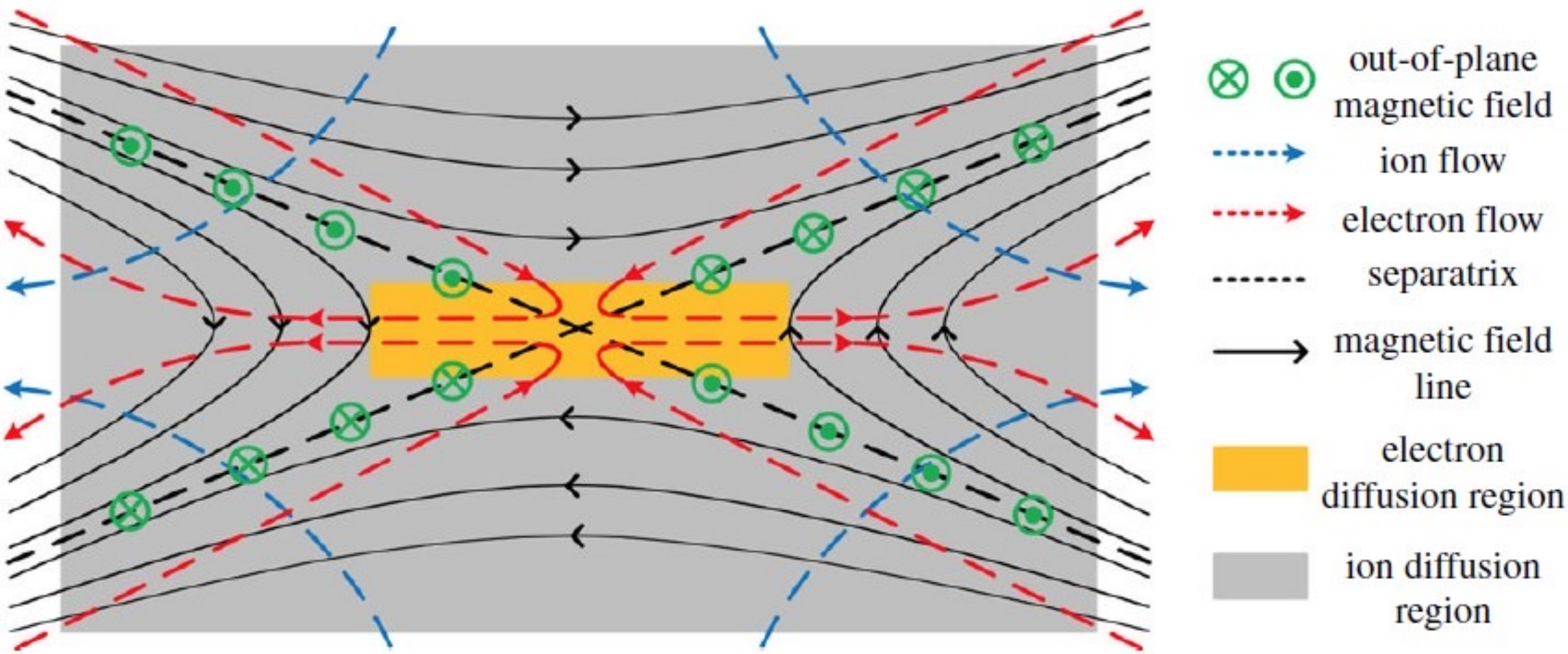

Figure 5. Schematic of two-fluid reconnection. Ions decouple from electrons in the ion diffusion region (grey colour). Electrons are frozen to the field lines until they reach the electron diffusion region (orange colour). The electron flow pattern creates a quadrupole out-of-plane magnetic field, a signature of the Hall effect.

Zweibel EG, Yamada M. (2016) Perspectives on magnetic reconnection. Proc. R. Soc. A 472: 20160479.
http://dx.doi.org/10.1098/rspa.2016.0479

Overview

- **Current sheets:** ***Magnetic field rotations [$J=\nabla\times B/\mu_0$] from the very wide Heliospheric Current Sheet to "narrow" M'pause***
- **Multi-spacecraft missions:** ***A brief introduction to tedrahedron formations and the Curlometer technique***
- **Near-Earth space regimes & boundaries**
- **The magnetic reconnection process at current sheets:**

  (a) Schematic overviews, 2D vs 3D & ion (di) scale

  (b) "To be or not to be" frozen-in? The G.O.L. vs Hall ☺

  (c) Reconnection rate v_{in}/v_{out}
- Observations of Reconnection Jets:

  (a) Cluster in the solar wind vs "timing normal" concept

  (b) MMS at the magnetopause: J from "curlB" vs J=Ne(Vi-Ve)
- Summary

Magnetic Reconnection Rate

How fast can a magnetic field B_i enter a diffusion region (DR) at an external inflow speed v_i? In other words, what is the “reconnection rate” v_{in}/v_{out} ratio?

$E = v_i B_i$ (just outside DR) *and* $E = J / \sigma$ (Ohm’s law inside DR) -> $v_i B_i = J / \sigma$
Using Ampere’s Law (inside DR) $J = B_i / (\mu_0 l)$ -> $v_i l = 1 / (\sigma\mu_0)$ (1)

Mass conservation implies that *inflow rate* (up & down) equals *outflow rate* *(left & right):*
$\rho v_i * 2L * 2 = \rho v_0 * 2l * 2$ or $v_o l = v_i L$ or $l = (v_i L)/v_o$ which combined with (1)
-> $v_i^2 = v_0 / L (\sigma\mu_0)$ *and using the Magnetic Reynolds number of the inflow plasma*
$R_m \equiv v_{Ai} L (\sigma\mu_0)$ -> $v_i^2 = v_0 v_{Ai} / R_m$ *where* v_{Ai} *is the Alfvén speed of the inflow plasma*.

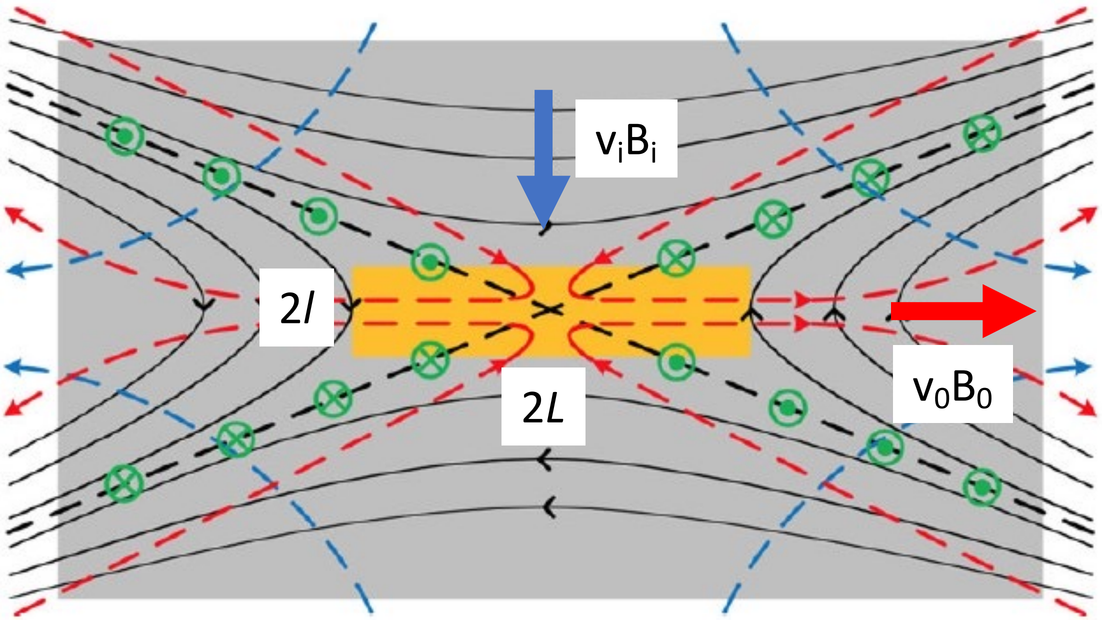

Magnetic Reconnection Rate

How fast can a magnetic field B_i enter a diffusion region (DR) at an external inflow speed v_i? In other words, what is the "reconnection rate" v_{in}/v_{out} ratio?

$v_i^2 = v_0 v_{Ai} / R_m$ (1) … but what is the outflow speed v_0?

Plasma Equation of Outflow Motion: $\rho\, d\mathbf{v}/dt = \mathbf{J}\times\mathbf{B}$ *where* $d\mathbf{v}/dt = \partial\mathbf{v}/\partial t + (\mathbf{v}\cdot\nabla)\mathbf{v}$

-> $\rho v_0^2/L = JB_0$ *(steady state) and using Ampere's law* $J = B_i / (\mu_0 l)$

-> $\rho v_0^2/L = B_0 B_i / (\mu_0 l)$

-> $v_0^2 = (L/\rho) * B_0 B_i / (\mu_0 l) = (L / l) * B_0 B_i / (\rho\mu_0)$

Now $(L / l) = (v_0/v_i)$ *from mass conservation and* $(v_0/v_i) = (B_i/B_0)$ *from magnetic flux conservation and* $v_0^2 = B_0 B_i / (\rho\mu_0) * (B_i/B_0)$ -> $v_0 = B_i / \mathrm{SQRT}(\mu_0\rho) = v_{Ai}$ (2)

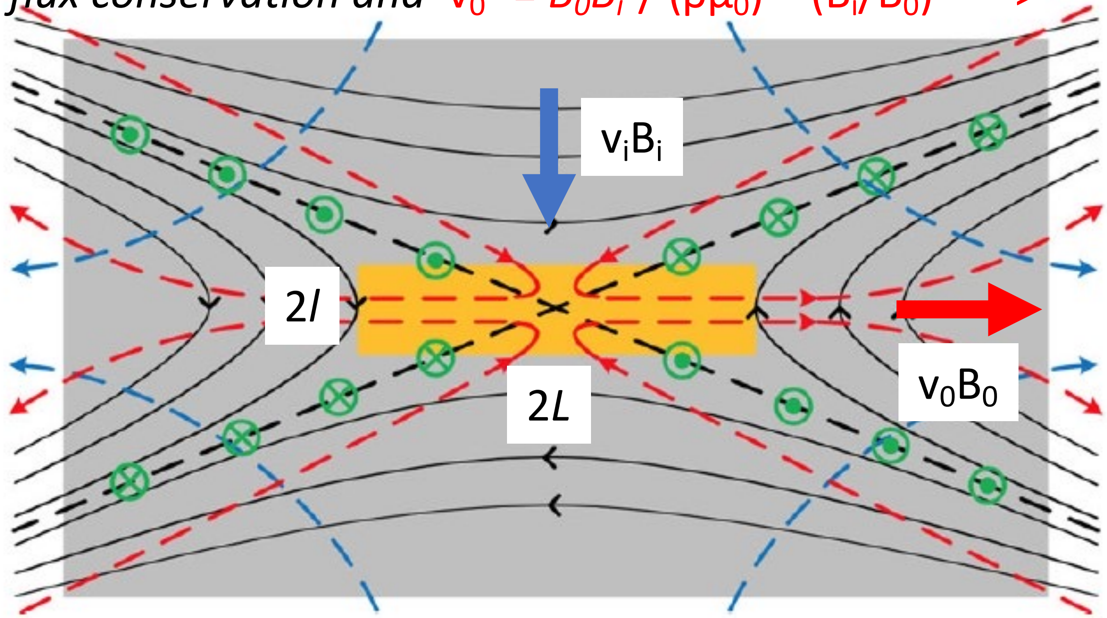

The original Sweet-Parker reconnection rate from (1) and (2):

$v_i = v_{Ai} / \mathrm{SQRT}(R_m)$

or

$v_i/v_{Ai} \sim 1/\mathrm{SQRT}(R_m)$

Magnetic Reconnection Rate

The original Sweet-Parker reconnection rate $v_{in}/v_{out} = v_i/v_{Ai} \sim 1/\mathrm{SQRT}(R_m)$ is **too slow** if the *dimension L along the current sheet* is **long compared with thickness δ** and this theory alone failed to explain reconnection associated with solar flares.

The famous “GEM reconnection challenge” set of papers in 2001, with an introduction by *Birn, J. et al.*, Geospace Environmental Modeling (GEM) Magnetic Reconnection Challenge (2001), https://doi.org/10.1029/1999JA900449, were instrumental in validating the importance of the **JxB Hall term** of the G.O.L. to obtain fast $v_i/v_A \sim 0.1$ rates.

BIRN ET AL.: GEM RECONNECTION CHALLENGE

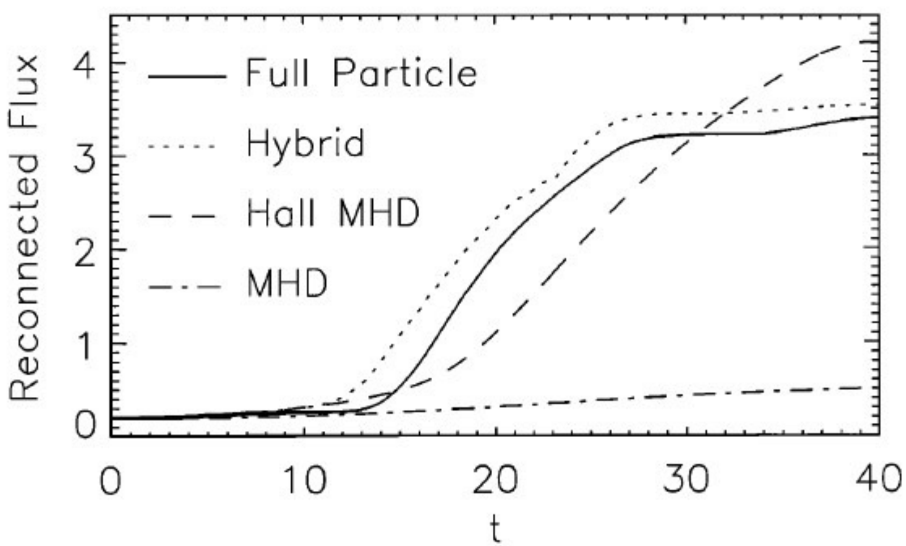

Figure 1. The reconnected magnetic flux versus time from a variety of simulation models: full particle, hybrid, Hall MHD, and MHD (for resistivity $\eta = 0.005$).

Overview

- **Current sheets:** ***Magnetic field rotations [$J=\nabla\times B/\mu_0$] from the very wide Heliospheric Current Sheet to "narrow" M'pause***
- **Multi-spacecraft missions:** ***A brief introduction to tedrahedron formations and the Curlometer technique***
- **Near-Earth space regimes & boundaries**
- **The magnetic reconnection process at current sheets:**
  - ***(a) Schematic overviews, 2D vs 3D & ion (di) scale***
  - ***(b) "To be or not to be" frozen-in? The G.O.L. vs Hall ☺***
  - ***(c) Reconnection rate v_{in}/v_{out}***
- **Observations of Reconnection Jets:**
  - ***(a) Cluster in the solar wind vs "timing normal" concept***
  - *(b) MMS at the magnetopause: J from "curlB" vs J=Ne(Vi-Ve)*
- Summary

Magnetic Reconnection - Observations

Magnetohydrodynamic (MHD) simulations

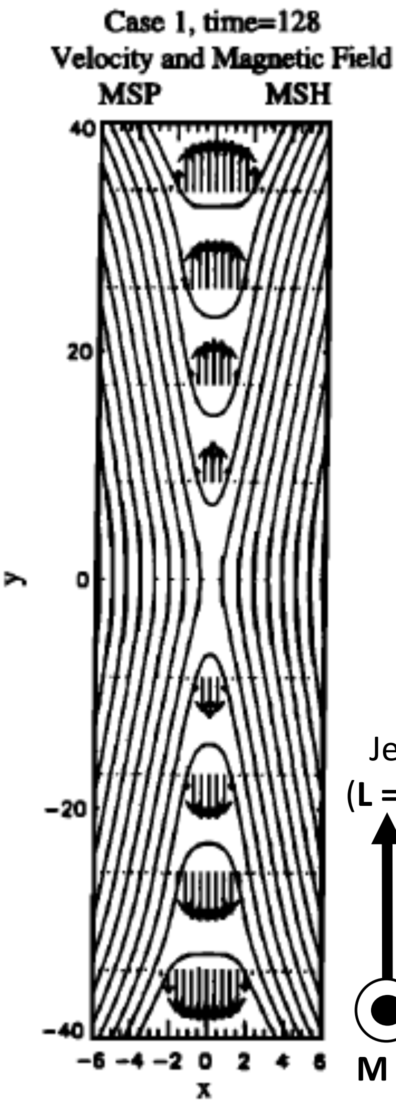

How do we find current sheets associated with reconnection jets in space?

(1) Find the "current sheet" – rotation of B.
"Easier" in an optimum "LMN" system (c.f. *simulation coordinates*).
Rotate from a measured frame (e.g. GSE, GSM, s/c frame etc)
into one defined as: **L** = maximum change in B,
N = normal to a current layer (various methods) and **M** = **N** x **L**

(2) Does the plasma (e.g. ion) velocity peak (+/-) across the layer?

(3) If it does, does the flow change satisfy ~Alfvén speed in a frame moving with the boundary?

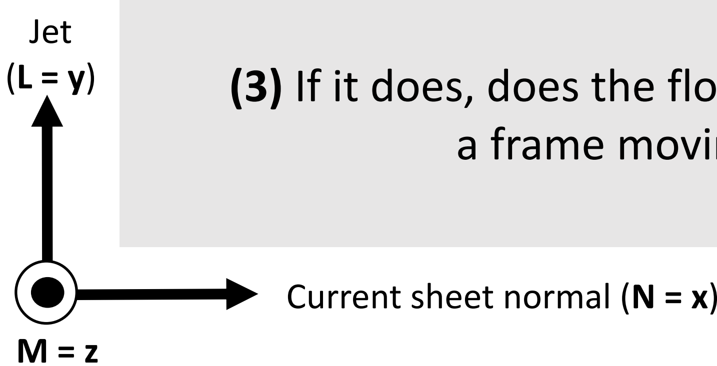

La Belle-Hamer et al., Magnetic reconnection in the presence of sheared flow and density asymmetry: Applications to the Earth's magnetopause, J. Geophys. Res., 1995

The four-spacecraft Cluster mission: Spacecraft separations

Year	Minimum (km)	Maximum (km)
2005	600	1700
2006	6000	12300
2007	400	12400
2008	40	10400
2009	3300	8500

Note: Solar wind density results in a most common *di* ~ 100 km

The four-spacecraft Cluster mission: Spacecraft separations

Year	Minimum (di)	Maximum (di)
2005	6	17
2006	60	123
2007	4	124
2008	0.4	104
2009	33	85

Note: Solar wind density results in a most common *di* ~ 100 km

Exploring Cluster in the solar wind

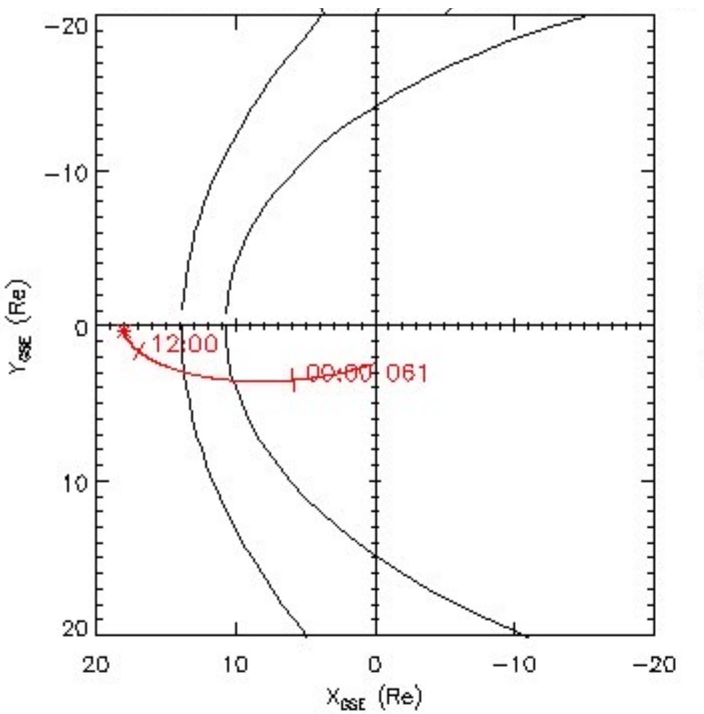

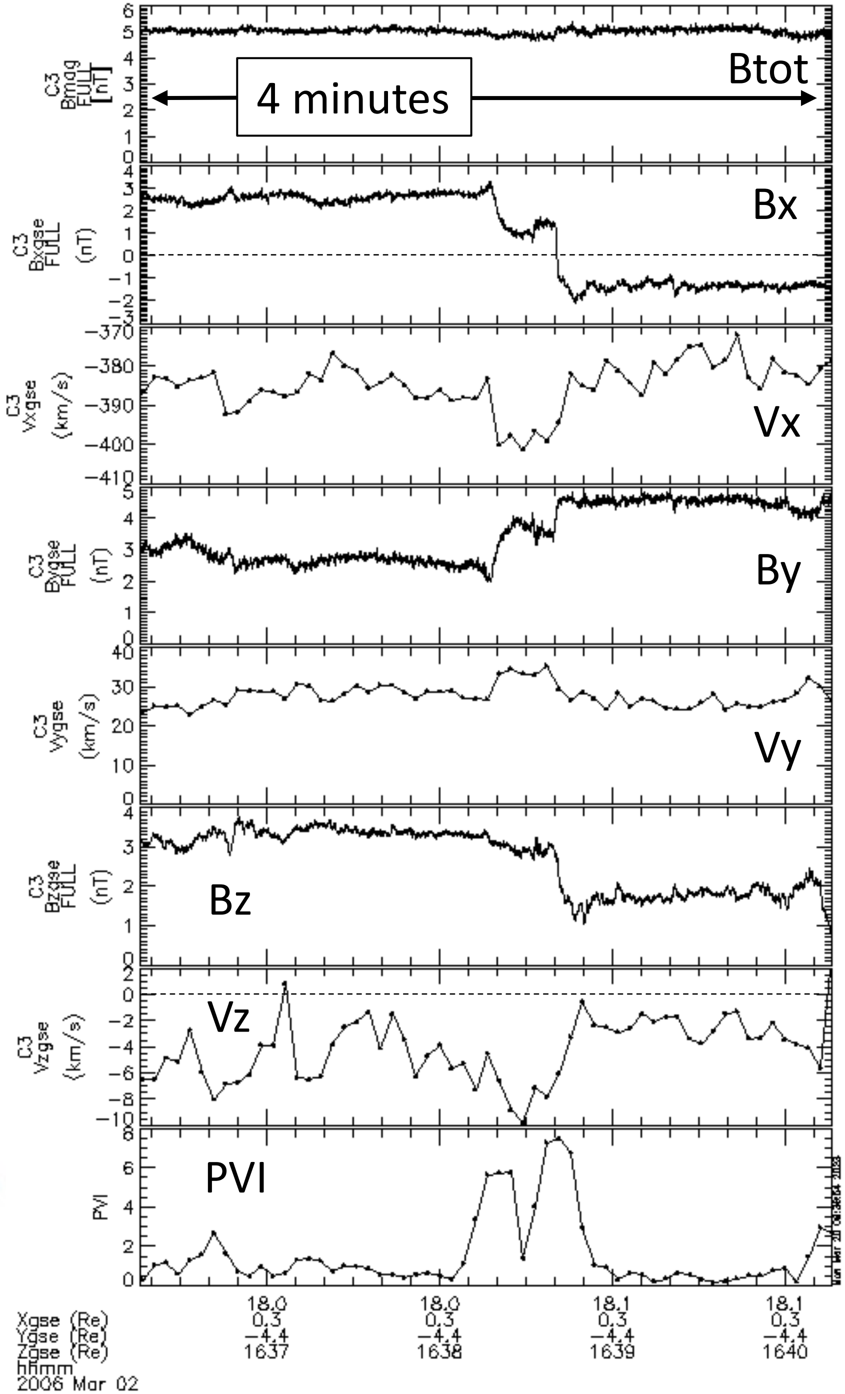

The PVI time series is defined in terms of the magnetic field increment vector $\Delta \boldsymbol{B}(t, \tau) = \boldsymbol{B}(t + \tau) - \boldsymbol{B}(t)$ (Greco et al. 2008):

$$\mathrm{PVI}(t, \tau) = \frac{|\Delta \boldsymbol{B}(t, \tau)|}{\sqrt{\langle |\Delta \boldsymbol{B}(t, \tau)|^2 \rangle}} \quad (1)$$

Greco et al., Ap. J. Lett., 2016, doi:10.3847/2041-8205/823/2/L39
THE COMPLEX STRUCTURE OF MAGNETIC FIELD DISCONTINUITIES IN THE TURBULENT SOLAR WIND

Exploring Cluster in the solar wind

We confirm a presence of an Alfvénic reconnection exhaust across a current sheet by using the so-called "Walén" relation (*Paschmann et al.*, 1986):

whether it may also satisfy the Walén relation $V_{\mathrm{WL}} = V_{\mathrm{L0}} \pm \Delta V_{\mathrm{AL}}$ as expected for a magnetic reconnection exhaust (Paschmann et al. 1986), where ΔV_{AL} is given as

$$\Delta V_{\mathrm{AL}} = \sqrt{\rho_0/\mu_0}\,(B_L/\rho - B_{L0}/\rho_0).$$

Here, $\mu_0 = 4\pi \times 10^{-7}$ Vs/Am is the permeability of free space and the other parameters indicated with a subscript "0" (V_{L0}, B_{L0}, ρ_0) correspond to the given external parameter at the start time of the Walén prediction, whether that is before the CS (leading side) or after the CS (trailing side). The positive and negative signs of ΔV_{AL} are chosen automatically according to the direction of the potential jet ($\Delta V_{\mathrm{L}} > 0$ or $\Delta V_{\mathrm{L}} < 0$).

Paschmann G., Papamastorakis I., Baumjohann W. et al., The magnetopause for large magnetic shear: AMPTE/IRM observations, JGR 91 11099, 1986

Eriksson et al., The Astrophysical Journal, 933:181 (21pp), 2022 July 10, https://doi.org/10.3847/1538-4357/ac73f6

Exploring Cluster in the solar wind

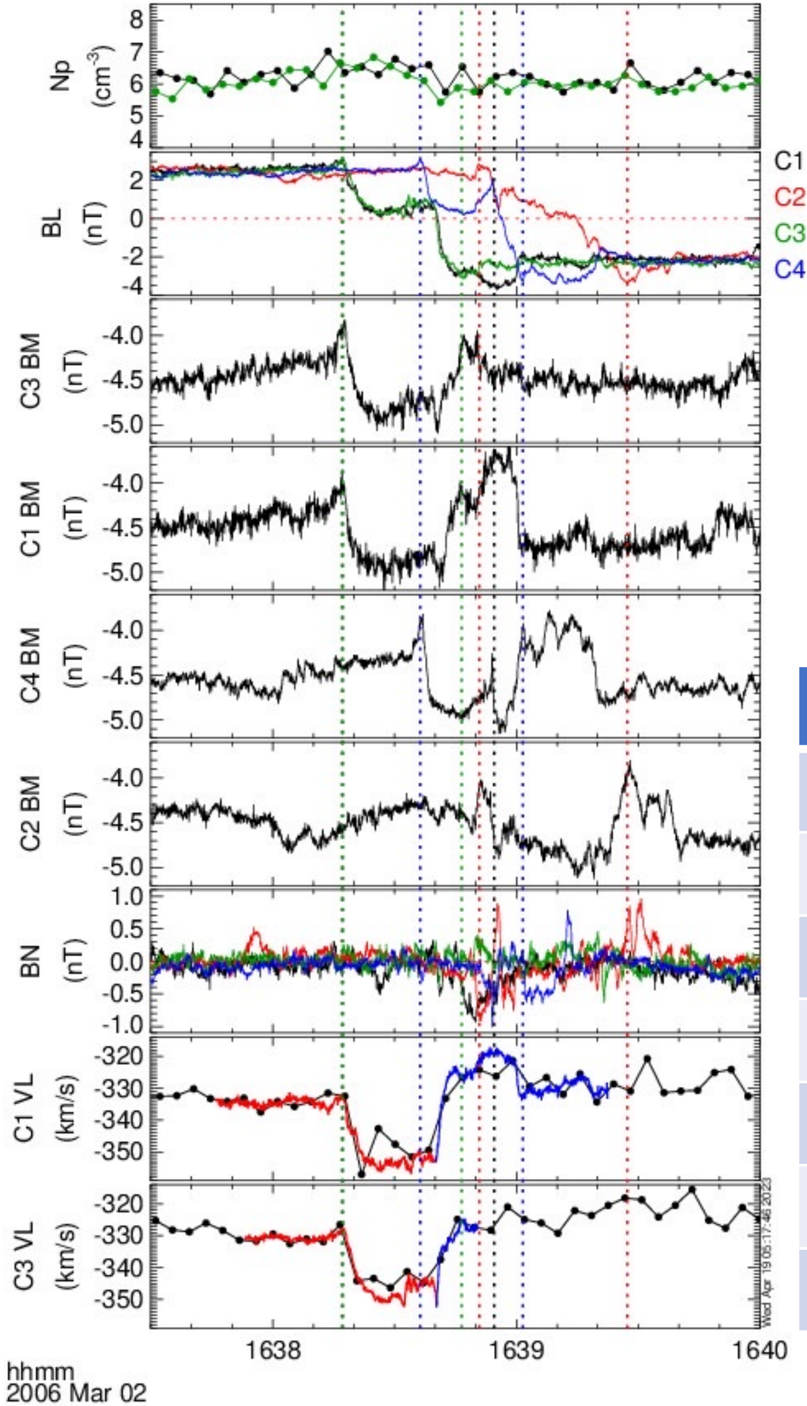

Event duration: 70.1 s (1.2 min)

Solar wind external flow:

$\langle V_L, V_M, V_N \rangle$ = [-329.8, 59.5, -194.8] km/s

$\langle di \rangle$=92.2 km

	C1	C2	C3	C4
Δt_{cs} (s)	37.3	36.4	29.3	25.3
ΔN (*di*)	79	77	62	53
ΔL (*di*)	133	130	105	90
ΔM (*di*)	24	24	19	16
B_{rot} (°)	79	75	74	78
B_{M1}/B_{L1}	1.6	1.7	1.7	1.9
B_{M2}/B_{L2}	2.2	2.3	1.9	2.1

Exploring Cluster in the solar wind

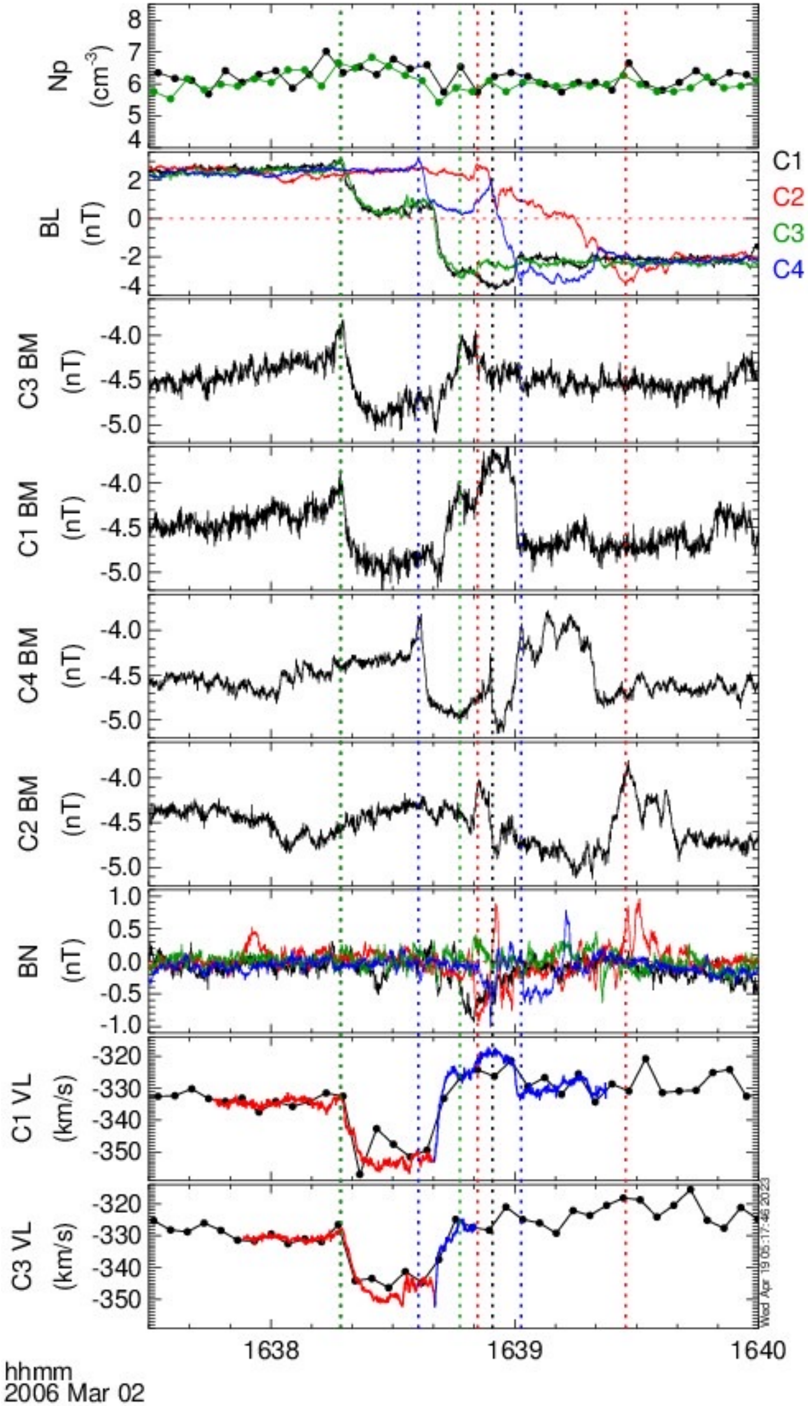

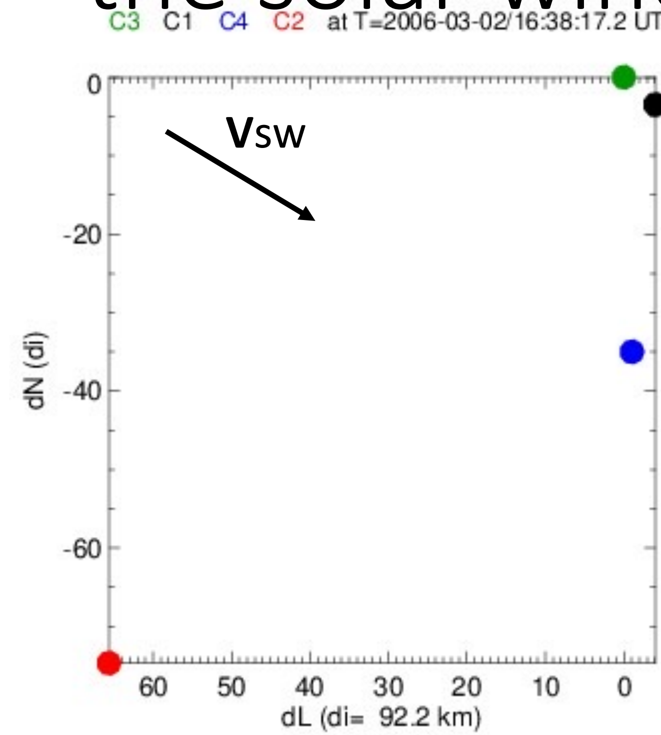

C3 R_{GSE}=(18.05 0.32 -4.37) R_E
N_{GSE}=(0.505808 0.434122 -0.745451)
L_{GSE}=(0.850924 -0.393063 0.348469)
M_{GSE}=(-0.141731 -0.810580 -0.568219)

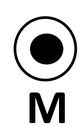

Exploring Cluster in the solar wind

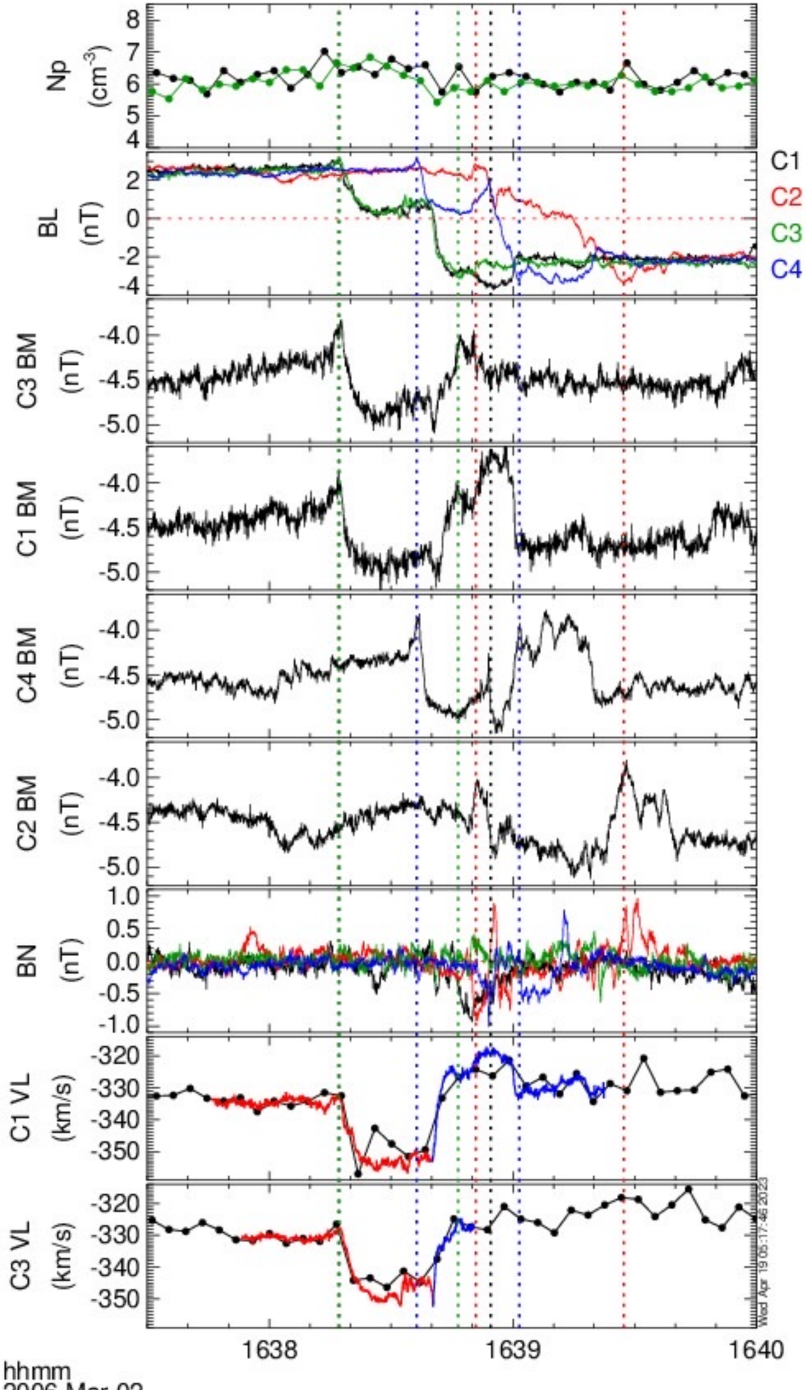

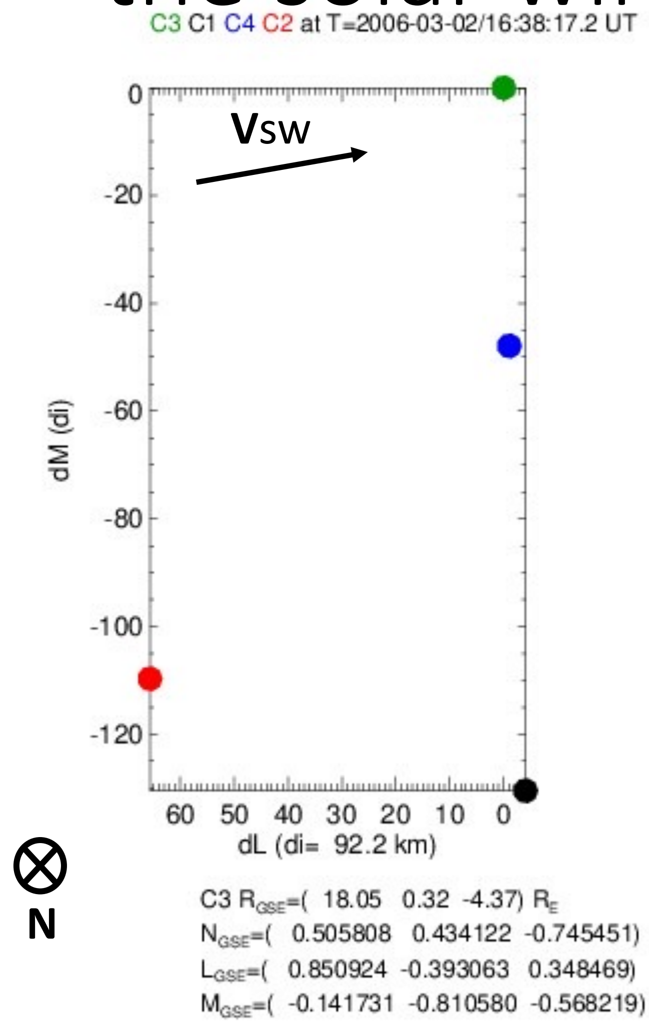

Timing Analysis

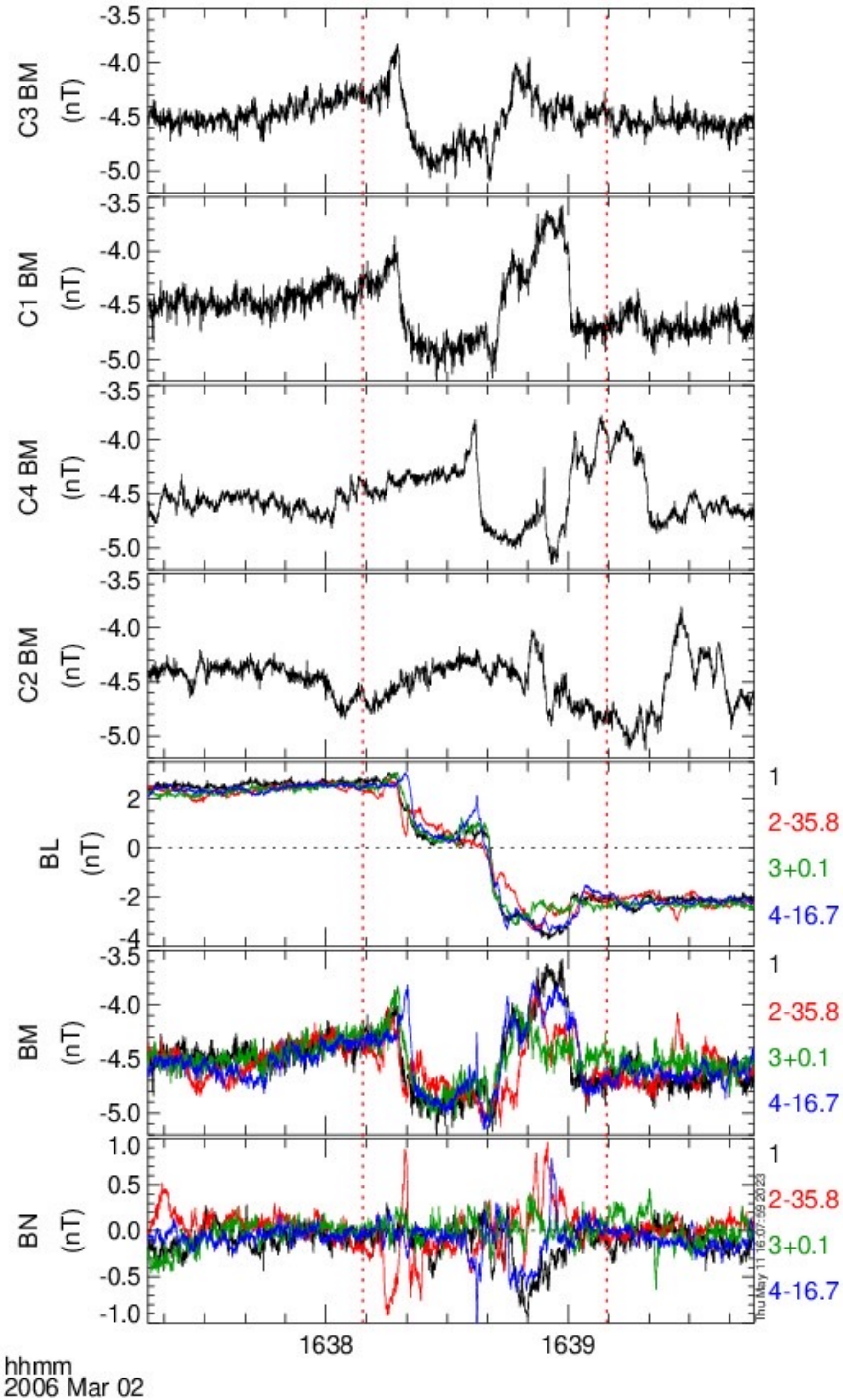

If you “only” had one s/c to go by …
you would not know what the **actual structure** of the current layer looks like.

A multi-formation mission demonstrates how the *same* current sheet has *important structure* in, e.g., BM and BN.

In this case, structure exists over the ~100 di separation.

Timing Analysis

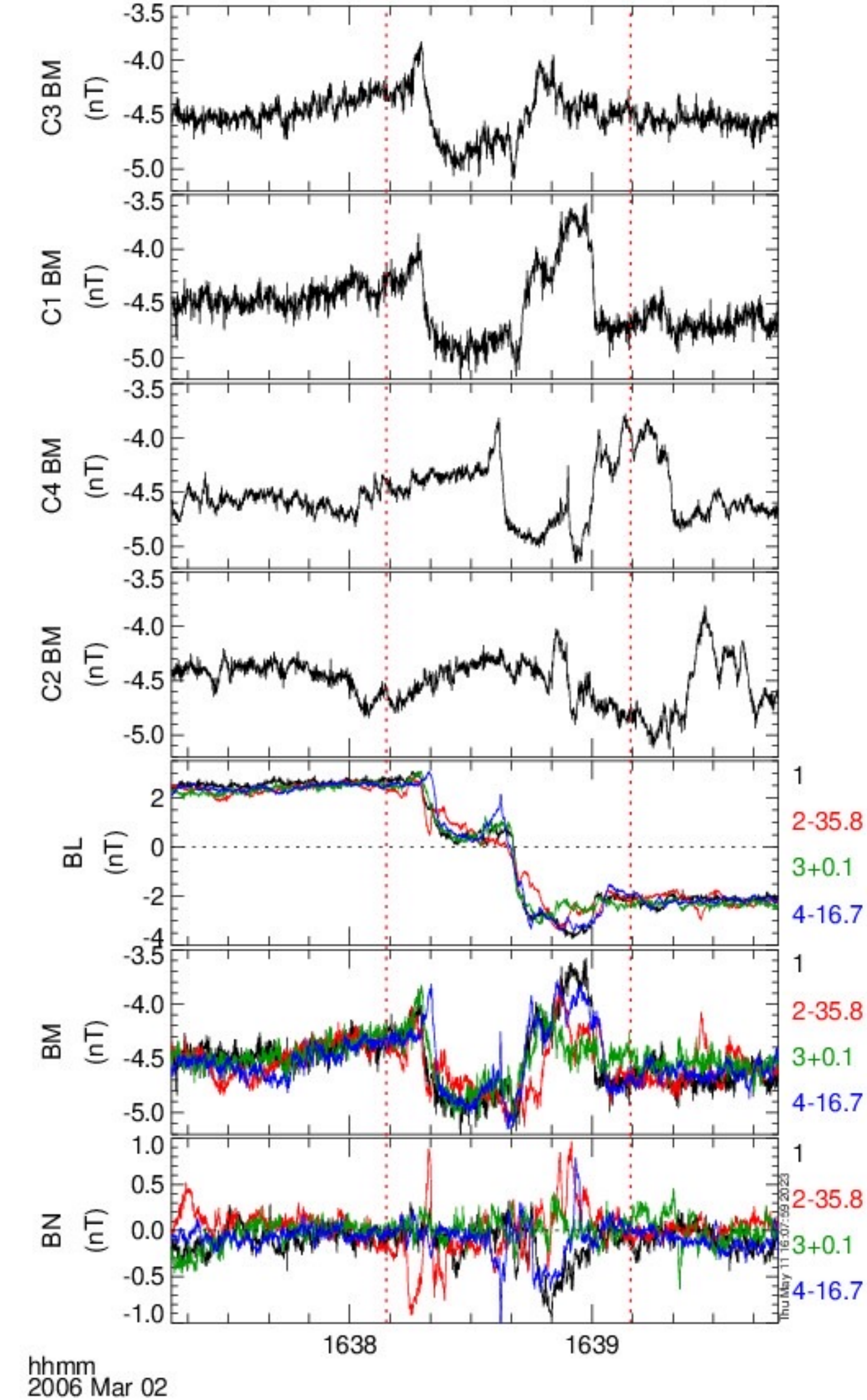

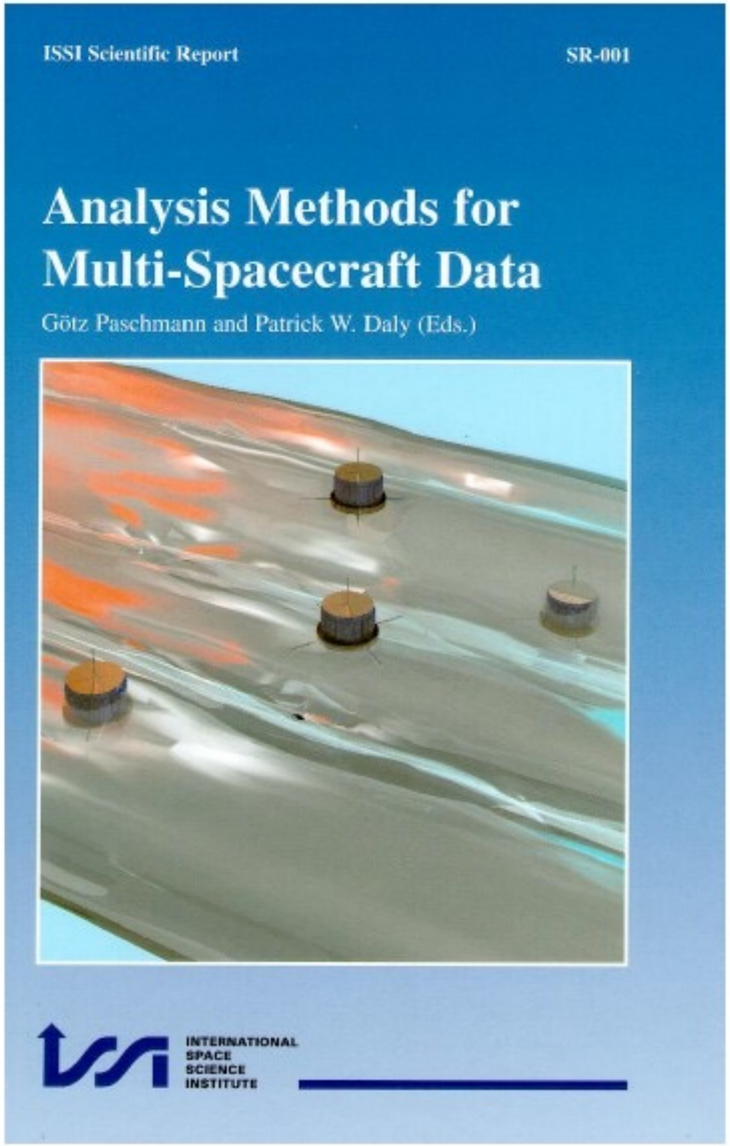

Ch.10 Shock & Discontinuity Normals… by Steven J. Schwartz

Timing Analysis

10.4.3 Multi-Spacecraft Timings

If the same boundary passes several spacecraft, the relative positions and timings can be used to construct the boundary normal and speed, since

$$(V_{\text{sh}}^{\text{arb}} t_{\alpha\beta}) \cdot \hat{n} = r_{\alpha\beta} \cdot \hat{n} \tag{10.19}$$

where $r_{\alpha\beta}$ is the separation vector between any spacecraft pair and $t_{\alpha\beta}$ the time difference between this pair for a particular boundary. Thus given 4 spacecraft, the normal vector and normal propagation velocity $V_{\text{sh}}^{\text{arb}} \equiv V_{\text{sh}}^{\text{arb}} \cdot \hat{n}$ are found from the solution of the following system:

$$\begin{pmatrix} r_{12} \\ r_{13} \\ r_{14} \end{pmatrix} \cdot \frac{1}{V_{\text{sh}}^{\text{arb}}} \begin{pmatrix} n_x \\ n_y \\ n_z \end{pmatrix} = \begin{pmatrix} t_{12} \\ t_{13} \\ t_{14} \end{pmatrix} \tag{10.20}$$

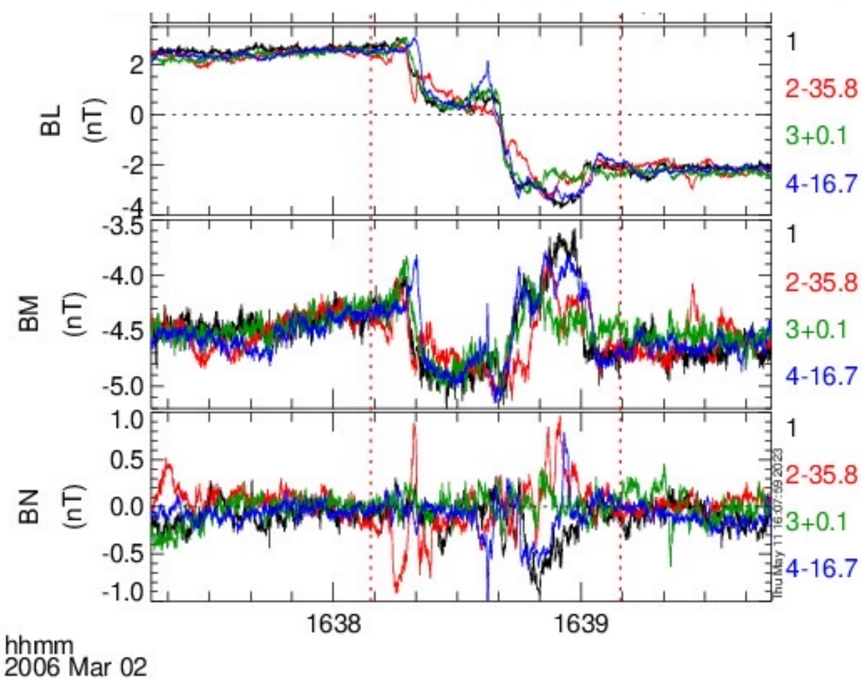

At 2006-03-02/16:38:41 UT :

$\mathbf{r}_{12}$=[1873, -6929, 6043] km

$\mathbf{r}_{13}$=[-1229, -9761, -6947] km

$\mathbf{r}_{14}$=[-2313, -7544, -2066] km

Relative C1 = [18.2, 1.8, -3.3] Re (GSE)

t_{12} = -35.8 s

t_{13} = +0.1 s

t_{14} = -16.7 s

Solving (e.g. inverting separation matrix):

$\mathbf{N}$t = ±[0.343745, 0.409645, -0.845003]

|$\mathbf{V}$t| = 58.5 km/s

Timing Analysis

10.4.3 Multi-Spacecraft Timings

If the same boundary passes several spacecraft, the relative positions and timings can be used to construct the boundary normal and speed, since

$$(V_{\rm sh}^{\rm arb} t_{\alpha\beta}) \cdot \hat{n} = \boldsymbol{r}_{\alpha\beta} \cdot \hat{n} \qquad (10.19)$$

where $\boldsymbol{r}_{\alpha\beta}$ is the separation vector between any spacecraft pair and $t_{\alpha\beta}$ the time difference between this pair for a particular boundary. Thus given 4 spacecraft, the normal vector and normal propagation velocity $V_{\rm sh}^{\rm arb} \equiv \boldsymbol{V}_{\rm sh}^{\rm arb} \cdot \hat{n}$ are found from the solution of the following system:

$$\begin{pmatrix} \boldsymbol{r}_{12} \\ \boldsymbol{r}_{13} \\ \boldsymbol{r}_{14} \end{pmatrix} \cdot \frac{1}{V_{\rm sh}^{\rm arb}} \begin{pmatrix} n_x \\ n_y \\ n_z \end{pmatrix} = \begin{pmatrix} t_{12} \\ t_{13} \\ t_{14} \end{pmatrix} \qquad (10.20)$$

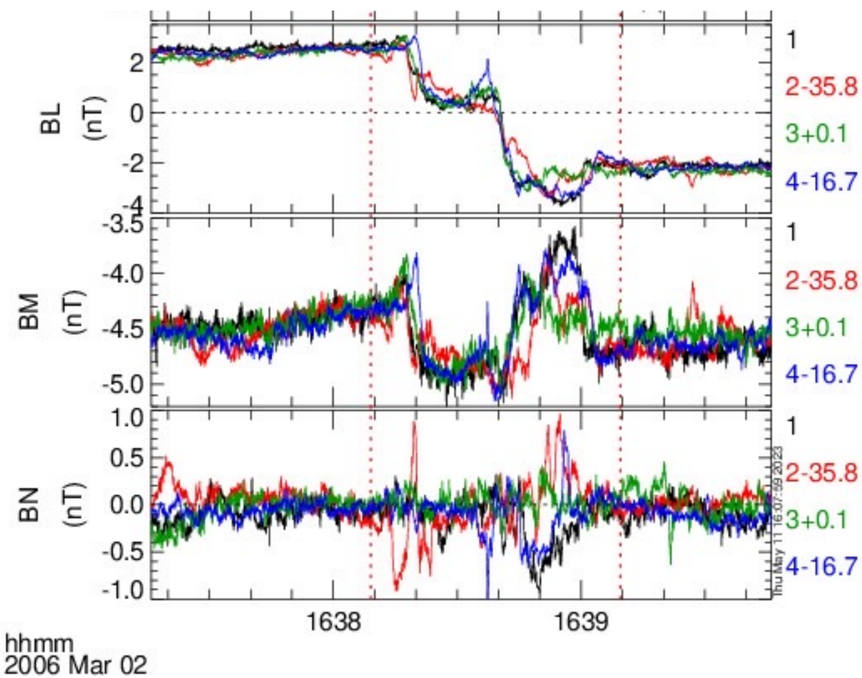

Nt = ±[0.343745, 0.409645, -0.845003]

|**V**t| = 58.5 km/s

Nc = $\mathbf{B}_1$x$\mathbf{B}_2$/|$\mathbf{B}_1$x$\mathbf{B}_2$| =

= [0.505808, 0.434122, -0.745451]

Angle difference: **N**t***N**c = 11^{o}

Caveats:

(1) Sharp signal gradient observed at all s/c

(2) Tetrahedron *formation* v.s. *s/c alignment* relative the (assumed) planar boundary

Overview

- **Current sheets:** ***Magnetic field rotations [$J = \nabla \times B/\mu_0$] from the very wide Heliospheric Current Sheet to "narrow" M'pause***
- **Multi-spacecraft missions:** ***A brief introduction to tedrahedron formations and the Curlometer technique***
- **Near-Earth space regimes & boundaries**
- **The magnetic reconnection process at current sheets:**
  - ***(a) Schematic overviews, 2D vs 3D & ion (di) scale***
  - ***(b) "To be or not to be" frozen-in? The G.O.L. vs Hall ☺***
  - ***(c) Reconnection rate v_{in}/v_{out}***
- **Observations of Reconnection Jets:**
  - ***(a) Cluster in the solar wind vs "timing normal" concept***
  - ***(b) MMS at the magnetopause: J from "curlB" vs J=Ne(Vi-Ve)***
- Summary

Exploring MMS at the Dayside Magnetopause: **GSM**

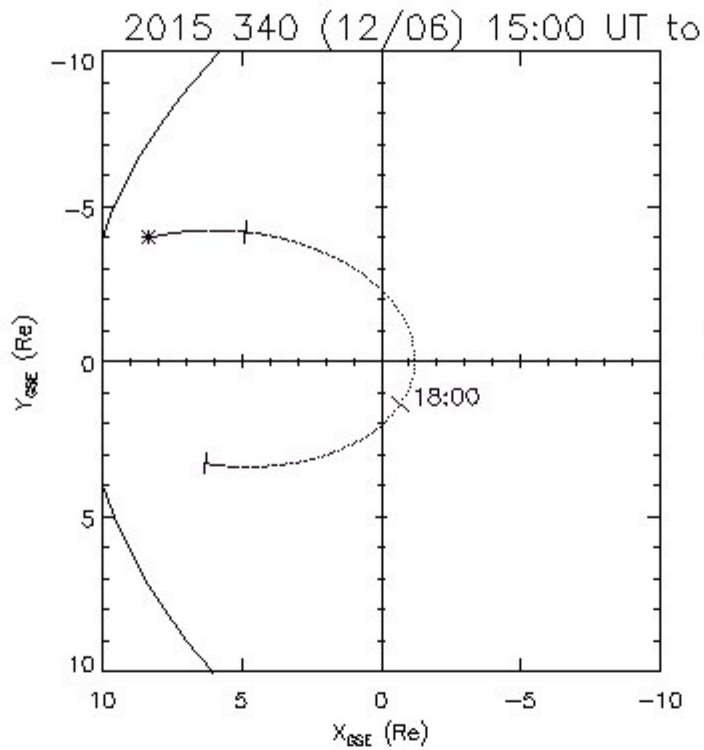

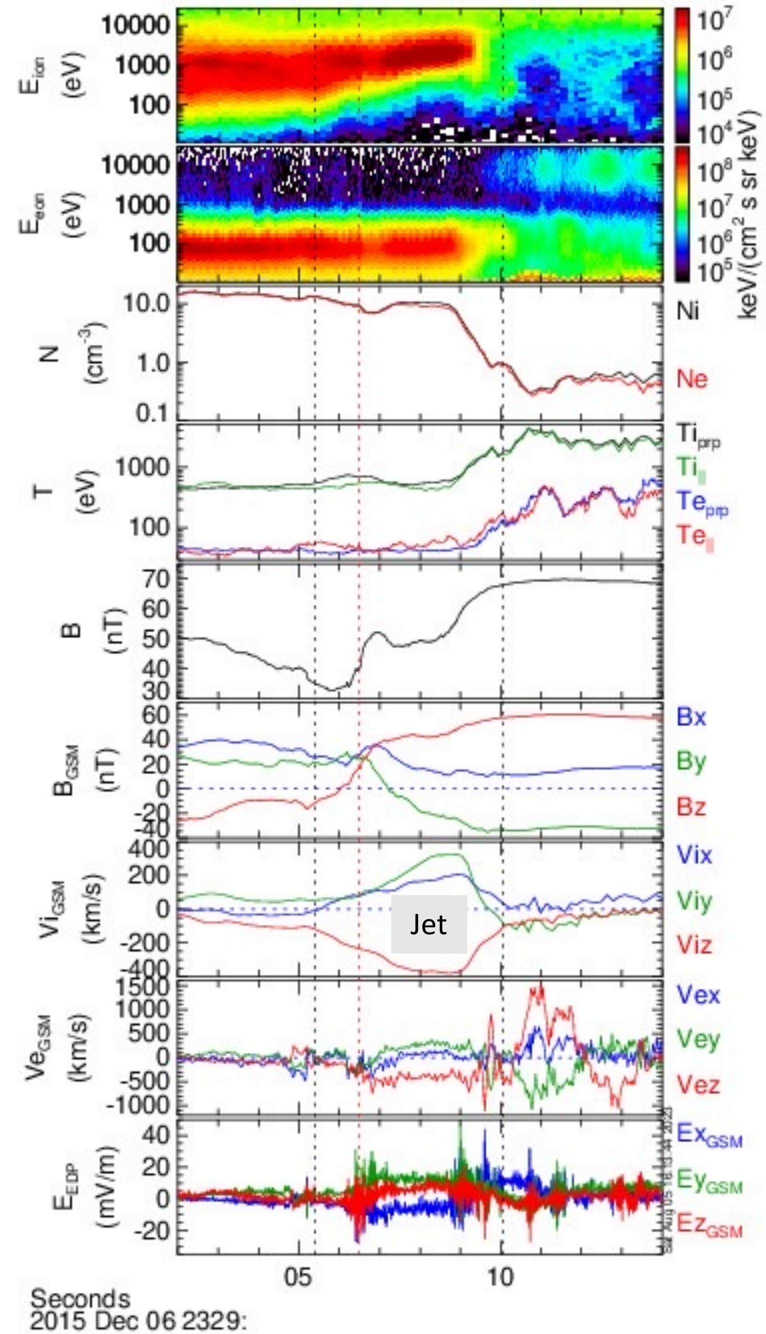

Exploring MMS at the Dayside Magnetopause: **GSM**

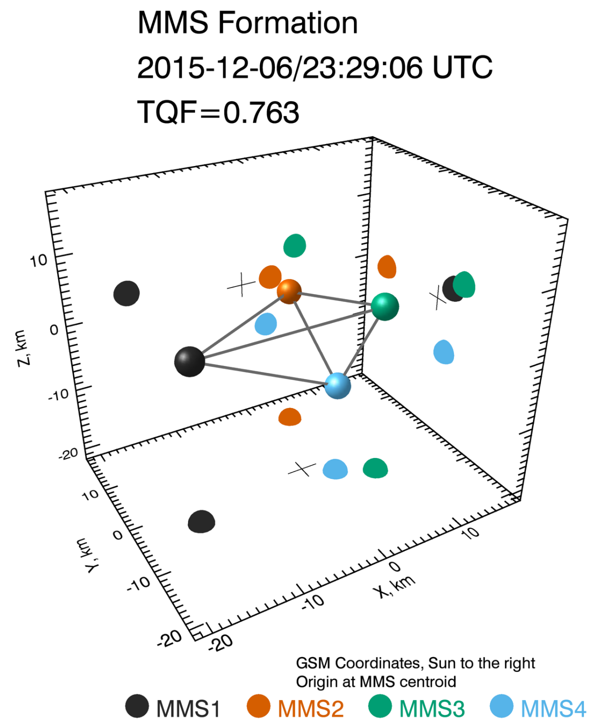

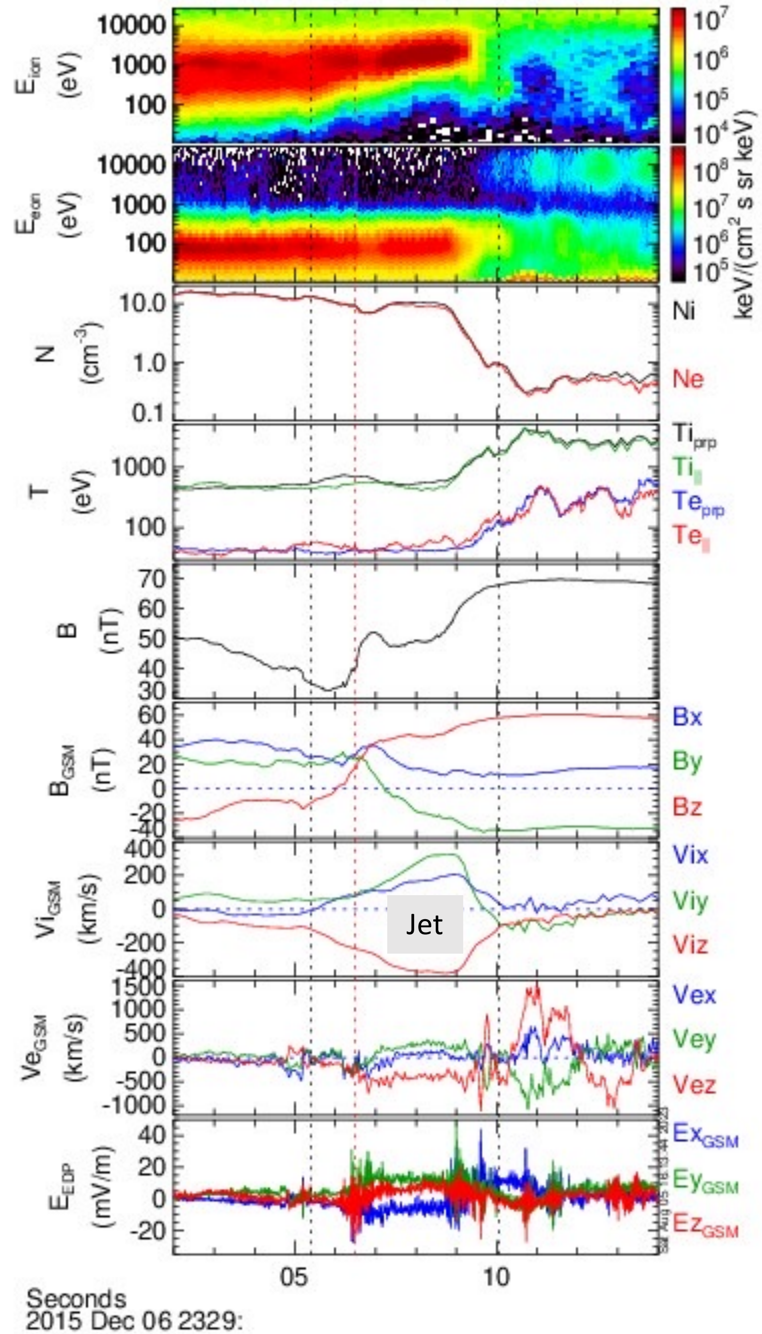

TQF = Tetrahedron Quality Factor

TQF = 1 <-> “regular” tetrahedron

Exploring MMS at the Dayside Magnetopause: **LMN & J=CurlB/μ_0**

vs J = Ne(Vi-Ve) = Jfpi

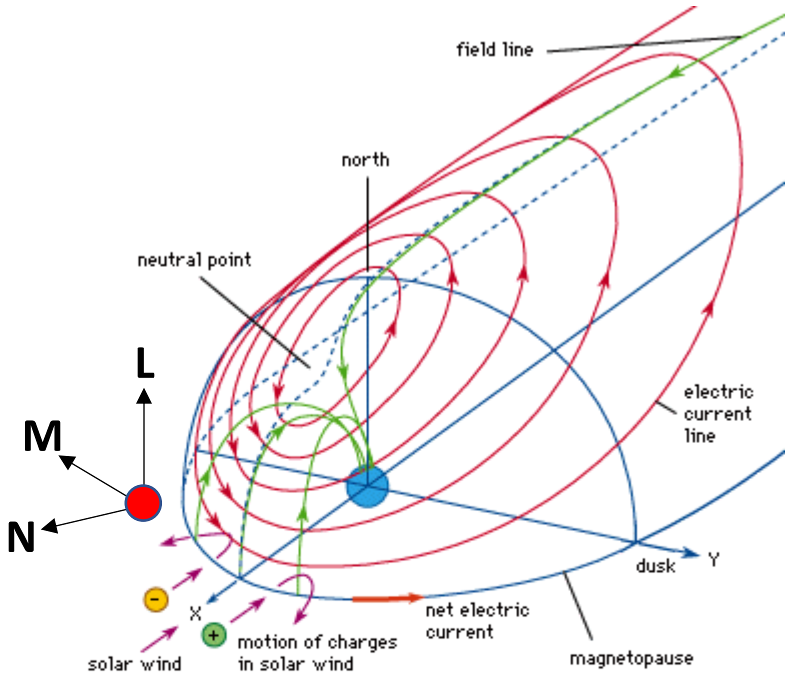

©1994 Encyclopaedia Britannica, Inc.

Lgsm = [-0.1598, -0.6770, 0.7185]
Mgsm = [-0.7211, -0.4170, -0.5533]
Ngsm = [0.6742, -0.6065, -0.4215]

Jcurl
(DIS res)

$\nabla \cdot B = 0$

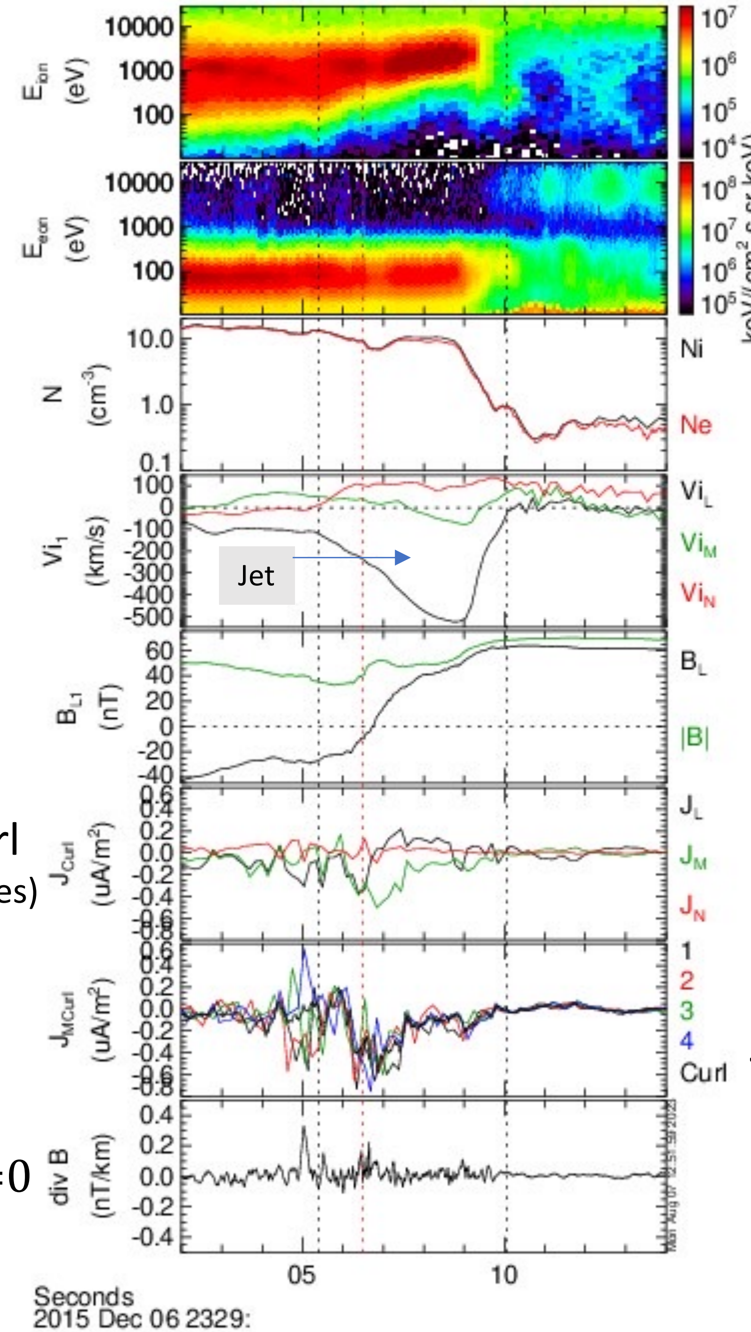

JMfpi
(DIS) vs
JMcurl
(brst)

Exploring MMS at the Dayside Magnetopause: LMN & J=CurlB/μ_0

vs J = Ne(Vi-Ve) = Jfpi

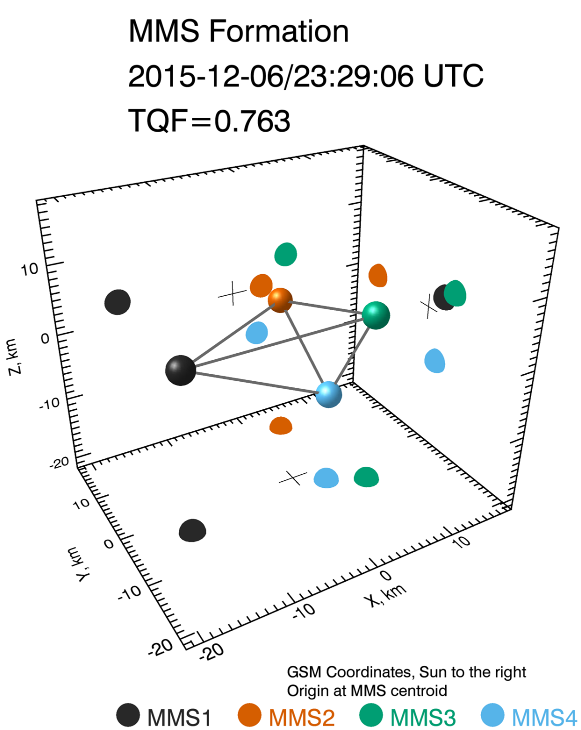

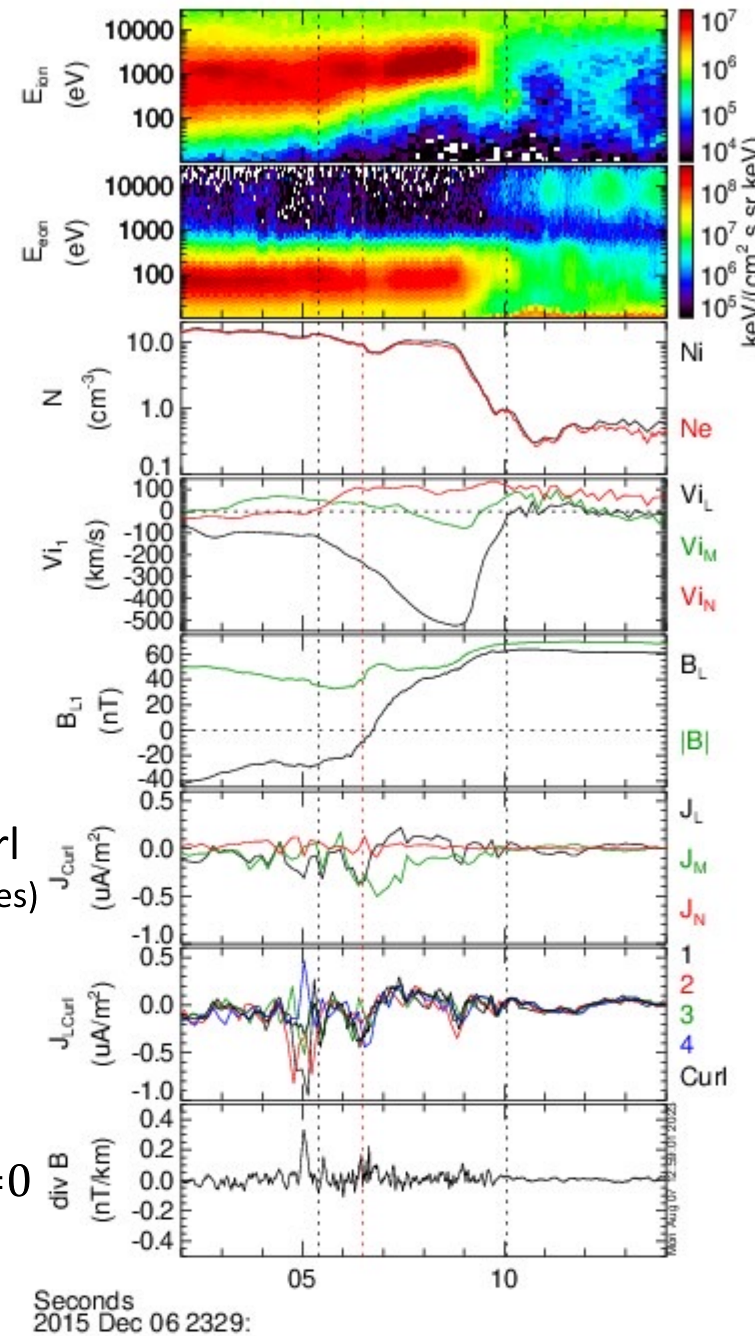

Jcurl (DIS res)

JLfpi (DIS) vs JLcurl (brst)

$\nabla \cdot B = 0$

Exploring MMS at the Dayside Magnetopause: LMN & J=CurlB/μ_0

vs J = Ne(Vi-Ve) = Jfpi

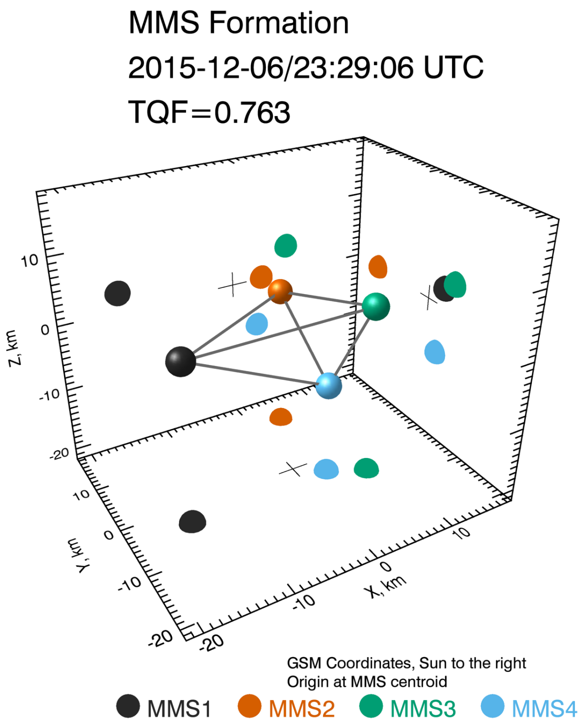

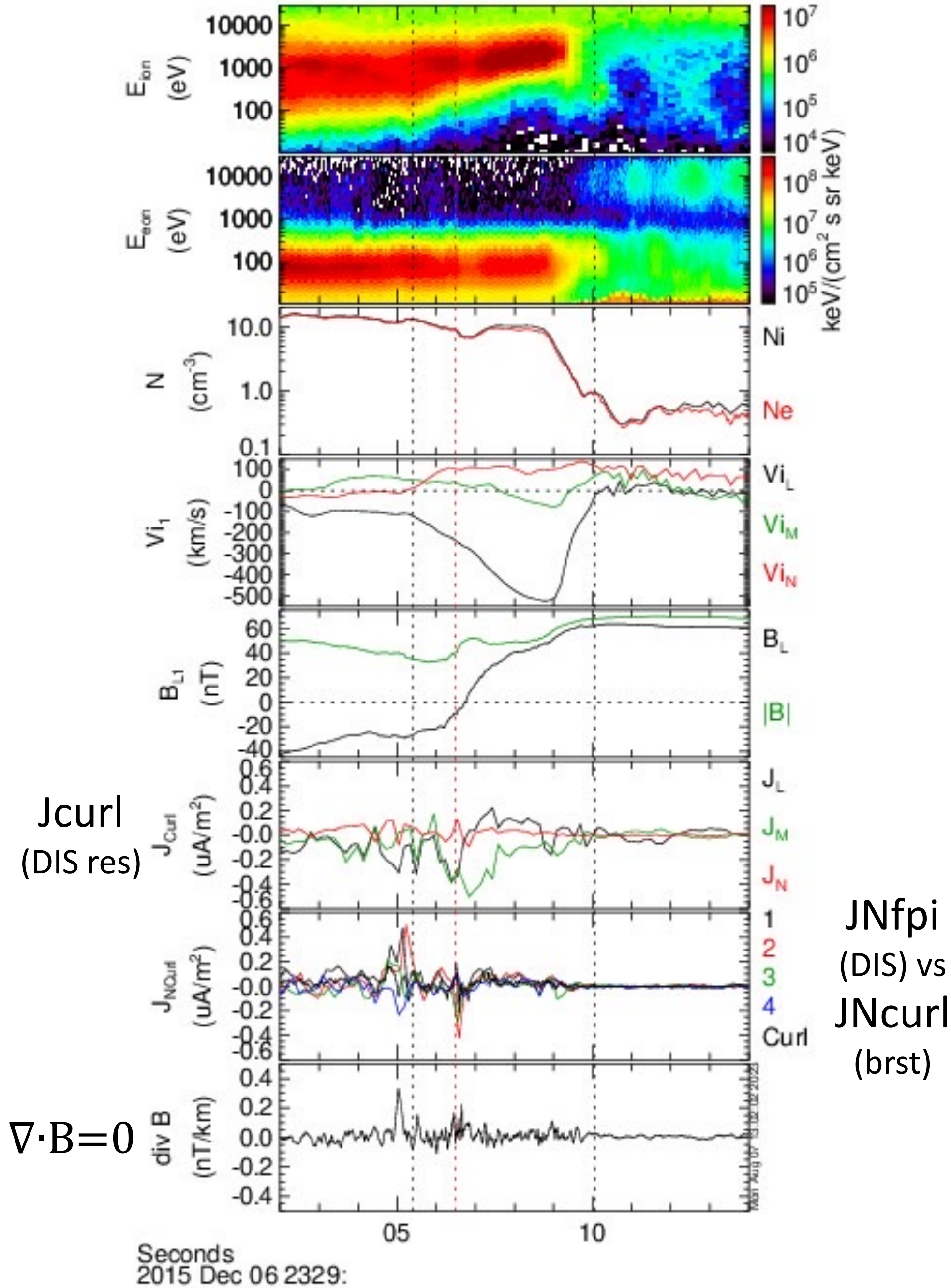

Tetrahedron conclusion:
Jcurl gives an average J.
Jfpi=Ne(Vi-Ve) is really good.
One may confirm if div(B)=0 …

Exploring MMS at the Dayside Magnetopause: **Reconnection $E'=E+V_exB$**

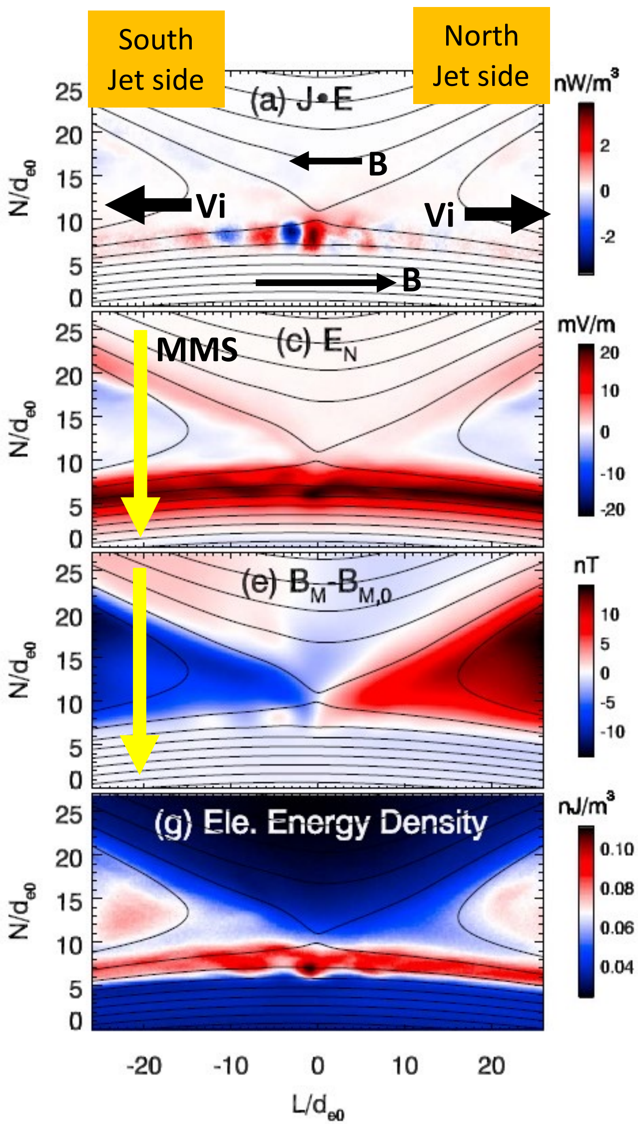

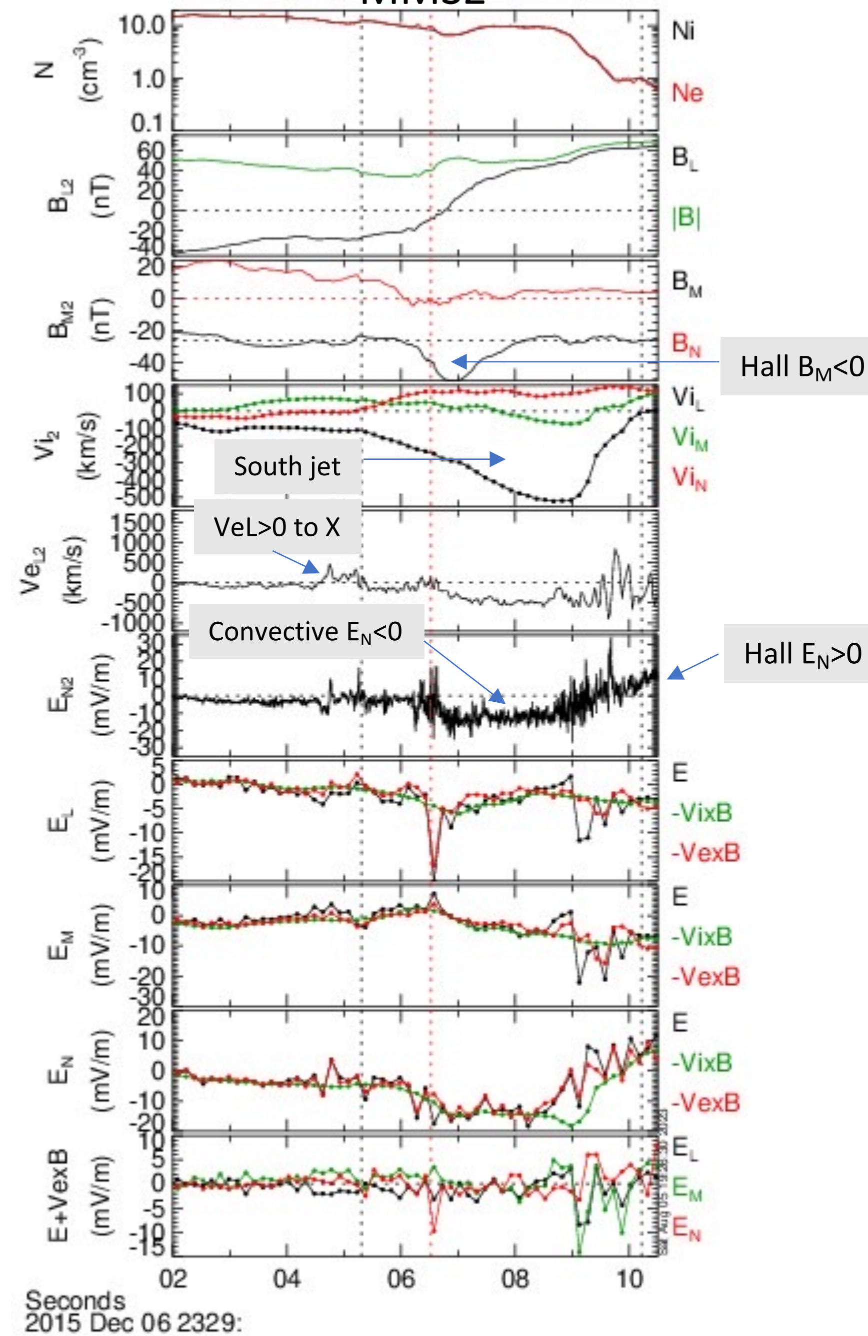

Exploring MMS at the Dayside Magnetopause: **Reconnection J·E'**

J · E' > 0 particles gain energy from EM
J · E' < 0 particles lose energy to EM

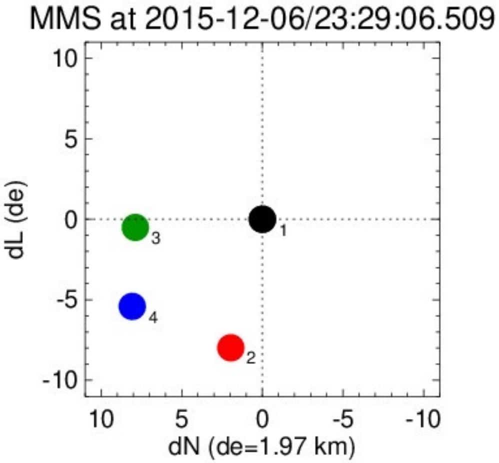

$MMS1_{GSM}$=[8.32 -3.96 -0.80] R_E
N_{GSM}=[0.674 -0.607 -0.421]
L_{GSM}=[-0.160 -0.677 0.718]
M_{GSM}=[-0.721 -0.417 -0.553]

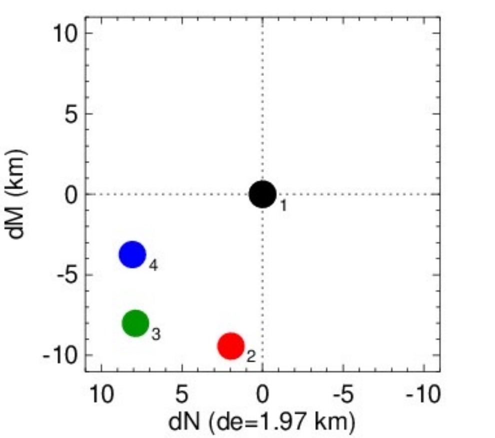

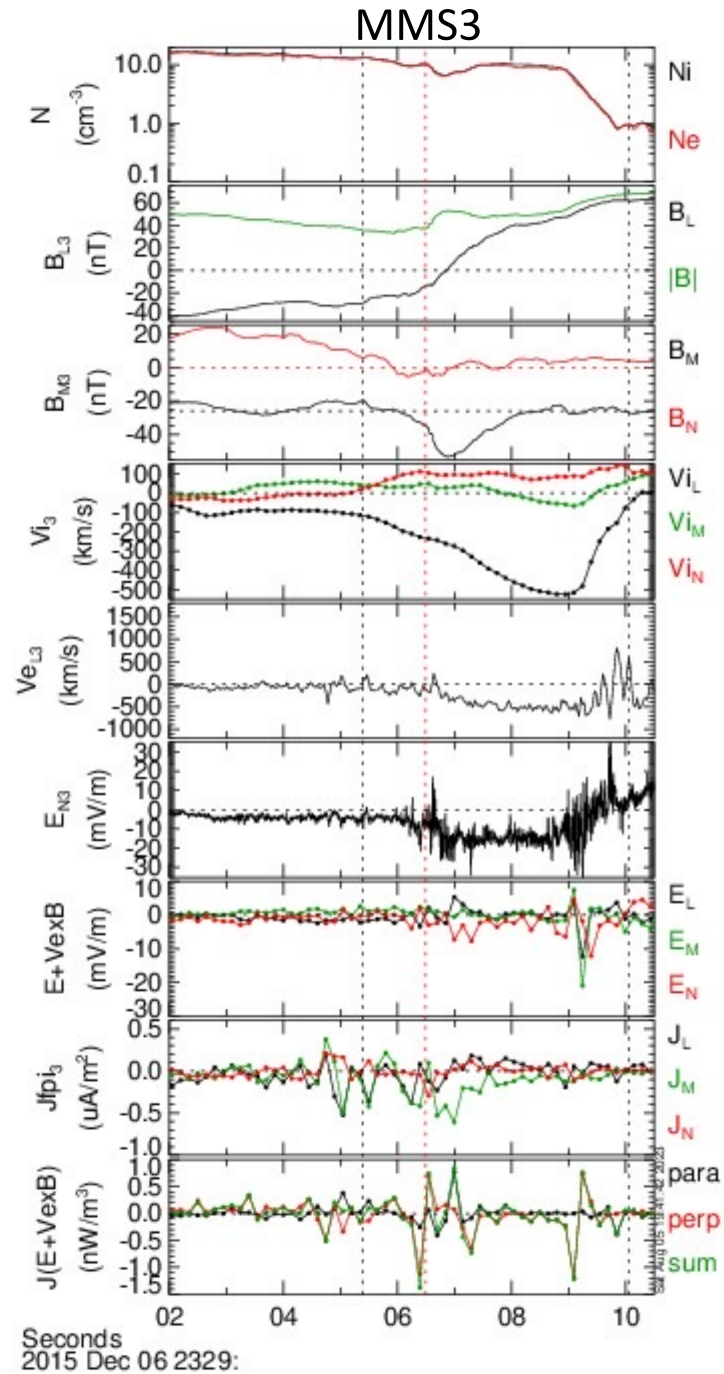

Exploring MMS at the Dayside Magnetopause: **Reconnection J·E’**

J · E’ > 0 particles gain energy from EM
J · E’ < 0 particles lose energy to EM

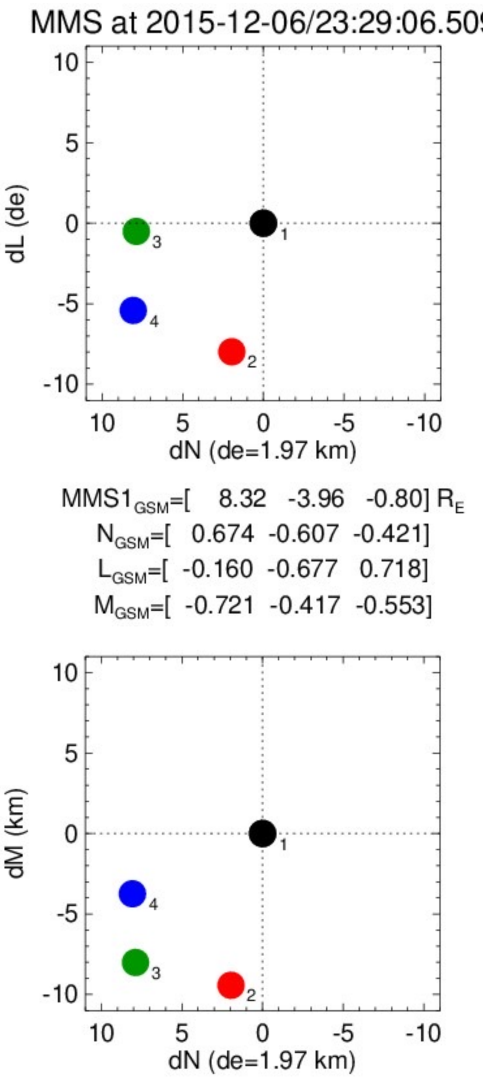

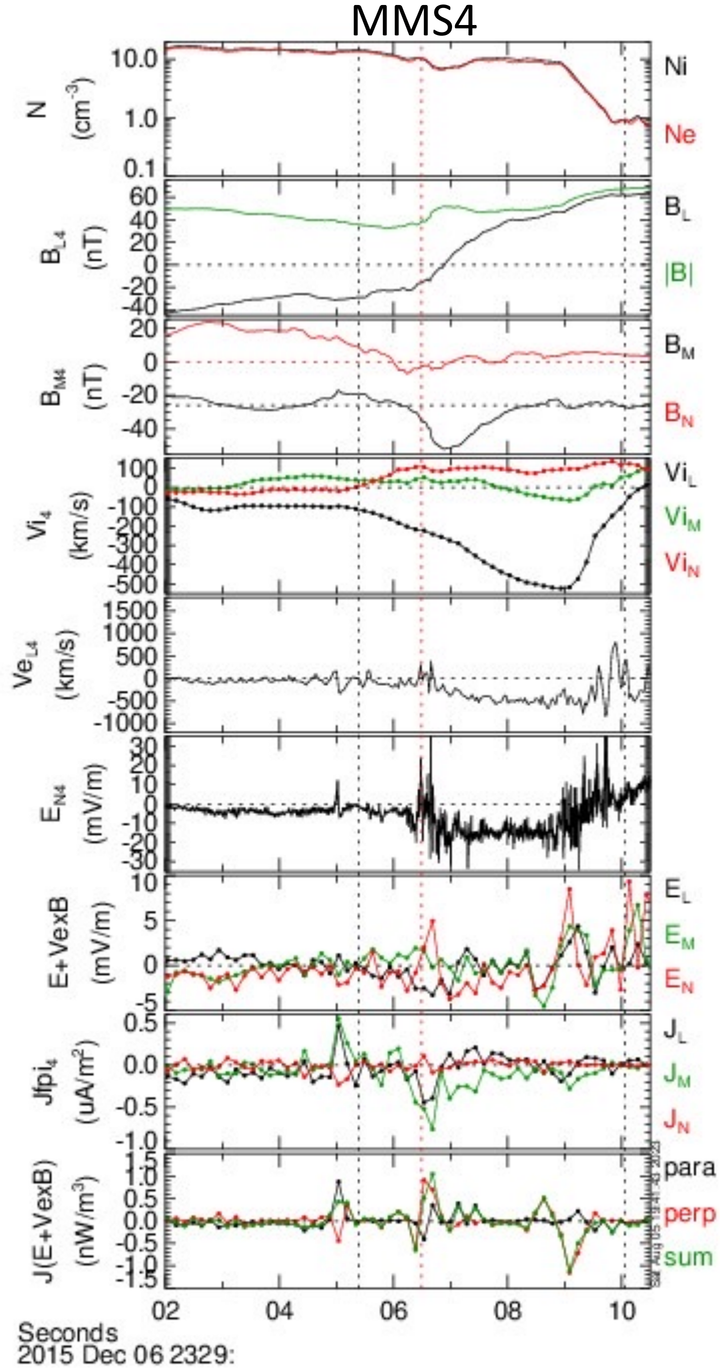

Exploring MMS at the Dayside Magnetopause: **Reconnection J·E'**

J · E' > 0 particles gain energy from EM
J · E' < 0 particles lose energy to EM

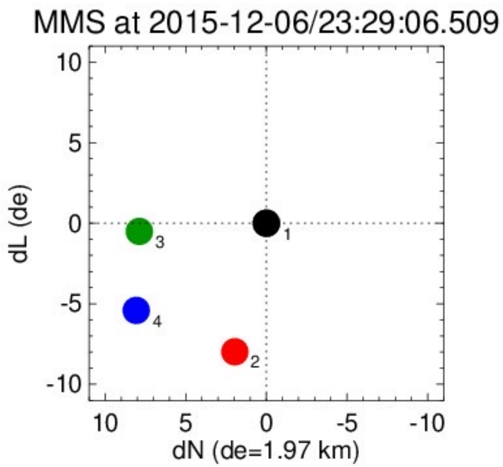

MMS1$_{GSM}$=[8.32 -3.96 -0.80] R_E
N$_{GSM}$=[0.674 -0.607 -0.421]
L$_{GSM}$=[-0.160 -0.677 0.718]
M$_{GSM}$=[-0.721 -0.417 -0.553]

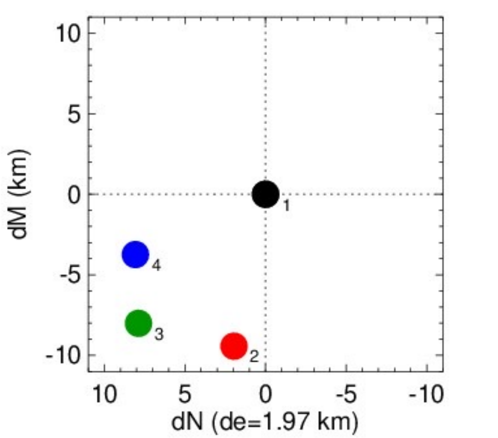

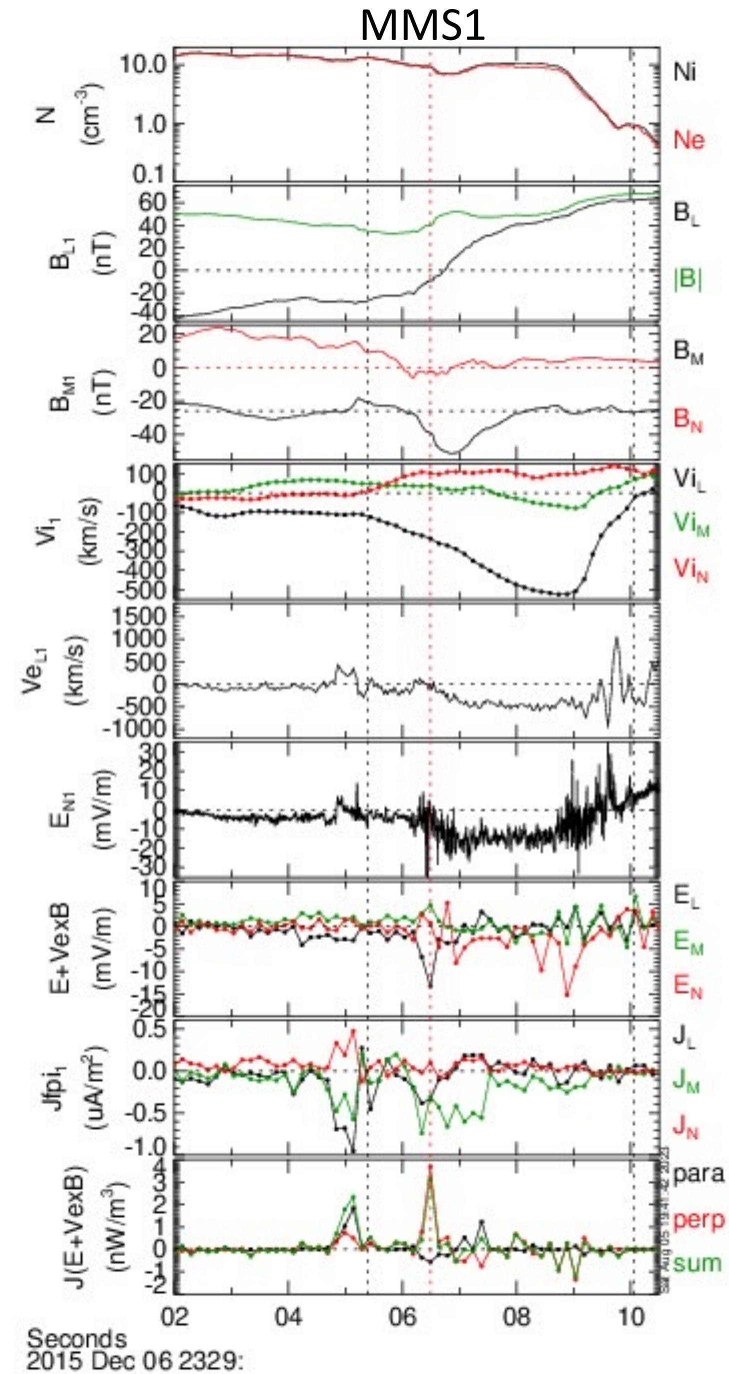

Exploring MMS at the Dayside Magnetopause: **Reconnection J·E’**

J · E’ > 0 particles gain energy from EM
J · E’ < 0 particles lose energy to EM

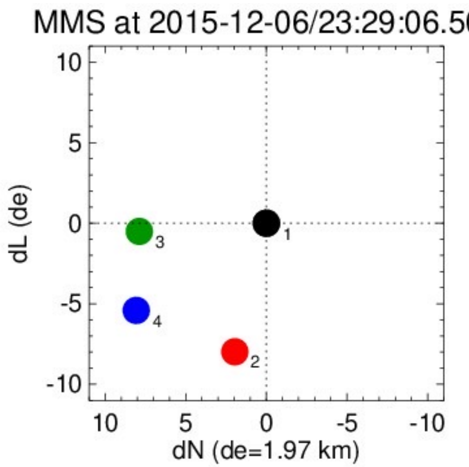

$MMS1_{GSM}$=[8.32 -3.96 -0.80] R_E
N_{GSM}=[0.674 -0.607 -0.421]
L_{GSM}=[-0.160 -0.677 0.718]
M_{GSM}=[-0.721 -0.417 -0.553]

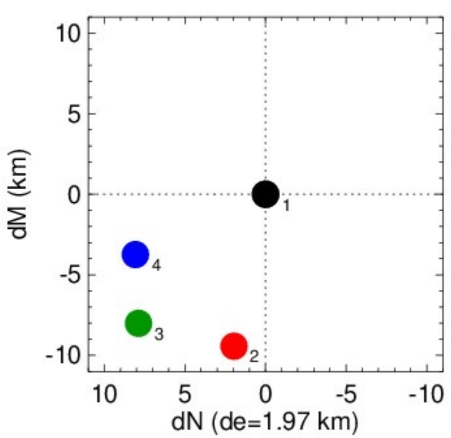

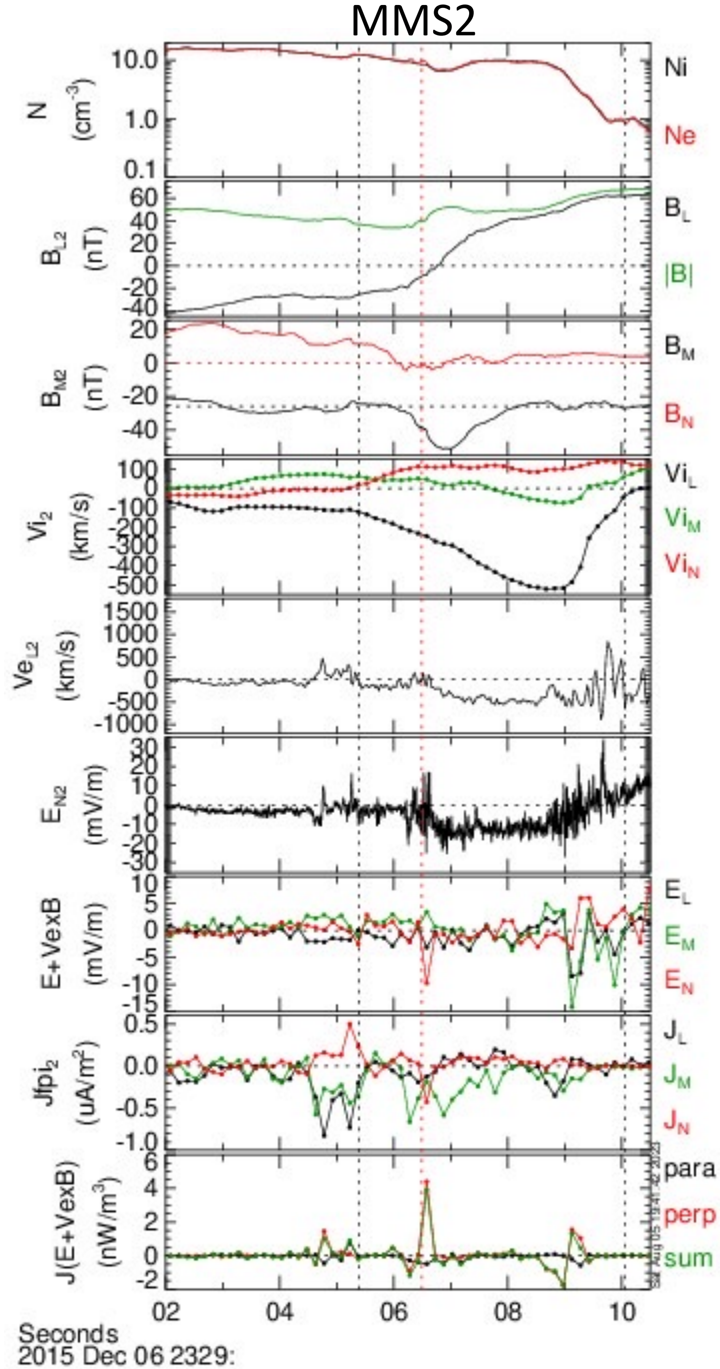

Exploring MMS at the Dayside Magnetopause: J·E' & ∇×(Ve)

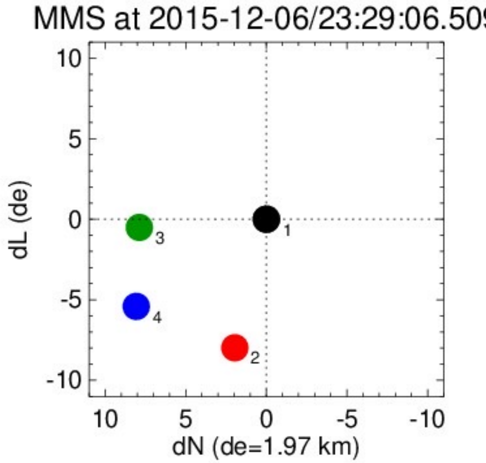

MMS1$_{GSM}$=[8.32 -3.96 -0.80] R_E

N$_{GSM}$=[0.674 -0.607 -0.421]

L$_{GSM}$=[-0.160 -0.677 0.718]

M$_{GSM}$=[-0.721 -0.417 -0.553]

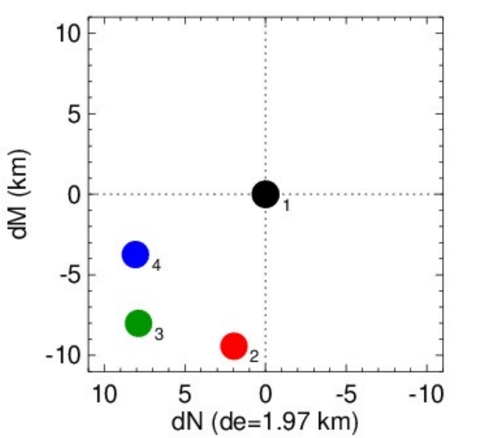

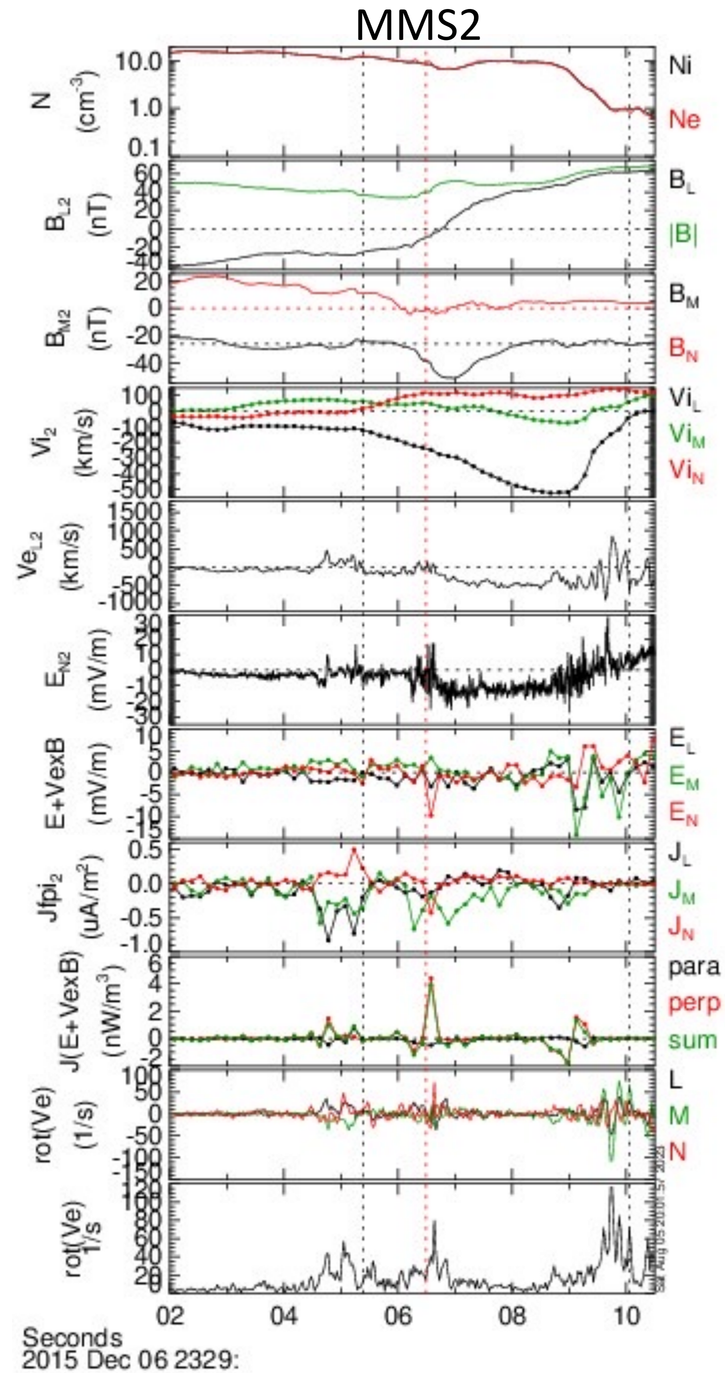

Exploring MMS at the Dayside Magnetopause: **J·E' & ∇×(Ve)**

MMS allows unprecedented examinations of kinetic (ions & electrons) physics associated with reconnection & space physics in general.

This example has demonstrated many predicted (PIC) signatures of reconnection at the asymmetric magnetopause.

It also demonstrated a case of electron flow vorticity at both separatrices & inside exhaust.

An extended ~8-10 d_e layer (L+M) exists inside the exhaust (ΔN~2d_e) with Jperp·E'>0 (mms2+mms1)

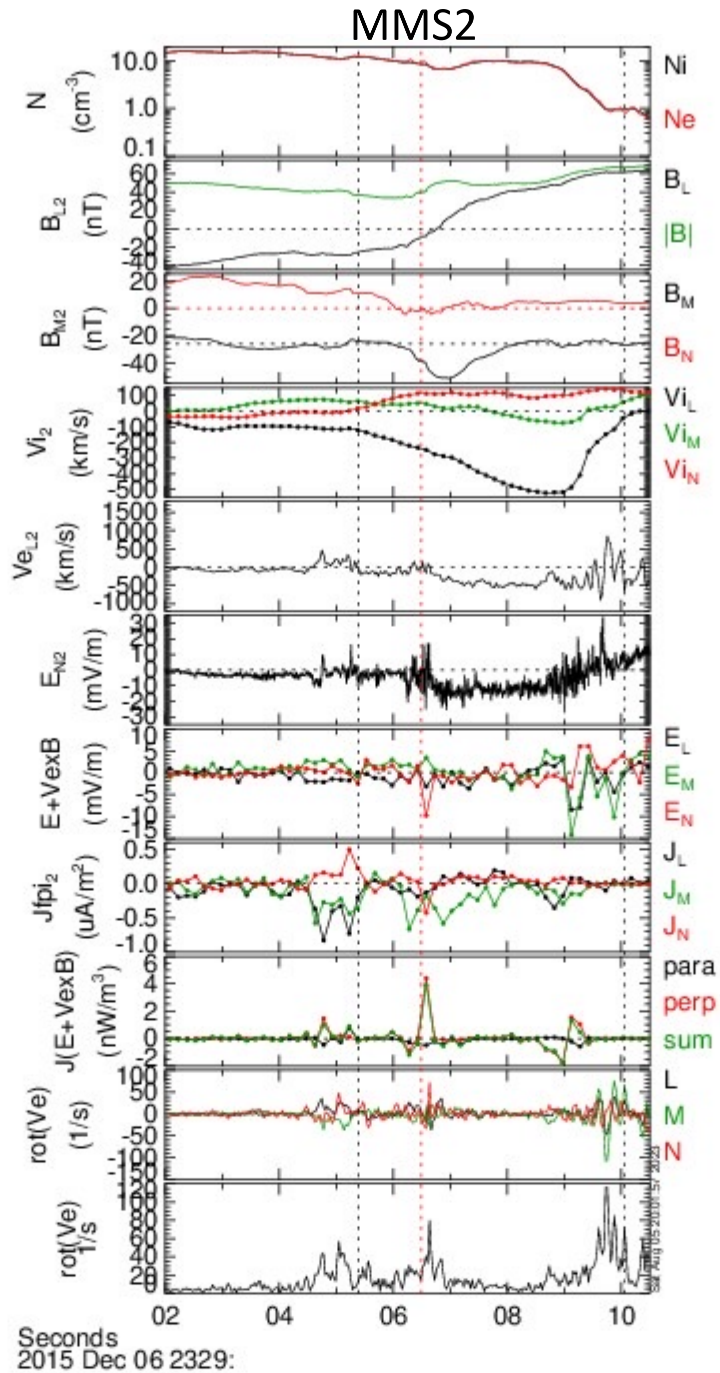

Summary

- Current sheets can become unstable and reconnect. Whether big or small… [Yes, many HCSs near the Sun support exhausts!]
- The Alfvenic jets along the CS are a major characteristic.
- Other Rx parameters include Hall B and if (!) there are good 3D electric field measurements, you should see the Hall E.
- Multi-spacecraft tetrahedron formations allow us to obtain spatial ***gradients***. Beware of "Tetrahedron Quality Factor"… *not all formations are "regular" (TQF=1) and div(B)≠0 !*
- The Generalized Ohm's Law helps us understand the plasma physics (particle motions) when **E** ≠ -**v** x **B** … e.g. Rx
- Showed observations of Alfvenic reconnection jets across two current sheets – one in the solar wind and one at the m'pause.

Summary

- *I did NOT cover how you find the crucial **L,M,N** orientation of current sheets in space.*

*Many methods exist. Often one truly only knows the direction of maximum variance (**L**)…* ☹

*Normals (**N**) found using…to name a few.*

*(1) minimum variance of **B*** *(ISSI Chapter 8, Sonnerup & Scheible, 1998)*

*(2) cross-product of **B** on either side* *(Knetter et al 2004, J. Geophys. Res., 109, A06102, doi:10.1029/2003JA010099)*

*(3) timing (**if** good s/c distribution – beware of poor alignments relative CS)* *(ISSI Chapter 10, Schwartz, 1998)*